STRENGTH PREDICTIONS OF HAT STIFFENED PLATE USING FINITE ELEMENT METHOD

A THESIS

Submitted by

MANOJ G. THARIAN

for the award of the degree of

DOCTOR OF PHILOSOPHY

(Faculty of Technology)

DEPARTMENT OF SHIP TECHNOLOGY
COCHIN UNIVERSITY OF SCIENCE AND TECHNOLOGY
KOCHI-682022, KERALA, INDIA

MARCH 2015

STRENGTH PREDICTIONS OF HAT STIFFENED PLATE USING FINITE ELEMENT METHOD

Thesis Submitted to

Cochin University of Science and Technology, Kochi

in fulfillment of the requirements for the award of the degree of

Doctor of Philosophy

(Faculty of Technology)

by

Manoj G. Tharian

Register No 3562 (2008 Admission)

under the supervision of

Dr. C. G. Nandakumar

Associate Professor

Department of Ship Technology

Cochin University of Science and Technology

Kochi-682022, Kerala, India

March 2015

Department Of Ship Technology
Cochin University of Science and Technology
Kochi 682022,
Kerala, India

CERTIFICATE

I hereby certify that, to the best of my knowledge, the thesis entitled ***'Strength Predictions of Hat Stiffened Plate Using Finite Element Method'*** *submitted by* ***Manoj G. Tharian****, Part time research student, Reg. No. 3562, to Cochin University of Science and Technology in partial fulfillment of the requirement for the award of Ph.D. degree in the faculty of technology is a bonafide record of the research work carried out by him under my supervision and guidance. The contents of this thesis have not been submitted to any other university or institute for the award of any degree. I also certify that all the relevant corrections and modifications suggested by the audience during the pre-synopsis seminar and recommended by the Doctoral Committee of the candidate have been incorporated in the thesis.*

Kochi-22
Date: 16.03.2015

Dr. C. G. Nandakumar
(Research Guide)
Associate Professor
Department of Ship Technology,
Cochin University of Science &
Technology,
Kochi-22
Email: *nandu@cusat.ac.in*

DECLARATION

I, hereby declare that the thesis entitled "**Strength Predictions of Hat Stiffened Plate Using Finite Element Method**" submitted to Cochin University of Science and Technology in partial fulfillment of the requirement for the award of the degree of Doctor of Philosophy in the Faculty of Technology is a bonafide record of the research work carried out by me under the supervision and guidance of **Dr. C. G. Nandakumar**, Department of Ship Technology, CUSAT. The contents of this thesis have not been submitted to any other university or institute for the award of any degree.

Kochi-22
Date: 16.03.2015

Manoj G. Tharian
Part time Research Scholar
Reg. No. 3562
Dept. of Ship Technology,
Cochin University of Science
& Technology,
Kochi – 21
Email: *mtharian2000@yahoo.co.in*

ACKNOWLEDGEMENTS

It is with immense gratitude that I acknowledge the support and inspiring guidance of my research guide, **Dr. C. G. Nandakumar**, Associate Professor, Department of Ship Technology. This work would not have been accomplished, but for his constructive reviews, constant encouragement and supervision throughout the course my research work.

I am thankful to **Dr. K. Sivaprasad**, HoD, Department of Ship Technology, Cochin University of Science and Technology for providing me with the opportunity to work in this area.

I express my sincere thanks to **Dr. E. M. Somashekharan Nair** for his advice and encouragement during the initial days of my research work and to **Dr. K. P. Narayanan** for his support and advice as doctoral committee member.

I thank all the faculty members of Department of Ship Technology who have given their valuable and fruitful suggestions. I greatly appreciate the support and advice received from my co-researchers **Bindumol T.V.** and **Smitha K. K.** during my research.

The services of the Office staff of Department of Ship Technology, Cochin University of Science and Technology are acknowledged with sincere thanks.

I express my sincere gratitude to **Rev. Fr. Dr. Antony Kariyil**, Director, Rajagiri Group of Institutions and **Msgr. Thomas Malekudy,** former Manager, Viswajyothi College of Engineering and Technology for facilitating this research work.

I also would like to thank many of my friends and colleagues who in various capacities have rendered their help. I greatly appreciate the support in proofreading received from my colleagues **Sonia Paul**, **Arun A. Balakrishnan** and **Jithin P. N.**

I am grateful to my mother **Smt. Mary Tharian** for her love, inspiration and appeal to the Almighty.

I would like to thank my wife **Archana** and my children **K. M. Tharian** and **K. M. Antony** for the understanding and patience shown by them during this period.

Above all, I express my indebtedness to the Almighty for all His blessing and kindness. All this would not have been possible without the grace of **GOD**.

Manoj G Tharian

CONTENTS

Page No.

ABSTRACT

KEYWORDS: Lightweight Ships, Hat Stiffened Plate, Finite Element Analysis, Representative Unit Cell, Orthotropic Plate Model, Superelement.

Hat Stiffened Plates are used in composite ships and are gaining popularity in metallic ship construction due to its high strength-to-weight ratio. Light weight structures will result in greater payload, higher speeds, reduced fuel consumption and environmental emissions. Numerical Investigations have been carried out using the commercial Finite Element software ANSYS 12 to substantiate the high strength-to-weight ratio of Hat Stiffened Plates over other open section stiffeners which are commonly used in ship building.

Analysis of stiffened plate has always been a matter of concern for the structural engineers since it has been rather difficult to quantify the actual load sharing between stiffeners and plating. Finite Element Method has been accepted as an efficient tool for the analysis of stiffened plated structure. Best results using the Finite Element Method for the analysis of thin plated structures are obtained when both the stiffeners and the plate are modeled using thin plate elements having six degrees of freedom per node. However, one serious problem encountered with this design and analysis process is that the generation of the finite element models for a complex configuration is time consuming and laborious. In order to overcome these difficulties two different methods viz., Orthotropic Plate Model and Superelement for Hat Stiffened Plate have been suggested in the present work.

In the Orthotropic Plate Model geometric orthotropy is converted to material orthotropy i.e., the stiffeners are smeared and they vanish from the field of analysis and the structure can be analysed using any commercial Finite Element software which has orthotropic elements in its element library. The Orthotropic Plate Model developed has predicted deflection, stress and linear buckling load with sufficiently good accuracy in the case of all four edges simply supported boundary condition. Whereas, in the case of two edges fixed and other two edges simply supported boundary condition even though the stress has been predicted with good accuracy there has been large variation in the deflection predicted. This variation in the deflection predicted is because, for the Orthotropic Plate Model the rigidity is uniform

throughout the plate whereas in the actual Hat Stiffened Plate the rigidity along the line of attachment of the stiffeners to the plate is large as compared to the unsupported portion of the plate.

The Superelement technique is a method of treating a portion of the structure as if it were a single element even though it is made up of many individual elements. The Superelement has predicted the deflection and in-plane stress of Hat Stiffened Plate with sufficiently good accuracy for different boundary conditions. Formulation of Superelement for composite Hat Stiffened Plate has also been presented in the thesis. The capability of Orthotropic Plate Model and Superelement to handle typical boundary conditions and characteristic loads in a ship structure has been demonstrated through numerical investigations.

LIST OF TABLES

LIST OF FIGURES

NOTATIONS

Latin Symbols

D_x, D_y, D_z	Rigidity of the orthotropic plate in the x, y and z directions respectively
E	Modulus of elasticity
E_x, E_y, E_z	Modulus of elasticity for the orthotropic plate in x, y and z directions respectively
F_x, F_y and F_z	Force along x, y and z axis
G	Modulus of rigidity for the parent Hat Stiffened Plate
G_{xy}, G_{yz}, G_{xz}	Modulus of rigidity for the orthotropic plate
H	Effective torsional rigidity of the orthotropic plate
I_r	Moment of inertia of the stiffener including the effective width of the attached plating
k'	Stiffness Matrix in local coordinates
k	Stiffness Matrix of Rectangular Shell Element having six degrees of freedom
k*	Stiffness Matrix of Rectangular Shell Element having five degrees of freedom
$k_{\mathbf{B}}$	Stiffness Matrix of Plate Bending Element
k_M	Stiffness Matrix of plane Stress Element
M_x, M_y & M_z	Moment about x, y and z axis respectively

q	Intensity of the uniformly distributed lateral load
R	Modified aspect ratio for the orthotropic plate
t	Thickness of the shell element
t_{op}	Thickness of the orthotropic plate
t_p	Thickness of the plate of Hat Stiffened Plate
t_r	Thickness of the stiffener of Hat Stiffened Plate
u,v & w	Translation degrees of freedom in the x, y and z direction respectively

Greek Symbols

ε	One thousandth of the smallest diagonal element of k_B and k_M
η, λ	Non dimensional parameters characterizing the material orthotropy
θ_x, θ_y & θ_z	Rotational Degree of Freedom about x, y and z axis respectively
ν	Poisson's ratio for an isotropic material
ν_x	Poisson's ratio, a unit extension in x direction is accompanied by lateral contraction $-\nu_x\sigma_x/E_x$
ν_y	Poisson's ratio, a unit extension in y direction is accompanied by lateral contraction $-\nu_y\sigma_y/E_y$
ν_z	Poisson's ratio, a unit extension in z direction is accompanied by lateral contraction $-\nu_z\sigma_z/E_z$
σ_x, σ_y	In-plane stress in the x and y directions respectively
Δ	Maximum deflection of the plate in the z direction under uniform lateral pressure q

Mathematical Symbols

[I]	Unit matrix
[T]	Transformation Matrix
{d}	Displacement vector in global coordinates
{d'}	Displacement vector local coordinates
{r}	Elemental load vector applied by an element to structure nodes in global coordinates
{r'}	Elemental load vector in local coordinates
[k]	Elemental stiffeness matrix in global coordinate

Variables used in the Computer programs

astif[ ][ ]	Contains the assembled stiffness matrix for the structure modeled using conventional element
def[ ]	Contains the structural values degrees of freedom
fx[]	Contains nodal values of forces in the x direction for the element
fy[]	Contains nodal values of forces in the y direction for the element
fz[]	Contains nodal values of forces in the z direction for the element
ldv[ ]	Contains the load vector for the structure
mx[]	Contains nodal values of moment about the x axis for the element
my[]	Contains nodal values of moment about the y axis for the element
mz[]	Contains nodal values of moment about the z axis for the element

nbdf[ ]	Contains the global numbering of structural degress of freedom
sastif[ ][ ]	Contains the assembled stiffness matrix for the structure modeled using Superelements
theetax[ ]	Contains the nodal values of rotational degree of freedom about the x axis
theetay[ ]	Contains the nodal values of rotational degree of freedom about the y axis
theetaz[ ]	Contains the nodal values of rotational degree of freedom about the z axis
u[ ]	Contains the nodal values of displacement degree of freedom in the x direction
v[ ]	Contains the nodal values of displacement degree of freedom in the y direction
w[ ]	Contains the nodal values of displacement degree of freedom in the z direction

ABBREVIATIONS

DNV	Det Norske Veritas
dof	Degrees of Freedom
FEA	Finite Element Analysis
FEM	Finite Element Method
FLS	Fatigue Limit State
FS	Two edges fixed and other two edges simply supported boundary condition.
HSP	Hat Stiffened Plate
IACS	International Association of Classification Societies
IMO	International Maritime Organization
ISO	International Organization for Standardization
OPM	Orthotropic Plate Model
RUC	Representative Unit Cell
SLS	Serviceability Limit State
SS	All four edges simply supported boundary condition.
ULS	Ultimate Limit State

CHAPTER 1

INTRODUCTION

1.1 MOTIVATION

Ship structure in general can be considered as a three dimensional frame work of stiffened plates, constituted by deck, side shells, bottom shell and bulkheads. A stiffened plate or panel is an assembly of stiffeners and plate where the stiffeners are welded on to one side of the plate in either one or both directions. Open sections like Flat Bar, Angle, Holland Profile (bulb-plate) and Tee are commonly used in ship structure. Trapezoidal or Hat shaped stiffener is a typical closed section stiffener which is commonly used in the case of composite structures but is not very common in metallic structures.

Construction of lightweight ships has been gaining popularity since it allows a greater payload for a given steel weight of the vessel and allows higher speeds to be achieved. In addition, lightweight ships result in reduced fuel consumption and environmental emissions for a given payload and distance travelled. The weight of a structure can be reduced significantly not only by the usage of lighter materials but also by improvements in structural configuration. Thus, introduction of Hat Stiffened Plate (HSP) in steel ship construction probably must have been an outcome of the attempts by ship designers to construct lightweight stiffened panels such as deck structures. The high strength-to-weight ratio of HSP has made it a choice for structural engineers in their attempt to design light steel deck structures for high speed vessels (Jia and Ulfvarson, 2005).

HSP has a number of closed profile stiffeners provided along the dominant direction as shown in Figure 1.1. In the case of steel structures, hat stiffeners are usually formed sections. The stiffeners are either welded or riveted to the plate and if riveted, flanges are provided for the stiffener. For composite structures, hat stiffeners are usually made by hand lay-up. The hat stiffeners are bonded to the plate through the flanges of the stiffeners.

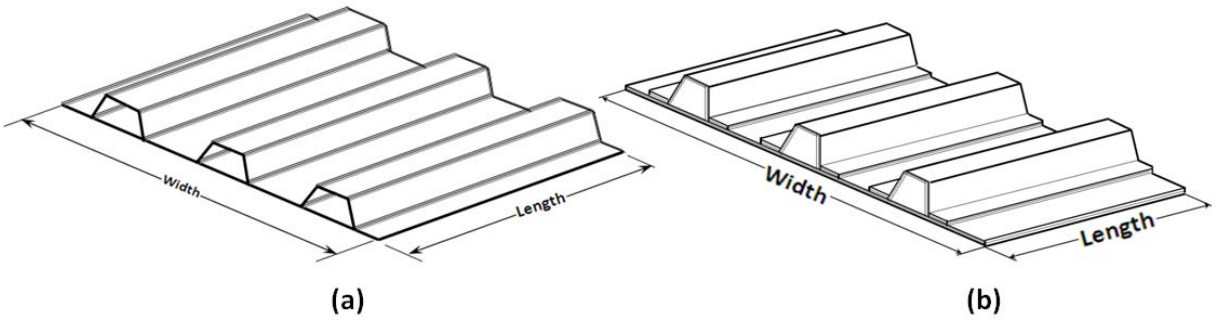

Figure 1.1 Schematics of a typical: (a) Metallic Hat Stiffened Plate (b) Composite Hat Stiffened Plate

The advantages of closed section stiffeners over the open section stiffeners both in the strength and economic point of view have been brought out by Dubas (1976). The closed section stiffeners have definite advantages over open section stiffeners, especially with regard to the torsional rigidity and strength-to-weight ratio. Closed section stiffeners provide a higher bending stiffness and thus allow a greater spacing of the stiffeners. The high Saint Venant torsional rigidity of closed section stiffeners enhances the ultimate strength of the stiffened plate. Moreover the geometrical configuration alone allows a greater spacing between the stiffeners due to their own width. The connection with the plate requires only two fillet welds which are no more than what is required for a single open section stiffener. The enclosed space between the stiffener and the plate in the case of closed section stiffeners can effectively be utilized as a duct for the passage of cables. However the cost of labor employed on the fabrication of these sections by the process of cold forming necessary for obtaining the required shape of section is slightly high when compared to open sections. In addition, closed sections provide restricted access to a portion of the plate which can affect the inspection for corrosion. In spite of this, closed sections stiffeners can be successfully employed in certain parts of ship structure.

Traditionally hat stiffeners have been used for stiffening the stool plates which support the corrugated bulkheads in bulk carriers. Trough shaped steel sections having the same shape as hat stiffeners are used as fenders on small ships (D'Arcangelo, 1969). HSPs are used as deck plate and bulkheads in ship structure. In addition, the hat shaped stiffeners are used in side panels of transit containers, sheet piles for various applications and structural panels.

Analysis of stiffened plate has always been a matter of concern for the structural engineers since it has been rather difficult to quantify the interaction between stiffeners and plating or rather the actual load sharing between these two. The interaction of beams and plating is an interaction between two modes of loading and response. Strain energy method has always remained as a solution strategy but of limited scope for actual stiffened plate problems. Application of matrix method and subsequent developments in the form of Finite Element Method (FEM) or Finite Element Analysis (FEA) has solved the complexities of analysis of stiffened plated structure. The single biggest development in ship structural design and analysis over the last few decades has been the introduction and acceptance of FEM as the structural analysis strategy. This tool offers both faster and more accurate solution to ship structural systems with complexities in geometry and boundary condition.

In ship structural design using FEM, analysis has been carried out at different scale levels viz., complete ship, hull module and principal members like stiffened panels, frames, girders etc. While using FEM, difficulties have been faced in the selection of elements, the choice of nodal positions and the method of connecting the beam and membrane elements. Best results using the FEM for the analysis of thin plated structures are obtained when both the stiffeners and the plate are modeled using thin plate elements having six degrees of freedom (dof) per node. However, one serious problem encountered with this design and analysis process is that the generation of the finite element models for a complex configuration is time consuming and laborious. Representing each stiffener individually while modeling a complete ship or hull module of a ship, is a tedious procedure and it will result in excessive amounts of storage. In order to overcome these difficulties two different methods viz., Orthotropic Plate Model (OPM) and Superelement for HSP have been suggested for the FEA of HSP in the present work. In the first method the HSP made of isotropic material and having geometric orthotropy has been replaced with an OPM having the same plan dimensions and having material orthotropy. The OPM can readily be modeled and analyzed using an orthotropic plate finite element available in the element library of any general finite element software. In the second method, the HSPs in the ship structure can be analyzed using Superelement developed without making any compromise on the accuracy. In the Superelement technique a portion of the structure is treated as a single element even though it

is made up of many individual elements. Both these methods will reduce the storage requirement and modeling efforts considerably.

The **objectives** of the present work have been listed below:

- To identify a Representative Unit Cell of Hat Stiffened Plate and substantiate the high strength-to-weight ratio of Hat Stiffened Plate by conducting numerical investigations
- To develop an **Orthotropic Plate Model** based on equal rigidity concept as a structural substitute for Hat Stiffened Plate to carry out linear elastic static analysis and linear buckling analysis
- To develop a **Superelement** for Hat Stiffened Plate for the geometric modeling and linear elastic analysis

1.2 LAYOUT OF THE THESIS

The geometrical features of a HSP, advantages and limitations of closed section stiffeners, applications of HSP and the scope of FEM for the analysis of stiffened plate have been explained in Chapter 1. In addition, objectives of the present work have been listed here. Chapter 2 gives the review of literature on classical methods for the analysis of HSP, FEA of stiffened plates including HSP and plate finite elements. In Chapter 3, numerical investigations have been carried out to quantify the structural advantages of HSP over plates stiffened with open section stiffeners. In Chapter 4, the development of an OPM for HSP based on equal rigidity concept has been explained and numerical investigations have been carried out to validate the OPM developed. In Chapter 5, formulation of Superelement for HSP has been explained and numerical investigations have been carried out to validate the Superelement developed. Chapter 6 contains summary and conclusions of the present work.

Orthotropic plate theory has been presented in Appendix A and analytical solution for the bending of orthotropic plate has been presented in Appendix B. The expressions for the stiffness coefficients for plate bending and plane stress elements have been given in Appendix C.

CHAPTER 2

LITERATURE REVIEW

2.1 GENERAL

A detailed study on various methods for the analysis of stiffened plates has been carried out to identify a suitable method for the analysis of HSP. Among all the solution strategies available, FEM has been found to be the most effective tool for the analysis of stiffened plates. In addition a detailed review of literature available on FEA of metallic as well as composite HSPs has been carried out. A detailed review of literature available on plate bending elements has been carried out for the selection of a suitable element to use as the constituent element for the development of Superelement for HSP.

A comprehensive review of literature has been presented under the following subheadings:

- Classical Methods for the Analysis of HSP
- Analysis of Stiffened Plates
- FEA of HSP
- Quadrilateral Plate Finite Elements

In the classical method for the analysis of HSP, a brief review of literature on orthotropic plate theory used for the analysis of stiffened plates and analytical solution for orthotropic plates has been presented. Analysis of stiffened plates contains review of literature on analysis of stiffened plates using energy formulations, analysis of stiffened plates using FEM and ultimate strength predictions using FEM. A brief review of literature on metallic HSPs and composite HSPs have been presented in the section 2.4. Review of literature on plate bending elements available has been presented in the section 2.5.

2.2 CLASSICAL METHODS FOR THE ANALYSIS OF HSP

The governing differential equation of equilibrium for the bending of anisotropic plates subjected to lateral loads and the expression for the determination of rigidities in some specific cases has been given by Timoshenko (1959). A complete treatise of the classical methods for the analysis of stiffened plates has been given by Troitsky (1976), where orthotropic plate theory has been used for the analysis of plates stiffened with various types of stiffeners. The expressions for the flexural rigidities of various types of stiffened plate including HSP have been presented here. Classical methods can be employed for the analysis of such orthotropic plates. Schade (1951, 1953) has brought out the importance of effective breadth in the determination of sectional properties for design purposes. Hughes (1988) has presented a graph which enables the determination of effective breadth in the calculation of effective geometrical properties of the stiffened plate section. Bao et al (1997) have presented a critical review of analytical solutions for bending and buckling of flat, rectangular, orthotropic plates. Orthotropic Rescaling Technique has been employed to simplify the analysis. Systematic comparisons with finite element solutions are made for the critical buckling load of a plate under in-plane compression and for deflection and stresses in a plate under out-of-plane uniform pressure.

2.3 ANALYSIS OF STIFFENED PLATES

Wang and Rammerstorfer (1996) have proposed finite strip analysis for the determination of effective breadth and effective width of stiffened plate by finite strip analysis. Stiffened plates under lateral loads have been analyzed by Bediar (1997a) using a methodology which takes into account the discrete nature of the structure. In addition Bediar (1997b) has investigated the elastic behavior of multi-stiffened plates using an energy formulation.

Applications of matrix method and subsequent developments in the form of FEM have empowered the analysts capable of solving much of the complexities of analysis of stiffened plates. FEM method has been used in ship structure analysis, since early seventies (Kawai, 1973) and the extensive application of this method for the overall ship structure (global)

analysis as well as for the hull module analysis prevails even nowadays. Hughes (1988) has presented the structural modeling and analysis of hull module of a ship structure using FEM, where techniques like lumping the stiffeners; orthotropic plate approach and using separate stiffener element have been employed for linear analysis. Satish and Mukopadhyay (2000) have carried out the dynamic analysis of ship structures using a new stiffened plate element. Prusty and Satsangi (2001) have carried out static analysis of stiffened panels using an eight noded isoparametric element for shell and a three noded curved beam element for the stiffener.

It has been proposed to carry out the limit state analysis of HSP in this thesis using ULS since it has become a part of the day-by-day design and strength assessment practice. IMO and ISO requirements have recognized the need for limit state approaches for the design and strength assessment of ships and ship shaped offshore structures. There are four types of limit states that are relevant viz., Serviceability Limit State (SLS), Ultimate Limit State (ULS), Fatigue Limit State (FLS) and Accidental Limit State (ALS) for ship structural design (ISO, 2007). The true margin of structural safety cannot be determined as long as the ultimate limit state remains unknown. Hence the limit state approach has been well recognized as a better basis for design and strength assessment than the traditional allowable working stress approach. It is essential to predict the ultimate strength accurately within the design framework since the true strength margin of safety can be determined by comparing the ultimate strength and the design working stress. In maritime industry, the ultimate limit state has been applied as a basis of structural design and strength assessment (IACS, 2006a. and IACS, 2006b).

Pu et al. (1997) have presented a formulation for predicting the ultimate strength of a stiffened plate. Paik et al. (2001) have used large deflection orthotropic plate approach to develop the ultimate strength formulations for steel stiffened panels under combined biaxial compression/tension and lateral pressure loads, considering the overall buckling collapse mode. The first review article on ultimate hull girder strength has been presented by Yao (2003). Experimental investigations have been carried out by Paik and Thayamballi (2003) to study the effect of loading speed on the ultimate strength of steel plates subjected to dynamic axial compressive loads. Sun and Soares (2003) have presented results obtained from

experimental investigations carried out for the determination of ultimate torsional strength of a ship-type hull girder with a large deck opening. The ultimate load of stiffened plates with initial imperfections under axial compression has been determined using FEA and semi-empirical solutions by Kumar et al (2004) and the analytical results obtained have been compared with the experimental data. Paik et al (2008a, 2008b, 2008c) have carried out benchmark study on various ULS assessment methods for marine structures including IACS common structural rules and using various computer programs like ANSYS nonlinear FEA, DNV's PULS, ALPS/ULSAP, ALPS/HULL. Unstiffened plates surrounded by longitudinal stiffeners and transverse floors subjected to biaxial compression and lateral pressure loads have been dealt with in Paik et al (2008 a). Ultimate limit state assessment of stiffened plates under combined biaxial compression and lateral pressure loads has been dealt with in Paik et al (2008b) and the progressive collapse analysis of the hull structure has been dealt with in Paik et al (2008c). Some useful insights on application of nonlinear FEM for the assessment of ultimate limit strength of steel stiffened plated structures subjected to combined biaxial compression and lateral pressure actions have been presented by Paik and Seo (2009a, 2009b). Plate elements surrounded by stiffeners has been dealt with in Paik and Seo (2009a) and stiffened plates surrounded by strong support members such as longitudinal girders and transverse frames has been dealt with in Paik et al (2009b).

2.4 FINITE ELEMENT ANALYSIS OF HAT STIFFENED PLATE

Ko and Jackson (1991) have performed buckling analysis of Hat Stiffened Panel subjected to uniaxial compression using classical shear buckling theory for flat plate. Both local buckling and global buckling analysis have been carried out. The predicted local buckling loads have been compared with both experimental data and FEA. Jia and Ulfvarson (2005) have presented FEA on static and dynamic behavior of a high tensile steel deck designed with trapezoidal stiffeners. Hofmeyer (2005a) has substantiated that the location and movement of the first yield line in a total hat section can be investigated by using a 2D strip of hat section. The analytical model presented by Hofmeyer (2005b) gives a good insight in the complex cross section crushing behavior of hat sections made of steel.

Jiang et al. (1997) have carried out the FEA for the bending and buckling of unstiffened, sandwich and hat stiffened orthotropic rectangular plates. Two different approaches for modeling the HSP have been shown by them. In the former, the middle surface of the stiffener flanges is attached to the middle surface of the plate using rigid beams and in the latter the flanges and the plate in the joining region are replaced by a single plate section with an effective thickness equal to the sum of the thicknesses of the flange and the original plate. They have concluded that for the HSP the method of stiffener to plate attachment in the finite element model significantly affect the results and the second approach has been found to give better results. Roberts et al. (1999) have carried out tests on solid unstiffened, sandwich and hat stiffened rectangular orthotropic FRP plates for buckling by in-plane compression and for stresses and deflection under uniform out-of-plane pressure. The test results have been compared with FEA and analytical solutions. For the HSPs the results have shown good agreement in buckling. However under out-of-plane pressure, FEA and experimental results for stress and deflection have been in poor agreement. A formulation based on the concept of equal displacements at the shell – stiffener interface has been used by Prusty (2003) for the linear static analysis of composite hat stiffened laminated shells. Prusty and Ray (2004) have performed free vibration analysis of laminated composite shell stiffened with hat stiffeners. A unified formulation for the development of rigidity matrix for the laminated hat shaped stiffeners has been presented. Chen and Soares (2007) have presented a systematic approach to estimate the longitudinal strength of ship hull in composite material stiffened with hat stiffeners under buckling, material failure and ultimate collapse of the deck structure. The finite element free vibration and buckling analysis of laminated hat stiffened shallow and deep shells using arbitrarily oriented stiffener formulation has been presented by Prusty (2008). Mittelstedt and Schroder (2010) have presented a closed-form analytical approach for the analysis of the local post buckling behavior of hat stiffened flat composite panels under transverse compression. The post-buckling behavior of different forms of the composite stiffened plates including hat stiffened plates has been studied by Fattaneh and Mohammad (2014).

2.5 RECTANGULAR FINITE ELEMENTS

A rectangular shell element formulated by superimposing a plate finite element with a plane stress element as proposed by Bathe (2004) has been used for the formulation of Superelement of HSP. The major task confronted has been the selection of a suitable plate element for the formulation of rectangular shell element. Best results will be obtained if the element selected have the five essential qualities viz., correctness, completeness, continuity, consistency and convergence. The early plate finite element formulations such as Adini and Clough (1960), Melosh (1961), Tocher (1962) and Clough and Tocher (1965) in the early 1960s were displacement based. By mid 1960s the importance of inter-element compatibility has been realized and the variational basis for the FEM had become better understood. Bogner et al. (1965) have developed rectangular plate bending element having 16 and 36 dof that exhibited inter-element compatibility and good convergence properties. Irons and Draper (1965) have substantiated that it is not possible to derive a conforming element using simple polynomials and three geometric dof.

Conforming plate elements have been difficult to obtain and researchers looked for alternative formulations. Researchers made use of the principle of minimum potential energy which resulted in equilibrium formulation and has been made use of to develop conforming plate elements. Here an interpolation function has been chosen for the stresses or moments within the element and this function has to satisfy equilibrium at every point in the structure and the stress conditions on the boundaries. Morley (1967, 1968) and Elias (1968) have simplified the use of equilibrium formulation and the latter implemented the use of element stress functions. Przemieniecki (1968) has presented the stiffness matrices for the rectangular plate bending element and the rectangular plane stress element in the closed form. Torbe and Church (1975) have formulated the stiffness matrix and consistent nodal load vectors for a general quadrilateral plate element for both in-plane and bending analysis. Finite element solutions using the principle of minimum complementary energy have been discussed in detail by Gallagher (1975) and Zienkiewicz (1977). The 1970s saw a reduction in the rate at which new elements were derived and one of the most significant developments which emerged from that decade was the use of the displacement formulation based on Mindlin plate theory and

reduced integration schemes. A brief review of developments in the field of plate finite elements has been presented by Hrabok and Hrudey (1984).

Kirchhoff plate bending theory was abandoned in favor of Reissner-Mindlin plate theory of moderately thick plates. The continuity requirement for the displacement assumption has been lowered to C^0 but the transverse shear becomes an integral part of the formulation. Successful quadrilateral C^0 elements have been developed by Hughes et al. (1977), Pugh et al. (1978), MacNeal (1978, 1982), Crisfield (1983), Dvorkin and Bathe (1984), Tessler and Hughes (1985), Stanley (1985) and Park and Stanley (1986).

Wilson (1974) has presented the application of static condensation technique. Cook and Shah (1978) have compared the computational cost of two different condensation algorithms. The technique of static condensation has been successfully applied to condense stiffener web and flange of stiffened shell and a computer program has been developed based on this technique for the rapid analysis of stiffened cylindrical hulls by Rajgopalan and Chettiar (1984). The communication by Bathe and Dvorkin (1985) discusses a 4-node plate bending element for linear elastic analysis which is obtained as a special case, from a general nonlinear continuum mechanics based on 4-node shell element formulation. Ibrahimbegovic and Wilson (1991) have presented a simple formulation of a flat shell element obtained by superimposing discrete Kirchhoff plate bending elements and the membrane elements with drilling dof. Griffiths (1994) has expressed the stiffness matrix of a plane four node quadrilateral element in the closed form and comparison of the processing speed of the explicit and numerical approaches has been made. A four noded quadrilateral discrete Kirchhoff finite element has been proposed by Kratzig and Zhang (1994) for thin plate bending analysis by employing an eight noded interpolation scheme. Zhou and Vecchio (2006) have presented closed form finite element stiffness formulations for the four noded quadrilateral element with a fully populated material stiffness suitable for the nonlinear analysis of reinforced concrete membrane structures.

The rectangular plate bending element and the rectangular plane stress element presented by Przemieniecki (1968) has been selected for the formulation of quadrilateral element having six dof per node. These rectangular elements have been found to be easy to

employ for the shell element formulation as compared to other elements mentioned since the stiffness matrices are available in the closed form.

2.6 COMMENTS

Knowledge and information base are available in analysis of stiffened plates in the form of books and volumes of research publications. However, the source is not exhaustive as far as HSPs are concerned since introduction of hat shaped stiffeners in marine structures is a recent development. A definite need has been felt to develop a structural substitute or a Superelement which reduce the modeling efforts, storage requirement, and computational requirement for the FEA of HSP. From the review of literature it has been noted that usage of HSP in ship structure is picking up especially in the construction of light weight ships. The expressions for the flexural rigidities of HSP and the analytical solution for the bending orthotropic plates available in the literature have been made use of for the development of OPM for HSP. A detailed review of plate elements have been carried out and a shell element having six dof per node has been formulated based on the information gathered from literature. This quadrilateral shell element has been used for the formulation Superelement for HSP.

CHAPTER 3

STRUCTURAL PERFORMANCE OF HAT STIFFENED PLATE

3.1 GENERAL

The key elements of a ship structure are bottom and side shell plating, deck plating, transverse bulkheads, fore end, aft end and super structure as shown in Figure 3.1. Bottom and side shell plating serves as a watertight envelop of the ship as well as a principal strength member. Deck plating and transverse bulkheads which contribute substantially to the strength of the structure may also serve as liquid tight boundaries of internal compartments. Fore end accommodate bulbous bow, aft end accommodates the propeller and super structure contain accommodation area and navigation bridge. Apart from the fore end, aft end and superstructure a ship structure in general is a three dimensional frame work of stiffened plates, constituted by deck, side shells, bottom shell and bulkheads.

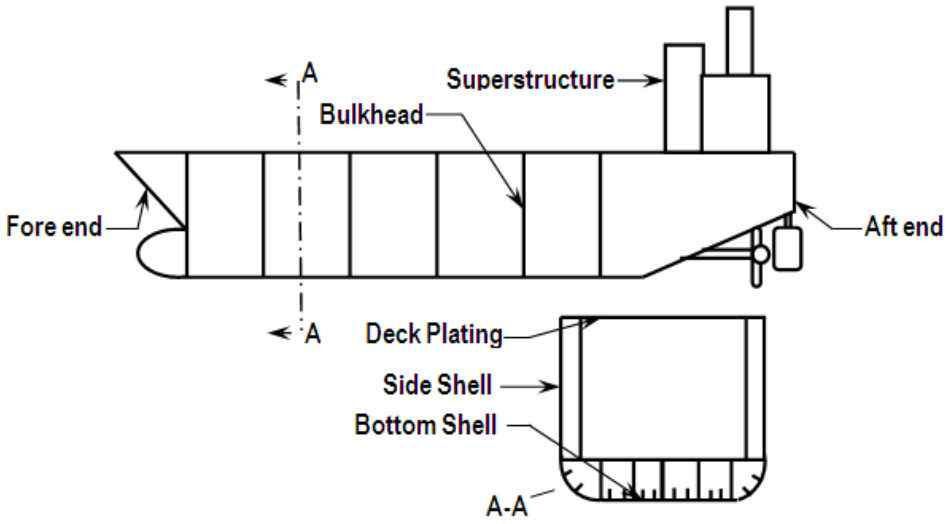

Figure. 3.1 Key structural elements of a ship

The stiffeners attached effectively to the plating contribute to the general longitudinal strength of the ship and will withstand the cargo and water pressure loads. In order to reduce their scantlings they are supported at locations other than bulkheads by deep transverse beams,

in the decks and by providing transverse floors in the bottom. The transverse bulkheads increase the transverse strength of the ship and have the same effect as the ends of a box. In a ship structure most of the lateral load acts initially on the plating. Through the action of plate bending, the plating transmits the lateral load to nearby stiffeners. The stiffeners in turn transmit the load to transverse beams and longitudinal girders.

A ship structure at sea is subjected to static and dynamic forces which causes the distortion of the structure. The ship structure is subjected to static forces, due to the water surrounding the ship, due to the weight of the cargo and due to the weight of the structure itself. The effect of these static forces is to cause a transverse distortion. For a ship floating in still water, although the total buoyant force is equal to the weight of the ship, due to the unalike distribution of the weight and the buoyancy along the length of the ship, it is subjected to shear force and bending moment. The bending moment causes the ship to bend in a longitudinal vertical plane like a beam. When the ship is moving amongst waves, distribution of weight remains unchanged but the distribution of buoyancy along the length is altered. This modification in the distribution of buoyancy causes a change in the shearing force and bending moment acting upon the ship in still water. The longitudinal bending causes compressive loading of stiffened plates. In addition to transverse loading and bending, a ship structure is subjected to torsion loads due to uneven distribution of cargo and by the action of waves. Torsion due to wave applied to a ship's structure like quartering sea causes twisting of the structure about the longitudinal axis.

The key interest in ship building is to design a structure having minimum weight and maximum strength. Ships which are built too strong are heavy, slow and cost extra money to build and operate since they weigh more, whilst ships which are built too weak suffer from minor hull damage and in some extreme cases catastrophic failure and sinking. So there has always been a constant strive among ship designers to design strong and lighter ships. The structural response of plates stiffened with hat stiffeners, flat bar, angle bar and Tee bar, subjected to lateral loading, in-plane loading and torsion loading has been investigated in the present chapter. ANSYS 12 has been used to carry out numerical investigations on plates stiffened with the selected stiffeners to establish the high strength-to-weight ratio of HSPs and the results have been presented in tabular form.

3.2 DESCRIPTION OF HAT STIFFENED PLATE

A section of the stiffened plate between two successive transverse deck beams of a conceptual lightweight ship deck on a pure car truck carrier vessel proposed by Jia and Ulfvarson (2005) having a span of 2.4 m has been selected for the various numerical investigation in this thesis.

3.2.1 Structural Characteristics

Geometry and dimensions of HSP having two stiffeners and the principal dimensions of the hat stiffener have been shown in Figure 3.2. The structure is made with EHS690 steel. The Poisson's ratio of the material is 0.3, the modulus of elasticity is 210 GPa, density is 7800 kg/m^3, and the yield stress is 690 MPa.

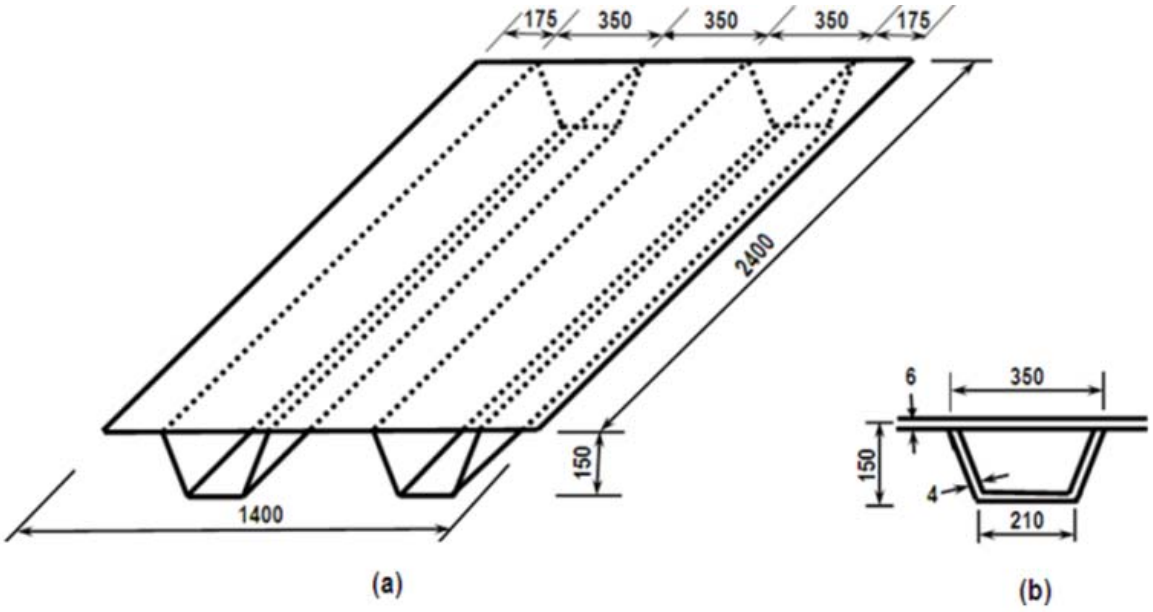

Figure 3.2 Geometry and dimensions of: (a) Hat Stiffened Plate having two stiffeners (b) Hat stiffener

3.2.2 Convergence Study

The structure has been modeled and analyzed using the finite element software ANSYS 12. Thin shell elements, shell 63 (4 noded) and shell 93 (8 noded) having six dof per node have been used to model the stiffener and the plate. The mesh density has been selected based

on convergence study carried out for HSP having two stiffeners as shown in Figure 3.2, using shell 63 and shell 93 elements. In-plane mesh densities 5 x 8, 8 x 16, 28 x 30 and 34 x 40 have been chosen for the convergence study. Simply supported boundary condition on all four edges and a uniformly distributed lateral pressure of 10 kPa has been applied on the HSP. The maximum deflection has been found out for various mesh densities. Plots of maximum deflection for various mesh densities has been made for shell 63 and shell 93 element and are shown in Figure 3.3. Shell 93 element show convergence for a mesh density of 28 x 30 and an aspect ratio of 1.8. Shell 93 and a mesh density of 28 x 30 have been adopted while modeling the HSP for further investigations in this chapter.

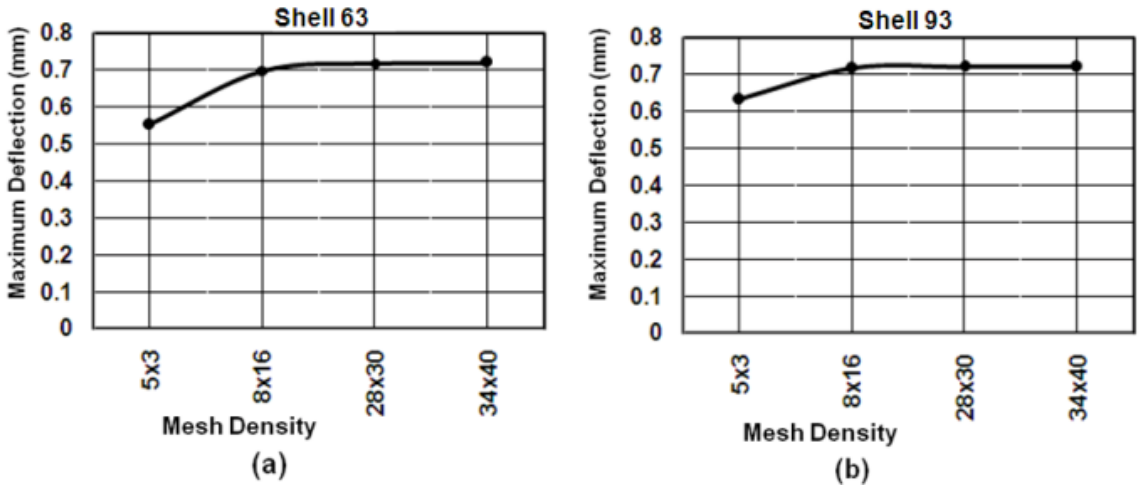

Figure 3.3 Plot of maximum deflection versus mesh density for: (a) For shell 63 element (b) For shell 93 element

3.2.3 Selection of Representative Unit Cell for Hat Stiffened Plate

The deck plate of ship or similar structural components strengthened with hat stiffeners may be measuring a few meters as a structural member and may consist of large number of hat stiffeners. For the structural analysis of such components, it will be convenient to have a Representative Unit Cell (RUC) which is a miniature of the original structure. An RUC of the HSP has been selected based on a linear static analysis carried out for HSP panels having two, three, four and five stiffeners. Geometry of these RUCs has been given in Figure 3.2 (a) and Figure 3.4. These plates have been modeled using shell 93 elements. Simply supported

boundary conditions are prescribed on edges perpendicular to the stiffeners and continuous boundary conditions have been imposed on edges parallel to the stiffeners. A uniformly distributed lateral pressure of 10 kPa has been applied on the HSP.

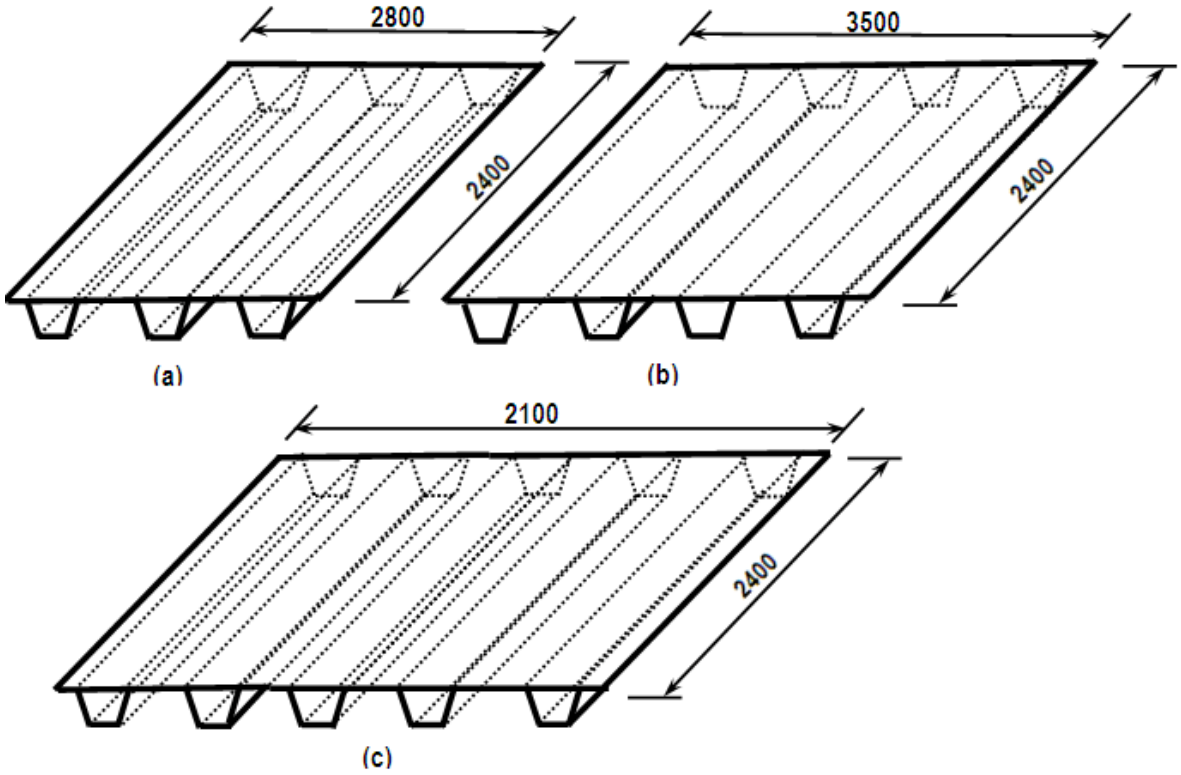

Figure 3.4 Geometry and dimensions of Hat Stiffened Plates having: (a) three stiffeners (b) four stiffeners and (c) five stiffeners.

Comparison of maximum deflection and maximum in-plane stress at the centre of HSP having two, three, four and five stiffeners has been presented in Table 3.1. Since the maximum deflection has been the same and the variation in stress has been less than 4%, HSP with two stiffeners as shown in Figure 3.2 has been selected as the RUC of HSP and will be used for subsequent investigations reported in this thesis.

Table 3.1 Comparison of maximum deflection and maximum in-plane stress at the centre of Hat Stiffened Plates having two, three, four and five stiffeners

No. of Stiffeners:	Two Stiffeners	Three Stiffeners		Four Stiffeners		Five Stiffeners	
			Percentage Variation		Percentage Variation		Percentage Variation
Maximum Deflection (mm) :	0.7093	0.7093	0	0.7093	0	0.7093	0
Maximum in-plane Stress (MPa.) :	10.09	9.70	3.87	10.09	0	9.70	3.87

3.3 STRENGTH OF STIFFENERS COMMONLY USED IN SHIPBUILDING

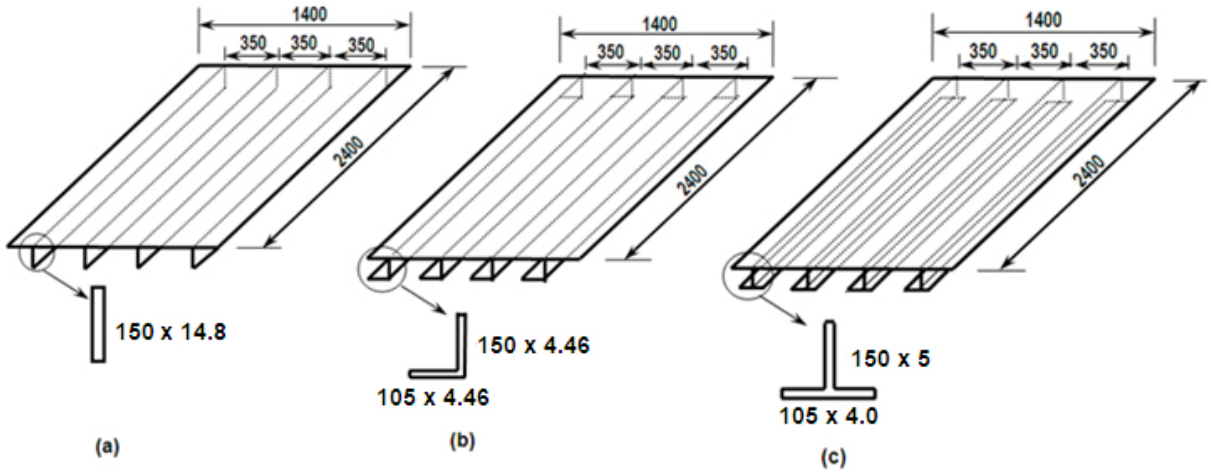

Figure 3.5 Geometry and dimensions of equivalent unit cells of plates stiffened with: (a) flat bar (b) angle bar and (c) tee bar

In order to quantify the strength-to-weight ratio of HSP, its structural response has been compared with that of plates stiffened with open section stiffeners commonly used in ship building, viz., flat bar, angle bar and tee bar. The equivalent unit cell of open section stiffeners has been arrived at based on the equivalent section modulus concept. The scantlings of the open section stiffeners are calculated such that HSP and open section stiffened plates have

equal section modulus and same plate dimensions. The dimensions of the equivalent RUCs of stiffened panels with flat bar, angle bar and tee bar are shown in Figure 3.5.

3.4 STRUCTURAL RESPONSE

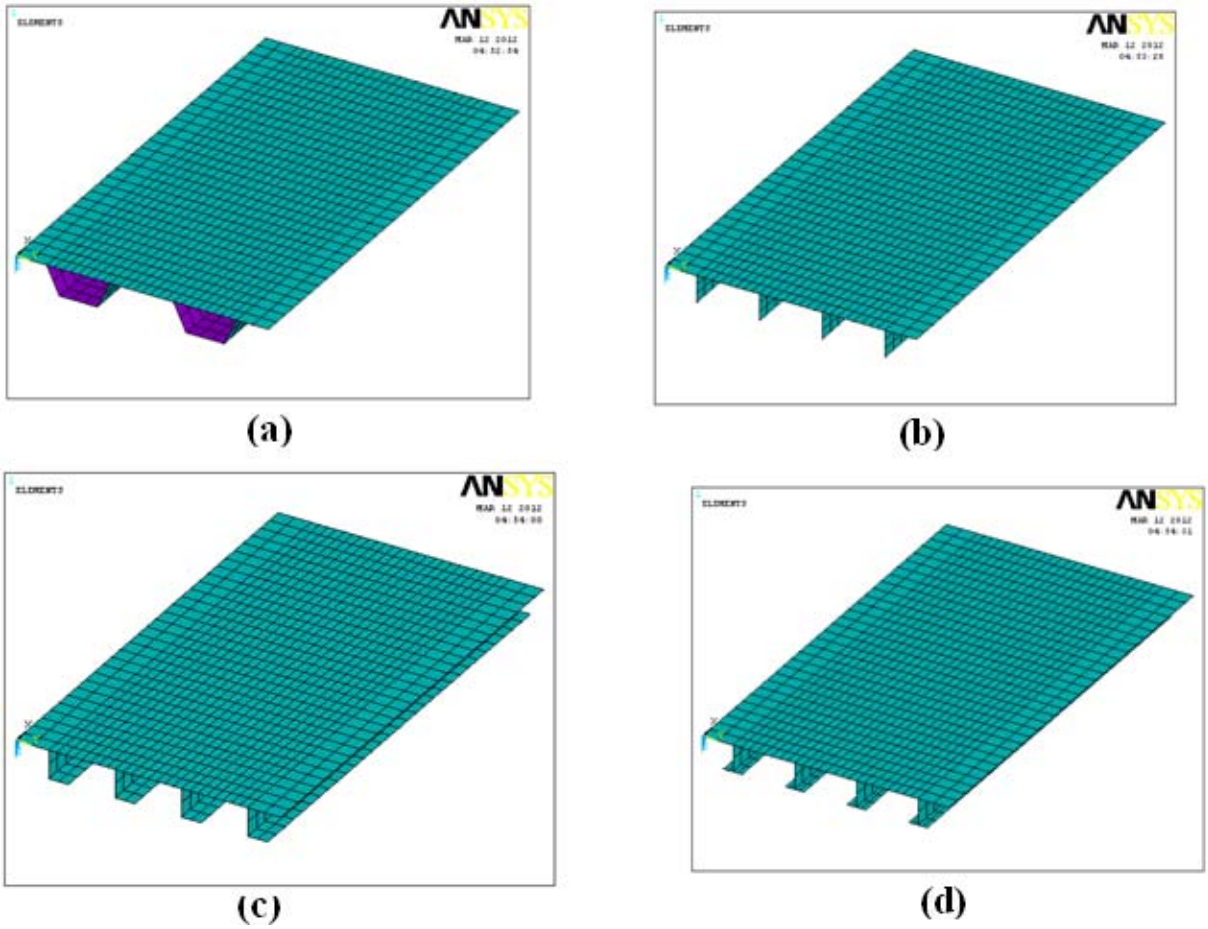

Figure 3.6 Finite element models of Representative Unit Cell of plate stiffened with: (a) hat stiffener, (b) flat bar, (c) angle bar and (d) tee bar

The structural response to lateral loading, in-plane loading and torsion loading of RUC of HSP and its equivalent open section stiffened plates have been estimated and compared. The analysis has been carried out using ANSYS 12 and finite element models of these components have been shown in Figure 3.6. The degree of rotational restraints at the plate boundary is neither zero nor infinite, the former being equivalent to simply supported condition and the latter corresponding to fixed condition. The restraints at the plate boundary

depends on torsional rigidity of support members which is neither zero nor infinity. For practical design purpose with the benefit of mathematical simplicity, the simply supported boundary condition (i.e., with zero rotational restraints) is often adopted in maritime industry when analytical or semi-analytical methods are applied (Paik and Seo, 2009a). In the present study simply supported boundary conditions has been applied on all four edges.

3.4.1 Lateral Loading

In a ship structure the stiffened plates are mainly subjected to lateral or transverse loads i.e., loads normal to the plane of the plate. Hydrostatic pressure acting on the bottom and side shells of the plate, cargo distributed on the deck etc. are examples for lateral loads acting on stiffened plates in the case of a ship structure. A lateral pressure of 10 kPa has been applied in each of the four cases. Linear static FEA has been carried out using ANSYS 12 and a comparison of maximum deflection and maximum principal stress have been made and presented in Table 3.2.

Table 3.2 Comparison of maximum deflection and maximum principal stress for the plates stiffened with four different types of stiffeners and subjected to lateral load

Sl No.	Stiffener shape	Weight Ratio	Section Modulus	Max Deflection	Max. Deflection Ratio	Max. Principal Stress	Max. Principal Stress Ratio
			cm^3	mm		MPa	
1	Hat	1.00	365.78	0.7207	1.00	26.50	1.00
2	Flat Bar	1.36	380.3	0.6348	0.88	25.37	0.96
3	Angle	1.01	382.2	1.3864	1.92	89.07	3.36
4	Tee	1.02	369.3	0.7061	0.98	27.60	1.04

From the table it has been seen that for same section modulus the plate stiffened with flat stiffener is 36% heavier as compared to HSP. The maximum deflection and the maximum principal stress for plate stiffened with angle stiffener have been very high as compared to HSP. The variation in maximum deflection and maximum principal stress for tee stiffener has

been found to be less than 4% as compared to that of HSP. Plate stiffened with tee bars exhibits comparable strength-to-weight ratio with that of HSP for lateral loading.

3.4.2 In-plane Compressive Loading

The top deck of ship's hull is subjected to bending compressive stress due to sagging bending moments and it is prone to buckling failure. The buckling mode for a stiffened plate depends on the relative geometric proportions of the plate and stiffener elements (Bediar, 1997a). For light stiffening, the plate buckles together with the stiffener giving rise to failure in overall buckling mode. If the stiffener is rigid in flexure and weak in torsion, buckling occurs in a local mode. The stiffeners in this case divide the plate into several sub-panels with longitudinal edges almost rotate freely. If the stiffener is both flexurally and rotationally stiff, another local mode results and the longitudinal edge of each panel in this case is fixed against rotation giving rise to a higher buckling load for each sub panel. Most ship panels must carry substantial lateral loads and this requirement usually produces stiffeners that are already larger and more rigid than the minimum sizes required by consideration of overall elastic buckling.

In-plane compressive load has been applied on the finite element models of stiffened plates shown in Figure 3.6 and linear buckling analysis has been carried out. The first buckling mode for all the four stiffened plates simply supported on all four edges and subjected to an axial compressive load has been shown in Figure 3.7.

The critical load for all the four stiffened plates has been presented in Table 3.3. From the table it can be seen that the plate stiffened with flat bar has got very low value for critical load. For plates stiffened with angle bar stiffeners and tee bar stiffeners the value of critical load is comparable with that of HSP.

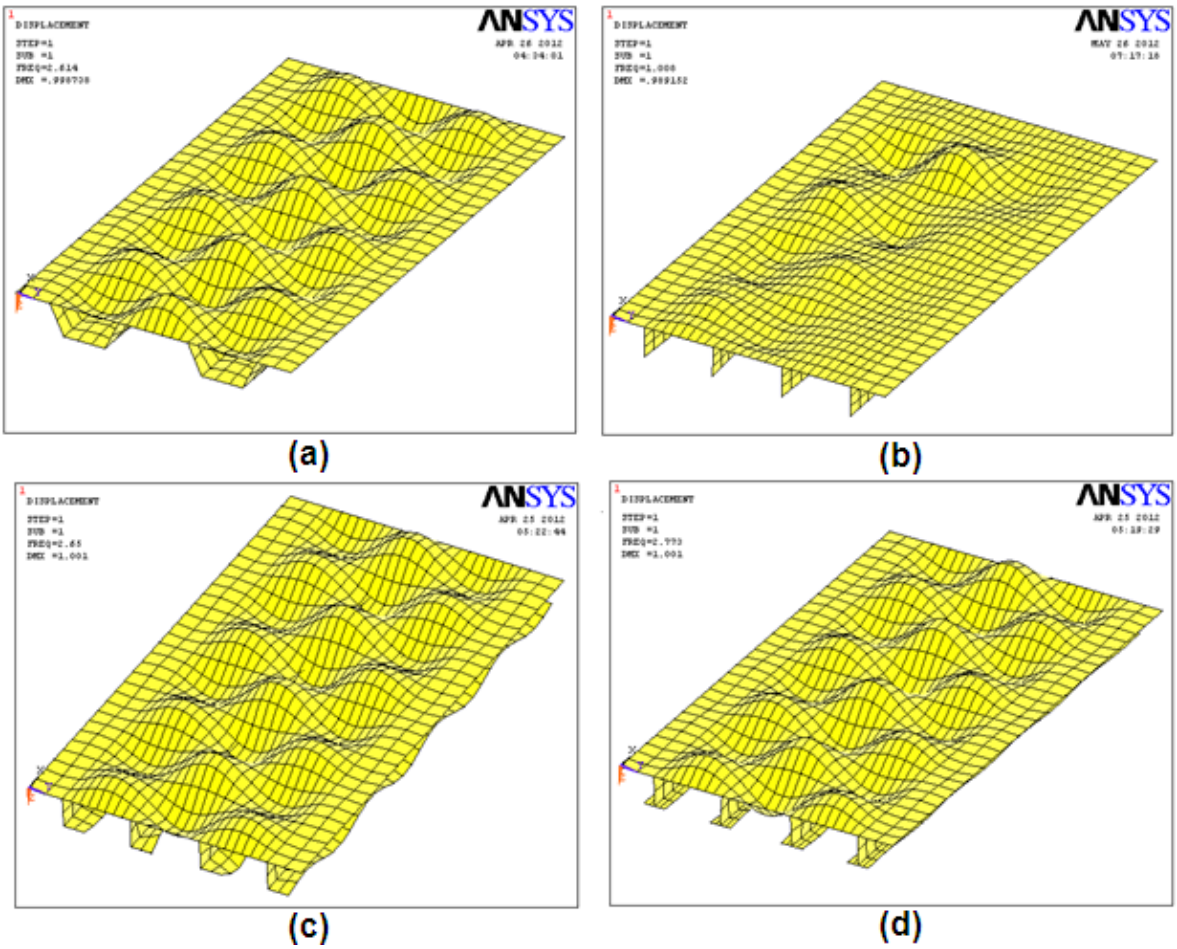

Figure 3.7 First buckling mode for plate stiffened with: (a) hat stiffener, (b) flat bar, (c) angle bar and (d) tee bar

Table 3.3 Comparison of critical load for the plates stiffened with four different types of stiffeners

Sl No.	Stiffener shape	Weight Ratio	Critical load
			MPa
1	Hat	1.00	287.35
2	Flat Bar	1.36	100.8
3	Angle	1.01	265.01
4	Tee	1.02	277.32

3.4.3 Torsion Loading

To compare the structural response to torsion loading, the finite element models shown in Figure 3.6 has been used. All dof on either ends of the stiffened panel have been arrested and a torsion load of 1 kN-m has been applied at mid-span. Warping stress, σ_x generated due to torsion and the significant shear stresses τ_{xy} and τ_{xz} obtained for all the four types of stiffeners have been compared and presented in Table 3.4. It has been seen that warping stresses in the case of plates stiffened with angle stiffener and tee stiffeners are extremely high as compared to that for HSP. Thus it has been seen that HSP exhibits extremely superior strength-to-weight ratio when the structural response to torsional load has been compared.

Table 3.4 Comparison of warping stress and shear stress for the plates stiffened with four different types of stiffeners and subjected to torsion load

Sl No.	Stiffener shape	Weight Ratio	Warping Stress		Shear Stress in the cross sectional plane.	
			Σx	Ratio	τ_{xy}	τ_{xz}
			MPa		MPa	MPa
1	Hat	1.00	24.95	1.00	9.43	1.73
2	Bar	1.36	25.75	1.03	9.61	3.78
3	Angle	1.01	51.69	2.07	19.55	3.67
4	Tee	1.02	120.58	4.83	29.92	9.05

3.5 RESULTS AND DISCUSSION

Table 3.5 Performance of plates stiffened with various types of stiffeners subjected to lateral load, in-plane load and torsion load

Sl No.	Stiffener shape	Weight Ratio	Response to lateral load	Response to in-plane load	Response to torsion load
			Max. PrincipalStress	Critical Load	Warping Stress
			MPa	MPa	MPa
1	Hat	1	26.5	287.35	24.95
2	Flat Bar	1.36	25.37	100.8	25.75
3	Angle	1.01	89.07	265.01	51.69
4	Tee	1.02	27.6	277.32	120.58

The stiffened plates in a ship structure are subjected to lateral, in-plane and torsion loading. The responses of RUC of HSP and commonly used open section stiffeners to these types loading have been investigated. The performance HSP and plates stiffened with open section stiffeners having the same section modulus subjected to various types of loading have been presented in Table 3.5. For lateral loading the strength-to-weight ratio of plates stiffened with HSP is high as compared to flat bar and angle bar. In buckling, the performance of HSP has been found much superior to plate stiffened with flat bar whereas plates stiffened with angle bar and Tee bar performs equally well as HSP. However, in torsion, the warping stress developed for plates stiffened with Tee bar is very high as compared to HSP. Hence it has been seen that the strength-to-weight ratio of HSP is much better as compared to that of commonly used open section stiffeners.

CHAPTER 4

ORTHOTROPIC PLATE MODEL FOR HAT STIFFENED PLATES

4.1 GENERAL

Orthotropic Plate Model (OPM) of the HSP has been proposed as an efficient structural substitute. In the OPM approach, the stiffened plate made of isotropic material and having geometric anisotropy due to stiffeners has been replaced by an unstiffened plate of the same plan dimensions and having material orthotropy. An OPM has been formulated as a structural substitute for HSP, which will make the structural analysis of HSP possible with the orthotropic plate elements available in the element library of any general purpose structural analysis software. This will significantly reduce the modeling efforts and storage requirement in the analysis of a complete ship or hull module using any commercial finite element software.

4.2 FORMULATION OF EQUIVALENT ORTHOTROPIC PLATE MODEL

The HSP made up of an isotropic material has been substituted by an elastically equivalent OPM. Geometric parameters of HSP and its equivalent OPM are shown in Figure 4.1. The flexural rigidities of HSP are available as given by eqn. 4.1 and eqn. 4.2.

$$D_x = \frac{EI_r}{b_1+b_2} \qquad D_y = \frac{Et_P^3}{12(1-\nu^2)} \qquad ---------- (4.1), (4.2)$$

I_r is the moment of inertia of the stiffener and the effective breadth used for calculating this generally depends on various parameters like the ratio $a_0/ (b_1+b_2)$, boundary conditions, cross sectional dimensions of the stiffeners and Poisson's ratio (where a_0 is the length between zero bending moment). Effective breadth ratio as proposed by Hughes (1988) has been taken for the calculation of moment of inertia of the stiffener. Dimensions a, b, b_1, b_2, t_r and t_p have been shown in Figure 4.1.

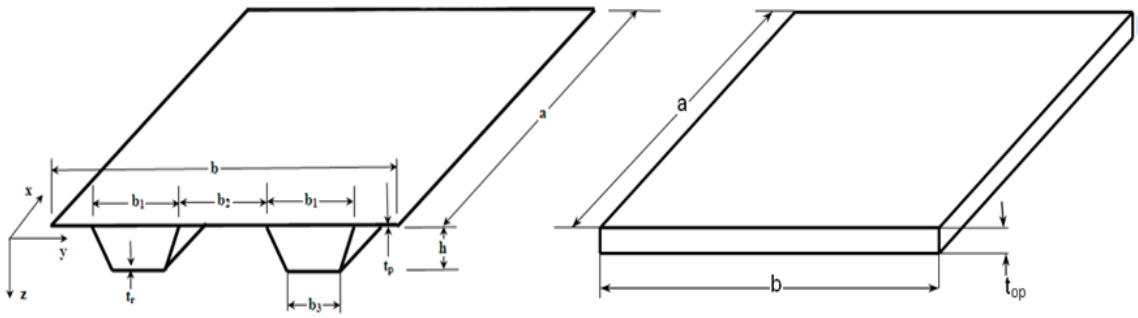

Figure 4.1 Geometrical parameters of Hat Stiffened Plate and its equivalent Orthotropic Plate Model

The orthotropic plate theory and the analytical solution for bending of orthotropic plate have been made use of for determining the material properties and thickness of the equivalent OPM for HSP and have been explained in Appendices A and B respectively. The length a, breadth b and the values of rigidities, D_x and D_y for the elastically equivalent OPM have been made the same as that of the parent HSP. The effective torsional rigidity, H has been found out using eqn. A5. Poisson's ratio ν_x for the equivalent OPM has been assumed to be same as that of the parent HSP. Substituting for D_x, D_y and ν_x in eqn. A6, ν_y has been found out and assuming D_z equal to D_y, ν_z is also calculated using eqn. A7. The characteristic non dimensional parameters, η, λ and the modified aspect ratio R for the OPM have been calculated using eqns. B1 and B2.

The thickness t_{op} for the equivalent OPM has been determined using the analytical expression for stress in an orthotropic plate by Bao et al. (1997) as given in eqns. B5, B7, B10 and B12. The first two eqns. are for all four edges simply supported boundary condition and the other two eqns. are for two edges fixed and two edges simply supported. These expressions involve the value of in-plane stress σ_x at the centre of an orthotropic plate due to a lateral pressure load and its thickness. The value of in-plane stress, σ_x necessary to substitute in eqn. B5 or B7 or B10 or B12 has to be realized from a linear elastic analysis of the RUC of parent HSP. E_x and E_y have been found out using eqn. A2 and E_z is assumed to be the same as E_y. G_{xy} has been calculated using eqn. A5 and $G_{yz} = G_{xz} = G_{xy}$. Poisson's ratio ν_{xy}, ν_{yz} and ν_{xz} have been found out using eqn. A8. Thus all the geometrical and material properties of an equivalent OPM have been found out and these can be modeled and analyzed using thin orthotropic plate elements.

A computer code in C language has been written based on eqn. B7 for all four edges simply supported and based on eqn. B12 for two edges fixed and other two edges simply supported condition of the plate. The program reads the values of q, a, b, D_x, H, D_y, ν_x and σ_x as the input and t_{op} for the equivalent OPM has been obtained as the output. Once the t_{op} is calculated, the material model for the orthotropic plate is complete with E_x, E_y, E_z, G_{xy}, G_{yz}, G_{xz}, ν_{xy}, ν_{yz}, ν_{xz} being known. This information can readily be used along with t_{op} for the analysis of OPM of the HSP using any general purpose finite element software.

4.3 NUMERICAL INVESTIGATIONS

The RUC of HSP identified in section 3.2.1 has been selected for the numerical investigations. The material properties of RUC of HSP are given in section 3.2.2. The RUC of HSP with two stiffeners and the elastically equivalent OPM has been shown in Figure 4.2.

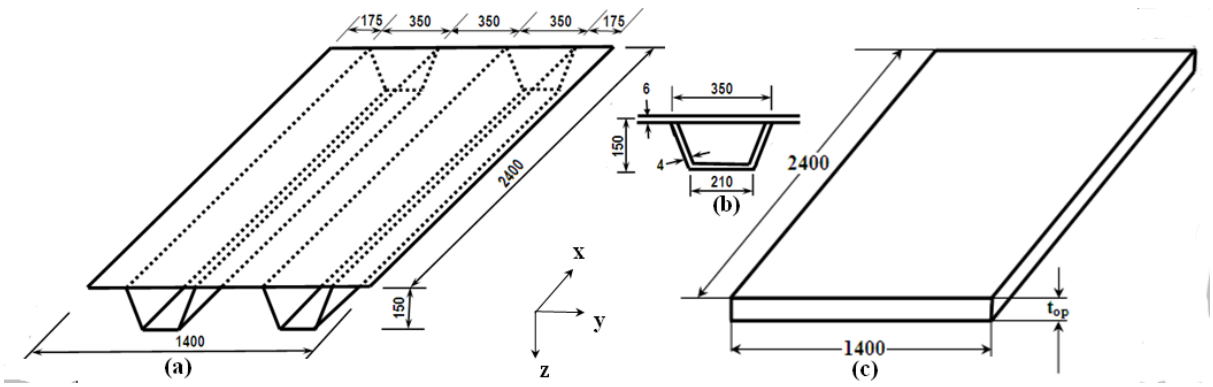

Figure 4.2 (a) Representative Unit Cell of Hat Stiffened Plate with two stiffeners. (b) Principal dimensions of hat stiffener, (c) Elastically equivalent Orthotropic Plate Model

For the two boundary conditions, Dx, Dy and H calculated for RUC of HSP has been given in Table 4.1. Linear static FEA of the RUC of HSP has been carried out using ANSYS 12. The structure has been modeled using isotropic thin shell elements and pressure load 10 kPa has been applied. For all edges simply supported boundary condition the maximum in-plane stress, σ_x has been obtained as 26.5 MPa and for two edges simply supported and the other two

edges fixed boundary condition, the maximum in-plane stress, σ_x has been obtained as 27.94 MPa. For the RUC of HSP, the input and output for the computer code for generating the t_{op} of equivalent OPM have been given in Table 4.2 for the two boundary conditions. Subsequently the material and geometric properties of equivalent OPM for the two specified boundary conditions are given in Table 4.3.

Table 4.1 Value of rigidity for Representative Unit Cell of Hat Stiffened Plate

RIGIDITIES	SS	FS
D_x (N-mm)	5.8648×10^9	4.866×10^9
D_y (N-mm)	4.1538×10^6	4.1538×10^6
H (N-mm)	1.5608×10^8	1.4218×10^8

SS: All four edges simply supported.
FS: Two edges fixed and other two edges simply supported.

Table 4.2 Input and output of the computer code for finding the thickness of equivalent Orthotropic Plate Model for the Representative Unit Cell of Hat Stiffened Plate

Boundary Condition:		SS	FS
Input	q (MPa)	0.01	0.01
	a (mm)	2400	2400
	b (mm)	1400	1400
	D_x (N-mm)	5.8648×10^9	4.866×10^9
	H (N-mm)	1.5608×10^8	1.4218×10^8
	D_y (N-mm)	4.1538×10^6	4.1538×10^6
	ν_x	0.3	0.3
	σ_x (MPa)	26.5	13.97
Output	t_{op} (mm)	39.8	32.14

SS: All four edges simply supported.
FS: Two edges fixed and other two edges simply supported.

Table 4.3 Geometric and material properties of equivalent Orthotropic Plate Model for the Representative Unit Cell of Hat Stiffened Plate

Boundary Condition:		SS	FS
Geometric Properties	a (mm)	2400	2400
	b (mm)	1400	1400
	t_{op} (mm)	39.8	32.14
Material Properties	E_x (MPa)	1.1162×10^6	1.7589×10^6
	$E_y=E_z$ (MPa)	790.6	1501
	$G_{xy} = G_{xz} = G_{yz}$ (MPa)	790.6	25470
	$\nu_{xy} = \nu_{xz}$	7.98×10^{-3}	8.76×10^{-3}
	ν_{yz}	2.1×10^{-4}	2.6×10^{-4}

SS: All four edges simply supported.
FS: Two edges fixed and other two edges simply supported.

4.3.1 Validation of Equivalent Orthotropic Plate Model with Bao's solution

The equivalent OPM has been modeled in ANSYS 12 using 8 noded orthotropic thin shell elements. An in-plane mesh density of 14 x 24 as shown in Figure 4.3(b) has been used and a uniform pressure load of 10 kPa has been applied. The material and geometric properties of the OPM given in Table 4.3 for the two boundary conditions has been used as the input. The deflection and the maximum stress at the centre for the equivalent OPM using the FEA have been compared with analytical solutions given by eqns. B3, B7, B11 and B12. The maximum deflection and stress at the centre are shown in Table 4.4. The comparison shows that the maximum variation in deflection is less than 6.5% and the maximum variation in in-plane stress, σ_x is less than 1%. Hence the procedure adopted for finding the thickness, modulus of elasticity, modulus of rigidity and Poisson's ratio for an orthotropic plate from the given values of plate rigidities has been found satisfactory. The structural response of the equivalent OPM of the HSP predicted using an orthotropic plate finite element has been validated herein with classical solution given by Bao et al. (1997).

Table 4.4 Comparison of deflection and maximum in-plane stress at the centre for the Orthotropic Plate Model found out using Finite Element Analysis and analytical solution

Response	Boundary Conditions	Analytical Solution	Finite Element Solution	Percentage Variation
Deflection (mm)	SS	0.7161	0.7339	2.49
	FS	0.1779	0.1890	6.24
Maximum in-plane stress (MPa)	SS	26.50	26.67	0.64
	FS	13.97	14.02	0.36

SS: All four edges simply supported.
FS: Two edges fixed and other two edges simply supported.

4.3.2 Validation of Orthotropic Plate Model as the structural substitute for Hat Stiffened Plate

The OPM of the HSP has been established as its structural substitute through FEA of RUC of HSP and its equivalent OPM. The finite element models of the RUC of the HSP and the equivalent OPM generated for this purpose modeled using ANSYS 12 have been shown in Figure 4.3. Eight noded isotropic thin shell elements (shell 93) has been used for modeling RUC of HSP and eight noded orthotropic thin shell element for the OPM. Both the models are analyzed for uniformly distributed pressure load of 10 kPa for the two boundary conditions mentioned in section 4.2.

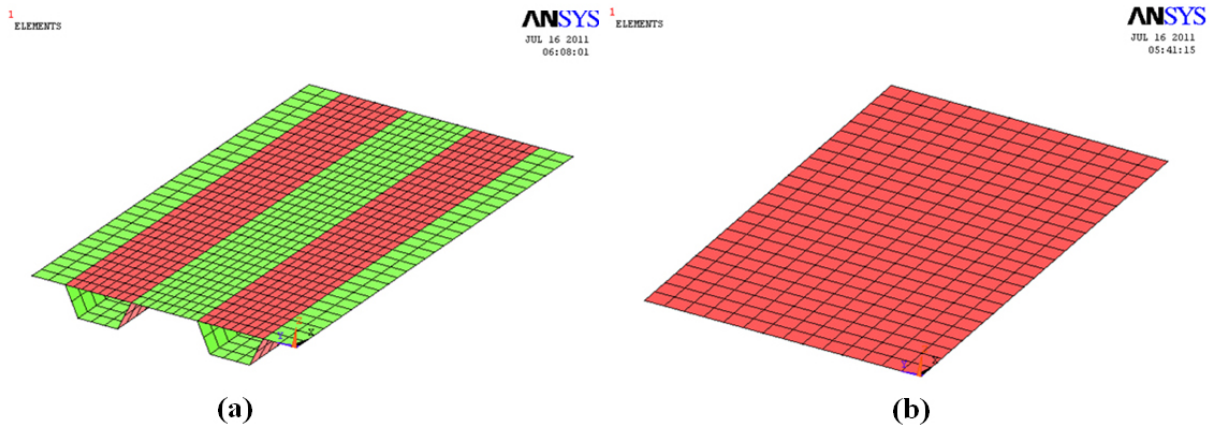

Figure 4.3 Finite element model of: (a) Representative Unit Cell of Hat Stiffened Plate (b) Equivalent Orthotropic Plate Model

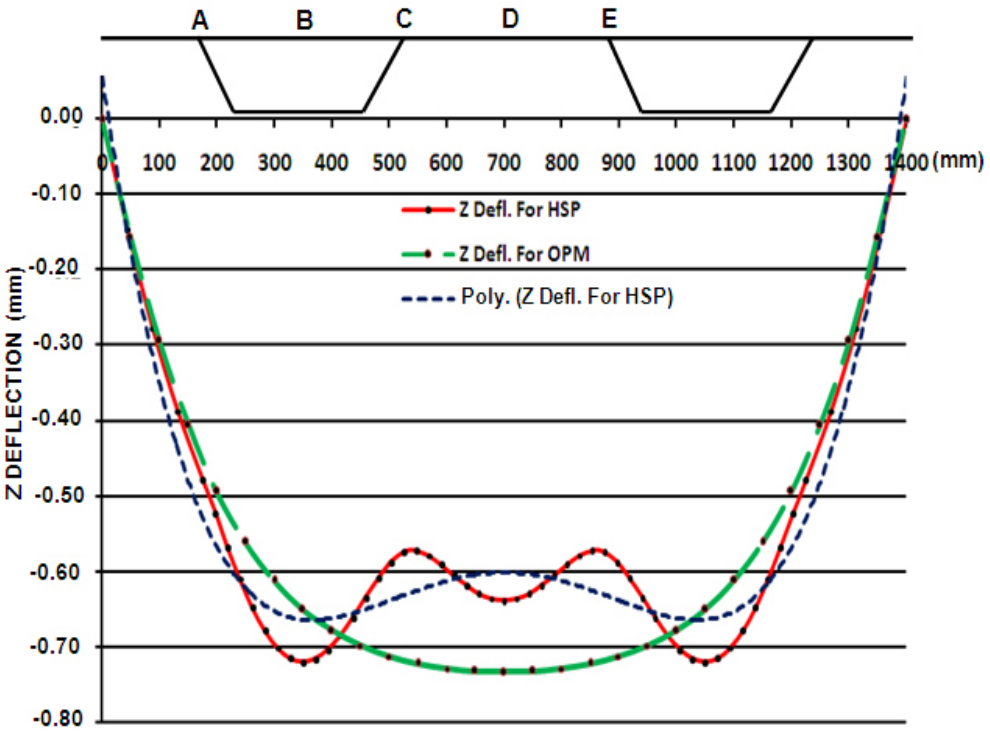

(a) All four edges simply supported boundary condition.

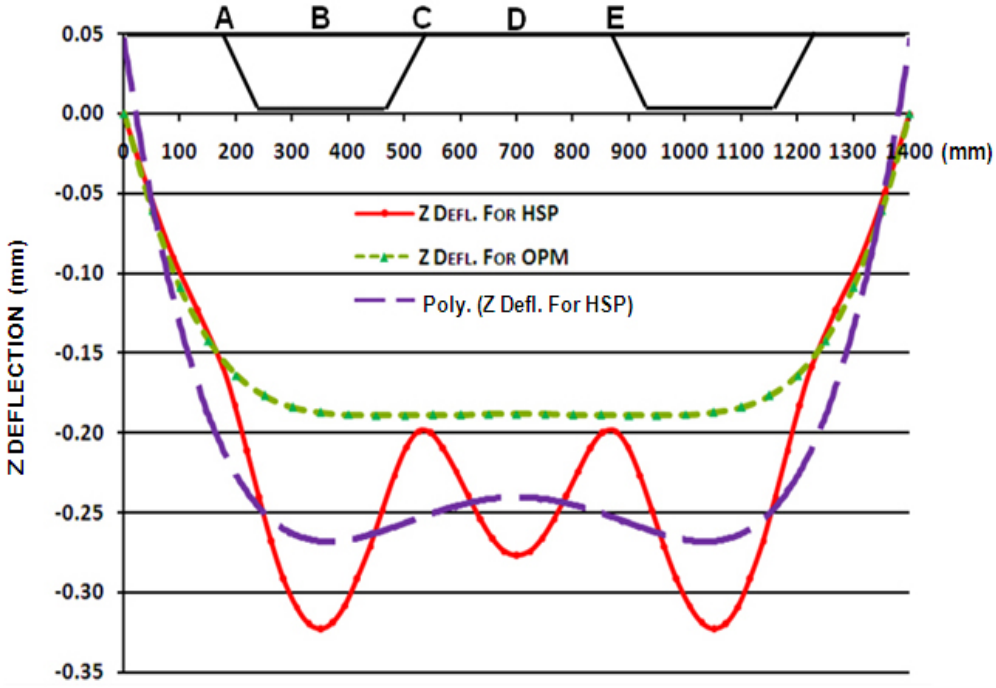

(b) Two edges fixed and two edges simply supported boundary condition.

Figure 4.4 Deflection-profile across width at mid-span for Hat Stiffened Plate and Orthotropic Plate Model

The deflection-profile across the width at mid-span has been plotted for the HSP and its equivalent OPM. Figure 4.4 (a) shows the deflection-profiles of HSP and its equivalent OPM with all four edges simply supported boundary condition and Figure 4.4 (b) shows the same for the two edges fixed and two edges simply supported boundary condition. Comparison of deflections at points A, B, C and D has been presented in Table 4.5.

Table 4.5 Comparison of deflections (in mm) at various locations across the width at mid-span for Hat Stiffened Plate and Orthotropic Plate Model

Boundary Condition	Location	HSP	OPM	Percentage Variation
SS	A	0.4791	0.4495	-6.2
	B	0.7207	0.6510	-9.7
	C	0.5747	0.7180	+2.5
	D	0.6391	0.7339	+14.8
FS	A	0.1586	0.1533	-3.3
	B	0.3230	0.1872	-42
	C	0.1989	0.1889	-5.0
	D	0.2768	0.1885	-32.0

SS: All four edges simply supported.
FS: Two edges fixed and other two edges simply supported.

It is evident from the Figure 4.4 as well as Table 4.5 that the deflection across the width of the plate considered at mid-span of the HSP shows oscillations. The maximum deflections occur at the quarter point (point B). These oscillations smoothened using a quadratic polynomial and is also shown in the same figure. The deflection at quarter point (B) is 12.7% and 16.7 % more than the mid-span (point D) deflection for the two boundary conditions. The maximum deflections predicted by the OPM differ by 7.5% and 31.7% when compared with smoothened value of HSP for the two boundary conditions.

The percentage variations in maximum in-plane stress and maximum von Mises stress for RUC of HSP and its equivalent OPM have been given in Table 4.6. The variation in maximum in-plane stress values which are generally of greater interest has been found to be

less than 1% in both the boundary conditions whereas, the maximum variation in von Mises stress is less than 3.5%.

Table 4.6 Comparison of maximum in-plane stress and maximum von Mises stress obtained for the Representative Unit Cell of Hat Stiffened Plate and its equivalent Orthotropic Plate Model

Response	Boundary Conditions	Hat Stiffened Plate	Orthotropic Plate Model	Percentage Variation
Maximum in-plane stress (MPa)	SS	26.50	26.67	0.64
	FS	27.94	28.05	0.39
von Mises stress (MPa)	SS	25.76	26.66	3.50
	FS	27.21	28.06	3.12

SS: All four edges simply supported.
FS: Two edges fixed and other two edges simply supported.

The location of maximum stress depends on the plate aspect ratio and material orthotropy for two edges fixed and two edges simply supported condition (Bao et al., 1997). Besides Bao et al. (1997) have commented on the limitations of scope of application of the orthotropy rescaling technique to plates with fixed edges. This feature has been reflected in the present study as well. OPM with two edges fixed and two edges simply supported condition has shown 42 % variation in deflection. Hence the OPM developed in the present study using orthotropy rescaling technique has been recommended for the predication of Critical Buckling Load and Ultimate Strength of HSP with all edges simply supported boundary condition.

4.4 PREDICTION OF CRITICAL BUCKLING LOAD

The stiffened plate and its equivalent OPM have been subjected to axial compressive load and simply supported condition has been applied on all four edges. Linear buckling analysis of RUC of HSP and its equivalent OPM has been carried out using ANSYS 12. The critical stress for HSP has been obtained as 287.35 MPa and the same obtained for equivalent OPM has been 287.26 MPa. The variation in critical stress has been found to be 0.03%. The

first buckling mode of HSP and its equivalent OPM have been shown in Figure 4.5 (a) and (b) respectively.

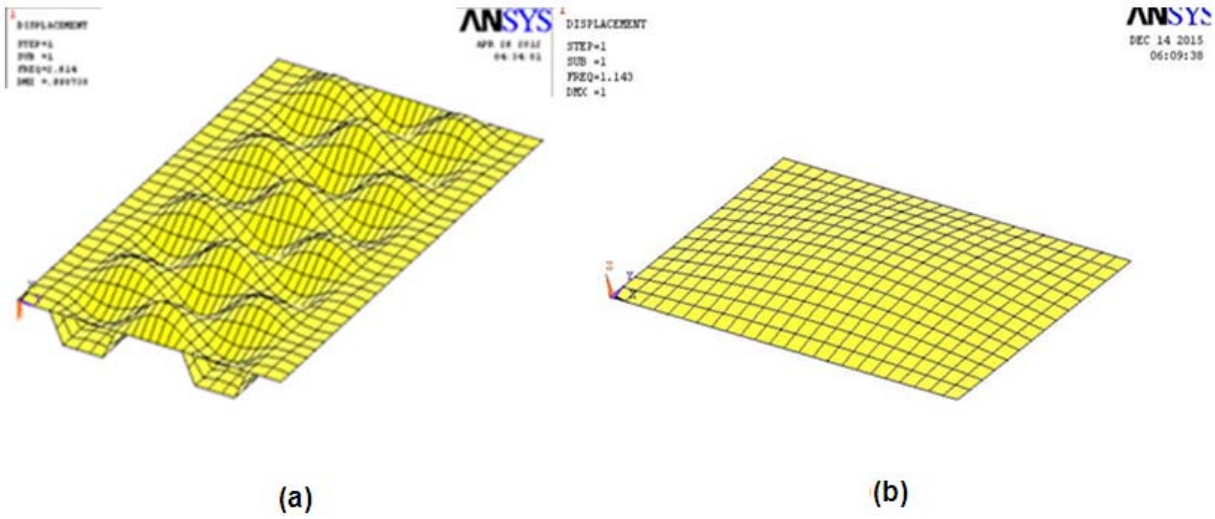

Figure 4.5 First Buckling mode of: (a) Hat Stiffened Plate and (b) Equivalent Orthotropic Plate Model

4.5 PREDICTION OF ULTIMATE STRENGTH

The ANSYS nonlinear FEA gives accurate solutions as long as the modeling technique applied is adequate enough in terms of representing actual structural behavior associated with geometrical nonlinearity, material nonlinearity, boundary condition, loading condition, mesh size and so on (Paik et al., 2008a). Failure of steel structures in conjunction with ULS is typically related to either one or both of the following nonlinear types of behavior viz., geometric nonlinearities associated with buckling or large deflection and material nonlinearities due to yielding or plastic deformation. Thus both geometric and material nonlinearities must always be taken into account in ULS assessment.

For ULS computations, it is essential to establish the material model in terms of stress-strain relationship. The present study adopts the elastic–perfectly plastic material model neglecting strain hardening effects for the purpose. In maritime industry this model has been well adopted for design and strength assessment of steel structures (Paik and Seo, 2009a). The material model for the present study has been shown in Figure 4.6.

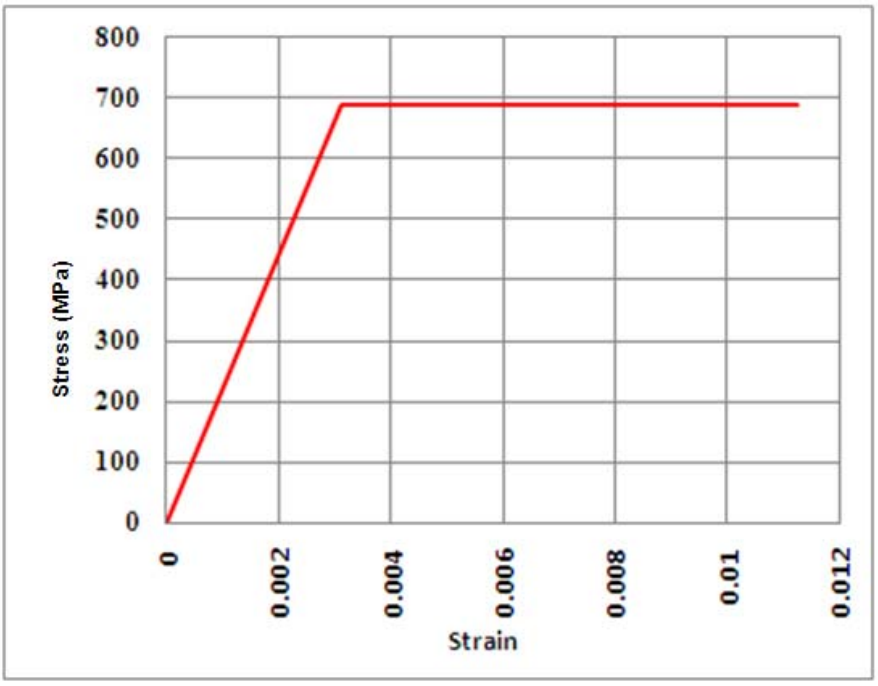

Figure 4.6 Elastic-perfectly plastic material model of EHS 690 steel used for ANSYS 12 non-linear FEA

The finite element models of HSP and its equivalent OPM as shown in Figure 4.3 have been used for the ultimate strength prediction. All four edges have been simply supported and in-plane compressive load has been applied incrementally. Combined non-linear FEA of the HSP and its equivalent OPM has been carried out using ANSYS 12. The ultimate strength behavior of RUC of HSP and its equivalent OPM has been determined from the load-deflection curve shown in Figure 4.7. The ultimate strength of RUC of HSP and its equivalent OPM has been found to be 340 MPa and 403 MPa respectively. The variation in ultimate strength has been found to be 18.5%.

The ultimate strength behavior of HSP shown in Figure 4.7 (a) is a typical stiffened plate behavior where the buckling of a local plate panel between stiffeners initially takes place and is followed by overall collapse due to excessive yielding or stiffener failure. The ultimate strength behavior of OPM shown in Figure 4.7 (b) is a typical plate behavior where buckling takes place at a critical value beyond which rigidity against applied load increases.

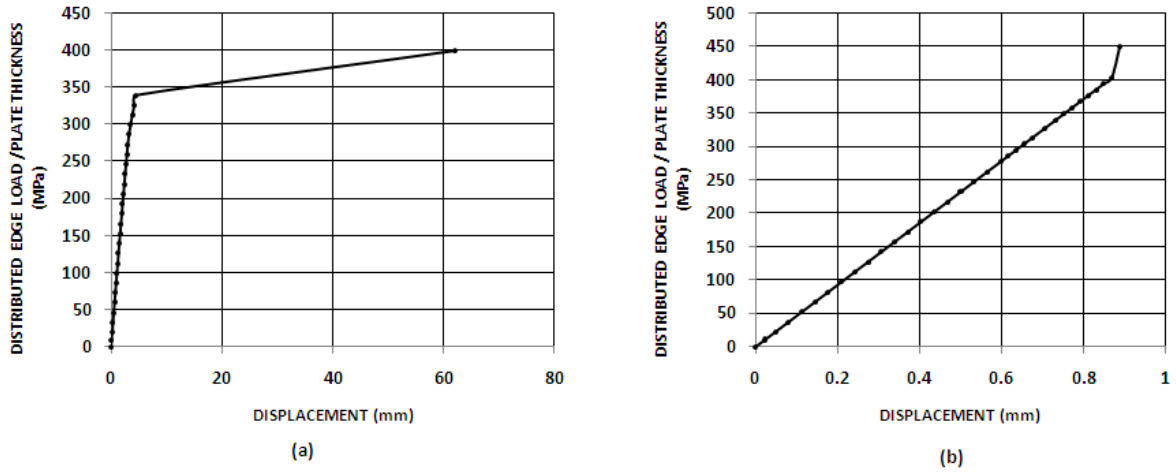

Figure 4.7 Ultimate strength behavior of: (a) Hat Stiffened Plate (b) Equivalent Orthotropic Plate Model

4.6 RESULTS AND DISCUSSION

A comparison of results obtained for RUC of HSP modeled using isotropic thin shell element and its equivalent OPM modeled using orthotropic thin shell element has been presented in Table 4.7 and Table 4.8. For simply supported boundary condition the OPM could predict the maximum deflection and maximum in-plane stress with good accuracy. For two edges fixed and other two edges simply supported boundary condition even-though the maximum in-plane stress could be predicted with sufficiently good accuracy the maximum deflection has shown a variation of 41.4%. In the Orthotropic Plate Model the rigidity is uniform throughout the plate whereas in the actual Hat Stiffened Plate the rigidity along the line of attachment of the stiffeners to the plate is large as compared to the unsupported portion of the plate. Therefore, the unsupported portion of the plate between the stiffeners shows large localized deflection. This behavior is highly pronounced in the case of two edges fixed and other two edges simply supported boundary condition. The deflection in the portion of the plate between the lines of attachment of stiffeners can be reduced if the width enclosed by the stiffener and the width between two adjacent stiffeners are reduced.

Table 4.7 Performance of Orthotropic Plate Model of Representative Unit Cell of Hat Stiffened Plate in the linear static analysis.

Boundary Condition	Max Deflection (mm)			In-plane Stress (MPa)		
	HSP	OPM	Percentage Variation	HSP	OPM	Percentage Variation
SS	0.7207	0.6977	3.2	26.50	26.67	0.64
FS	0.3230	0.1890	41.4	27.94	28.05	0.39

SS: All four edges simply supported.

FS: Two edges fixed and other two edges simply supported.

Table 4.8 Performance of Orthotropic Plate Model of Representative Unit Cell of Hat Stiffened Plate in linear buckling and ultimate strength analysis

Boundary Condition	Buckling Load (MPa)			Ultimate Strength (MPa)		
	HSP	OPM	Percentage Variation	HSP	OPM	Percentage Variation
SS	287.35	287.26	0.03	340	403	18.5

SS: All four edges simply supported.

The OPM could predict the linear buckling load with good accuracy and the ultimate strength of HSP could be predicted with an accuracy of 18.5% only.

CHAPTER 5

SUPERELEMENT FOR HAT STIFFENED PLATE

5.1 GENERAL

The Superelement technique is a method for treating a portion of the structure as if it were a single element even though it is made up of many individual elements. Ideally a structure should be analyzed and designed as a single unit to account for all of structure's interaction. Complexities in modeling the complete structure and limitations in computational means are the two main difficulties while analyzing a large structure as a single unit. In large structures, portion of structure containing several elements occurs repeatedly in various locations. This repetition provides an opportunity for introducing Superelement technique, leading to reduction in modeling efforts, storage requirement and computation requirement. The substructure of the large structure which repeats itself is considered as a single element called Superelement. The element stiffness matrices of individual elements constituting the substructure have been assembled in the same way as done for the complete structure to obtain the stiffness matrix for the Superelement. While generating the finite element model of the complete structure, the assembly of the substructure needs to be performed only once and the Superelement generated can be used at locations where the substructure appears. This will result in substantial reduction in time and computation required for the assembly of elements when the Superelement occurs repeatedly. The Superelement technique is of primary importance in the analysis of a large complex three dimensional structure and becomes even more important when the analysis forms a part of a rationally-based structural design process (Hughes, 1988). In this chapter the formulation and implementation of a Superelement which can model a HSP has been described. The Superelement has been formulated with the advantage of modeling HSP as a quadrilateral which will result in the reduction of man-hour required for modeling a large structure having HSPs. Superelement for HSP will reduce the man-hour and computation-time required in the modeling and analysis of a complete ship having HSPs without any compromise in accuracy.

5.2 DESCRIPTION OF SUPERELEMENT FOR HAT STIFFENED PLATE

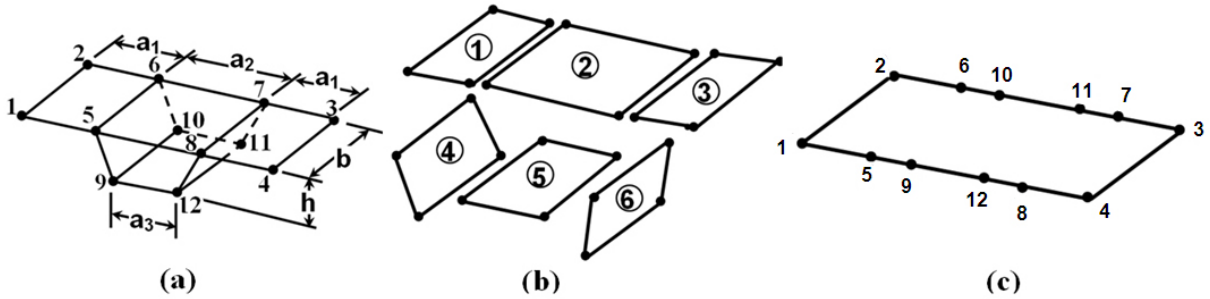

Figure 5.1 (a) Substructure of Hat Stiffened Plate (b) Six constituent elements of substructure. (c) Superelement of Hat Stiffened Plate

The RUC of HSP described in section 3.2.1 is a repetition of the substructure shown in Figure 5.1 (a). The geometric parameters of the substructure a_1, a_2, a_3, b and h have been shown in Figure 5.1 (a). The substructure of HSP is an assembly of six conventional four noded rectangular shell element as shown in Figure 5.1 (b). The stiffness matrices of the six conventional shell elements are added according to the nodal connectivity to obtain the stiffness matrix of the substructure. The geometry of the substructure and the locations of the nodes in the substructure have been made use of to represent the substructure by a Superelement as shown in Figure 5.1 (c). The Superelement for HSP is a single element with twelve nodes on its boundary. Node numbers one to eight are on the plate and node numbers nine to twelve corresponding to stiffener. Generally for a HSP loads are applied only on the plates. In the case of Superelement for HSP all the twelve nodes are on the boundary and serve as connection points between the Superelement and the rest of the structure. Since all the twelve nodes in Superelement for HSP are boundary nodes static condensation is not possible for reducing the size of the Superelement. This turns out to be advantageous as compared to a statically condensed Superelement since the tedious calculations like finding condensed stiffness matrix, condensed load vector and recovery of internal dof can be avoided. Thus usage of the Superelement described here is simple to use.

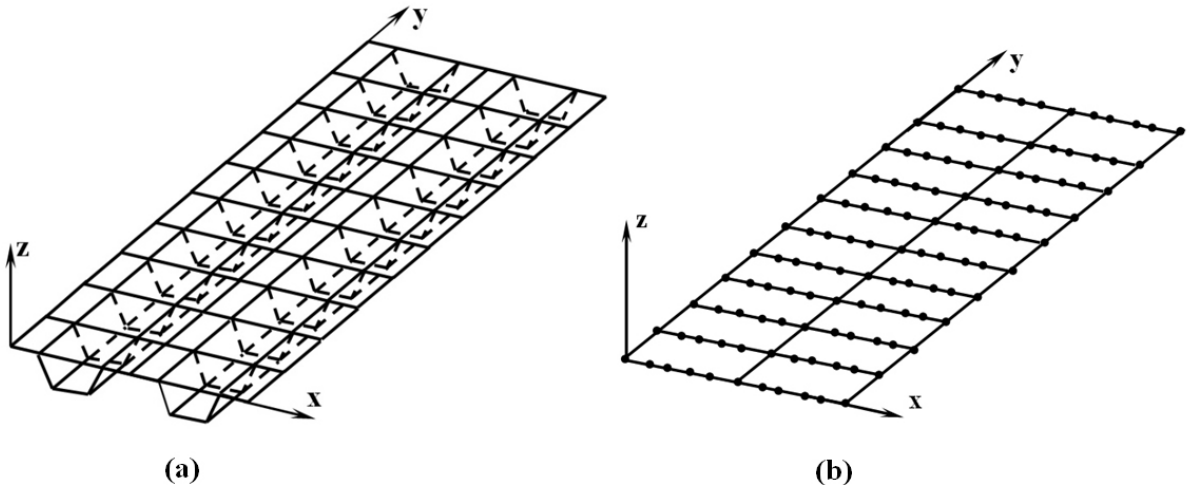

Figure 5.2 Finite Element model of Hat Stiffened Plate modeled using: (a) Shell elements (b) Superelement

The finite element model for RUC of HSP modeled using four noded shell element and the same modeled using Superelement are shown in Figure 5.2 (a) and (b) respectively. In the finite element model using shell elements the number of areas to be generated is seven and the number of elements is one hundred and twenty. Whereas, in the finite element model using Superelement the number of areas to be generated is one and the number of elements is twenty. In the case of RUC of HSP modeled using Superelement only twenty elements have been assembled whereas in the case of shell elements, one hundred and twenty elements have been assembled. Thus there is a significant reduction in modeling-efforts and computation requirement while using Superelement for HSP.

5.3 DESCRIPTION OF SUPERELEMENT FOR COMPOSITE HAT STIFFENED PLATE

HSP has got wide application in ships made of composite materials. The procedure for the formulation of Superelement has been extended for composite HSP. Figure 1.1 (b) shows a HSP made of composite material. The hat stiffeners for composite structures are bonded to the plate through the flanges of the stiffeners. While modeling, the flanges and the plate in the joining region are replaced by a single plate section with an effective thickness equal to the sum of the thicknesses of the flange and the plate.

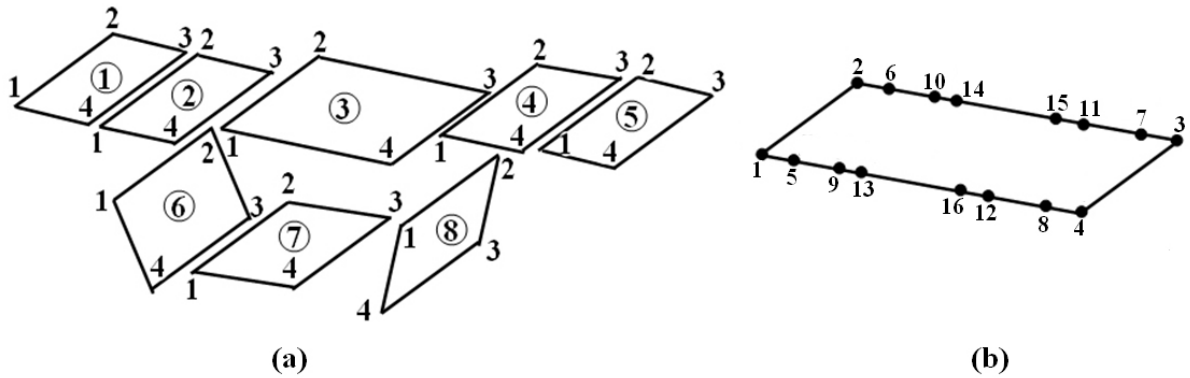

Figure 5.3 Composite Hat Stiffened Plate: (a) Eight constituent composite shell elements of substructure (b) Superelement

The substructure of composite HSP is a combination of eight conventional four noded rectangular composite shell elements as shown Figure 5.3 (a). The thickness of element numbers two and four is equal to the sum of the thicknesses of plate and stiffener flange. The stiffness matrices of the eight composite shell elements are added according to the nodal connectivity to obtain the stiffness matrix of the substructure. The Superelement for a composite HSP is a single element with sixteen nodes on its boundary as shown in Figure 5.3 (b). Node numbers one to twelve are on the plate and node numbers thirteen to sixteen corresponding to stiffener. All the sixteen nodes of Superelement for composite HSP are on the boundary and serve as connection points between the Superelement and the rest of the structure.

5.4 FORMULATION AND VALIDATION OF SHELL ELEMENTS

A flat rectangular shell element having six dof per node as shown in Figure 5.4 has been taken as the constituent element for the assembly of substructure of HSP. The rectangular flat shell element formulated herein can be effectively used for the analysis of HSP since the structure contains only flat plates. The three translational dof, u, v, w and three rotational dof, θ_x, θ_y, θ_z have been shown in Figure 5.4 (a). The nodal loads are three forces F_x, F_y, F_z, and three moments M_x, M_y, M_z. The nodal loads have been shown in Figure 5.4 (b). The element stiffness relation has been given by eqn. 5.1.

$$[\mathbf{k}]\{\mathbf{d}\} = -\{\mathbf{r}\} \quad ---------- \quad (\mathbf{5.1})$$

where, [k] is the elemental stiffness matrix, {d} is the elemental dof and {r} is the elemental load vector applied by an element to structure nodes.

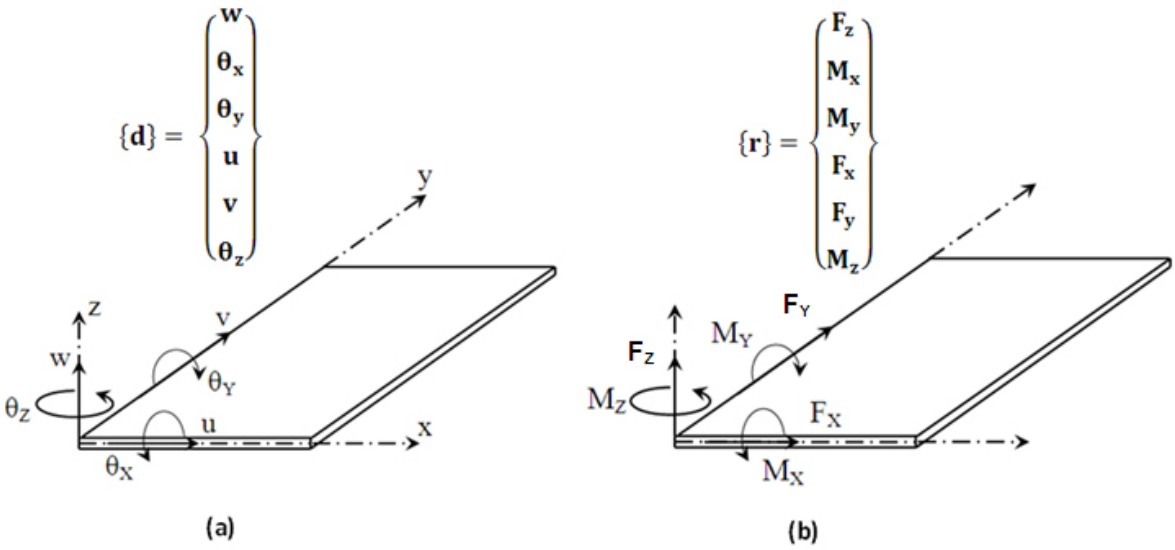

Figure 5.4 Shell Element: (a) Nodal degrees of freedom (b) Nodal loads

5.4.1 Generation of Stiffness Matrix

The flat rectangular shell element having six dof has been formulated as proposed by Bathe (2004), by superimposing plate bending element having three dof and a plane stress element having two in-plane dof. A four noded rectangular plate bending element and a plane stress element whose stiffness matrices have been given in the closed form by Przemieniecki (1968) have been used for the formulation of rectangular shell element. The rectangular plate bending element has one out-of-plane translation and two out-of-plane rotational dof per node viz., w, θ_x and θ_y. The positive directions of these dof have been indicated in the Figure 5.5 (a). The displacement function used to calculate stiffness properties of the rectangular plate bending element ensures that the deflection on the boundary of adjacent plate elements are compatible. However, rotations of the element edges on a common boundary are not

compatible and hence discontinuities in slopes exist across boundaries. The plane stress element selected has two in-plane translational dof per node viz., u and v whose positive directions are the same as the positive directions of the x and y axes as indicated in the Figure 5.5 (b). Stiffness properties of the plane stress element have been calculated using displacement functions which satisfy the assumption of linearly varying boundary displacements thereby the compatibility of displacements on the boundaries of adjacent elements has been satisfied. The expressions for the stiffness coefficients of plate bending elements and plane stress element have been given in Appendix C.

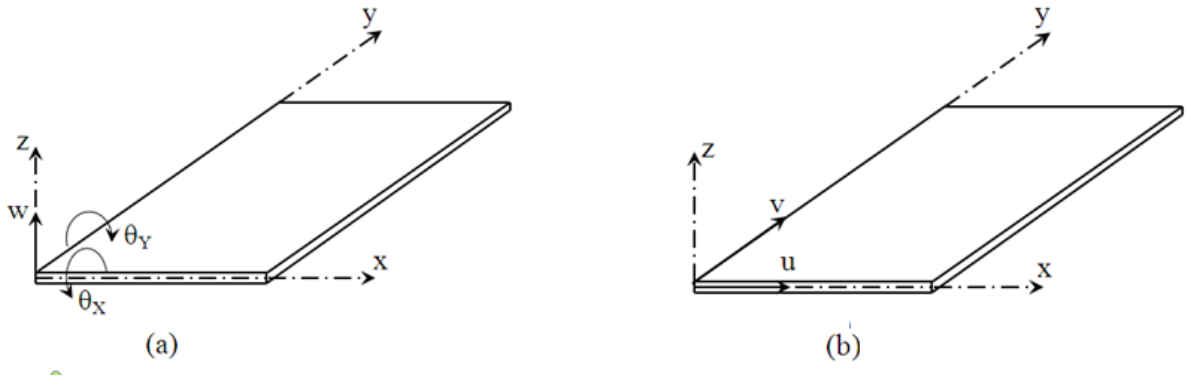

Figure 5.5 (a) Plate Bending Element with Three degrees of freedom (b) Plane Stress Element with Two degrees of freedom

The stiffness matrix k^* of the rectangular shell element having five dof has been obtained by superimposing the plate bending element and the plane stress element using eqn. 5.2.

$$\left[\frac{\mathbf{k}^*}{(\mathbf{20\ x\ 20})}\right] = \begin{bmatrix} \dfrac{\boldsymbol{k_B}}{(\mathbf{12\ x\ 12})} & \mathbf{0} \\ \mathbf{0} & \dfrac{\boldsymbol{k_M}}{(\mathbf{8\ x\ 8})} \end{bmatrix} \quad -------- \quad (\mathbf{5.2})$$

where, k_B and k_M are the stiffness matrices of plate bending element and the plane stress element respectively. Coefficients of k_B and k_M have been given in appendix C. The rectangular flat shell element obtained has five dof per node viz., w, θ_x, θ_y, u and v. The in-

plane rotation, θ_Z is not included in the dof. The stiffness coefficients corresponding to the local rotation about z axis at the nodes, θ_Z has been added to k* and the stiffness matrix of the rectangular shell element having six dof per node has been obtained. A small stiffness coefficient corresponding to the θ_Z rotation has been added to $[k^*]$. The stiffness coefficient corresponding to θ_Z has been taken as one thousandth of the smallest diagonal element of k_B and k_M. Thus the element rotation θ_Z at a node has not been measured and hence its contribution to the strain energy stored in the element is negligibly small. The stiffness matrix for the rectangular shell element having six dof per node viz., w, θ_X, θ_Y, u, v and θ_Z has been obtained using eqn. 5.3.

$$\left[\frac{\mathbf{k}}{(\mathbf{24\ x\ 24})}\right] = \begin{bmatrix} \dfrac{\mathbf{k}^*}{(\mathbf{20\ x\ 20})} & \mathbf{0} \\ \mathbf{0} & \dfrac{\boldsymbol{\varepsilon}.[\mathbf{I}]}{(\mathbf{4\ x\ 4})} \end{bmatrix} \quad ------ \quad (\mathbf{5.3})$$

where, ε is one thousandth of the smallest diagonal element of k_B and k_M and [I] is the unit matrix. The stiffness matrix for the flat shell element obtained has been a 24 x 24 symmetric matrix.

5.4.2 Transformation Matrix

Consider an arbitrarily oriented flat shell element which is lying in the x'y' plane of a local coordinate system x'y'z' which is arbitrarily oriented in a global coordinate system xyz as shown in Figure 5.6. w', θ_x', θ_y', u', v' and θ_z' are the dof in local coordinate system and w, θ_x, θ_y, u, v and θ_z are the dof in the global coordinates. The element stiffness relation in local coordinates has been given by the eqn. 5.4.

$$[\mathbf{k}']\{\mathbf{d}'\} = -\{\mathbf{r}'\} \quad ---------- \quad (\mathbf{5.4})$$

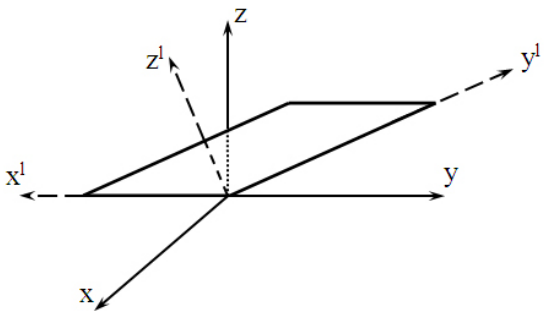

Figure 5.6 Global and Local Coordinate System for the Flat Shell Element.

The relation between local and global dof, nodal loads and stiffness matrices has been given by eqns. 5.5, 5.6 and 5.7 respectively.

$$\{\mathbf{d}'\} = [\mathbf{T}]\{\mathbf{d}\} \quad (\mathbf{5.5})$$

$$\{\mathbf{r}\} = [\mathbf{T}]^{\mathbf{T}}\{\mathbf{r}'\} \quad (\mathbf{5.6})$$

$$[\boldsymbol{k}] = [\boldsymbol{T}]^{\boldsymbol{T}}[\boldsymbol{k}'][\boldsymbol{T}] \quad (\mathbf{5.7})$$

If l_1 m_1 n_1, l_2 m_2 n_2 and l_3 m_3 n_3 are the direction cosines of the local x', y' and z' axes with respect to the global coordinate system xyz, the expression for transformation matrix [T] has been given by eqn. 5.8.

$$[\boldsymbol{T}] = \begin{bmatrix} \boldsymbol{\Lambda} & \mathbf{0} & \mathbf{0} & \mathbf{0} \\ \mathbf{0} & \boldsymbol{\Lambda} & \mathbf{0} & \mathbf{0} \\ \mathbf{0} & \mathbf{0} & \boldsymbol{\Lambda} & \mathbf{0} \\ \mathbf{0} & \mathbf{0} & \mathbf{0} & \boldsymbol{\Lambda} \end{bmatrix} \quad (\mathbf{5.8})$$

where,

$$[\Lambda] = \begin{bmatrix} n_3 & 0 & 0 & l_3 & m_3 & 0 \\ 0 & l_1 & m_1 & 0 & 0 & n_1 \\ 0 & l_2 & m_2 & 0 & 0 & m_1 \\ n_1 & 0 & 0 & l_1 & m_1 & 0 \\ n_2 & 0 & 0 & l_2 & m_2 & 0 \\ 0 & l_3 & m_3 & 0 & 0 & n_3 \end{bmatrix}$$

5.4.3 Finite Element Analysis Using Shell Element

The rectangular shell element formulated has been used for the analysis of plated structures. The structure to be analyzed has been discretised using the shell element and the stiffness matrices for the elements have been calculated in local coordinates. External loads have been applied on the structure nodes. The element stiffness matrices have been transformed from local coordinates to global coordinates using the transformation eqn. 5.7. The element stiffness matrices in the global coordinates have been assembled according to the nodal connectivity and boundary conditions have been applied. This will give a set of equations that describes the structure and has been given as eqn. 5.10.

$$[\mathbf{K}]\{\mathbf{D}\} = \{\mathbf{R}\} \quad ---------- \quad (\mathbf{5.10})$$

where, [K] is the assembled stiffness matrix for the structure, {D} is the structural dof and {R} is external structural loads.

The structural equations are solved using Gauss elimination method to obtain the global dof. The elemental dof in global coordinates for each element can be extracted from the global dof of the structure. These elemental dof in the global coordinates are transformed to local coordinates using eqn. 5.5 and the elemental load vector has been obtained using eqn. 5.4. The normal stresses along the x and y directions in the top and bottom layer at each node of the element have been calculated using eqns. 5.11 and 5.12.

$$\boldsymbol{\sigma_x} = \pm\frac{\mathbf{12M_y}}{\mathbf{bt^2}} \pm \frac{\mathbf{2F_x}}{\mathbf{bt}} \quad ---------- \quad (\mathbf{5.11})$$

$$\sigma_y = \pm\frac{12M_x}{at^2} \pm \frac{2F_y}{at} \quad \text{- - - - - - - - - - - - - - -} \quad (5.12)$$

5.4.4 Description of Computer Code

A computer program for the linear elastic FEA of a structure using rectangular flat shell element developed herein has been coded in C programming language. The program can run in a personal computer with Linux operating system. The schematic flow diagram of the software has been shown in Figure 5.7. The computer program consists of a main and nine functions. The program reads the input data from the data file ***INFILE*** and the output of the program has been written in the data file ***OUTFILE***.

The input data file ***INFILE*** contains the detailed description of the problem viz., the number of nodes, number of elements, number of nodes per element, dof per node, material properties – Young's modulus and Poisson's ratio, nodal coordinates, element connectivity, boundary condition, structural nodal loads and element number whose nodal stress values have to be calculated. Detailed problem description i.e., echo of the input, nodal values of displacements at each structural nodes in global coordinates, force resultants on the nodes of element specified in the local coordinates and stress values in the top and bottom layer at the four nodes of element specified have been written in the file ***OUTFILE***.

The main program calls the functions in the order **indata( ), numbdof( ), ldvect( ), asmbly( ), gauss( )** and **stressrec( )**. The description of the problem has been read from the data file ***INFILE***. Unconstrained dof of the structure have been numbered. Load vector for the structure has been generated corresponding to the unconstrained dof. The stiffness matrix for each element in the structure has been generated in local coordinate system. The stiffness matrix in local coordinate system has been transformed to global coordinate system. The elemental stiffness matrices in global coordinates have been assembled according to nodal connectivity to obtain the structural stiffness matrix. The structural equations have been solved to obtain the nodal values of dof in global coordinates. The stress values at the top and bottom layer have been computed at nodal points of the element specified in the input file. Working of the nine functions has been described subsequently.

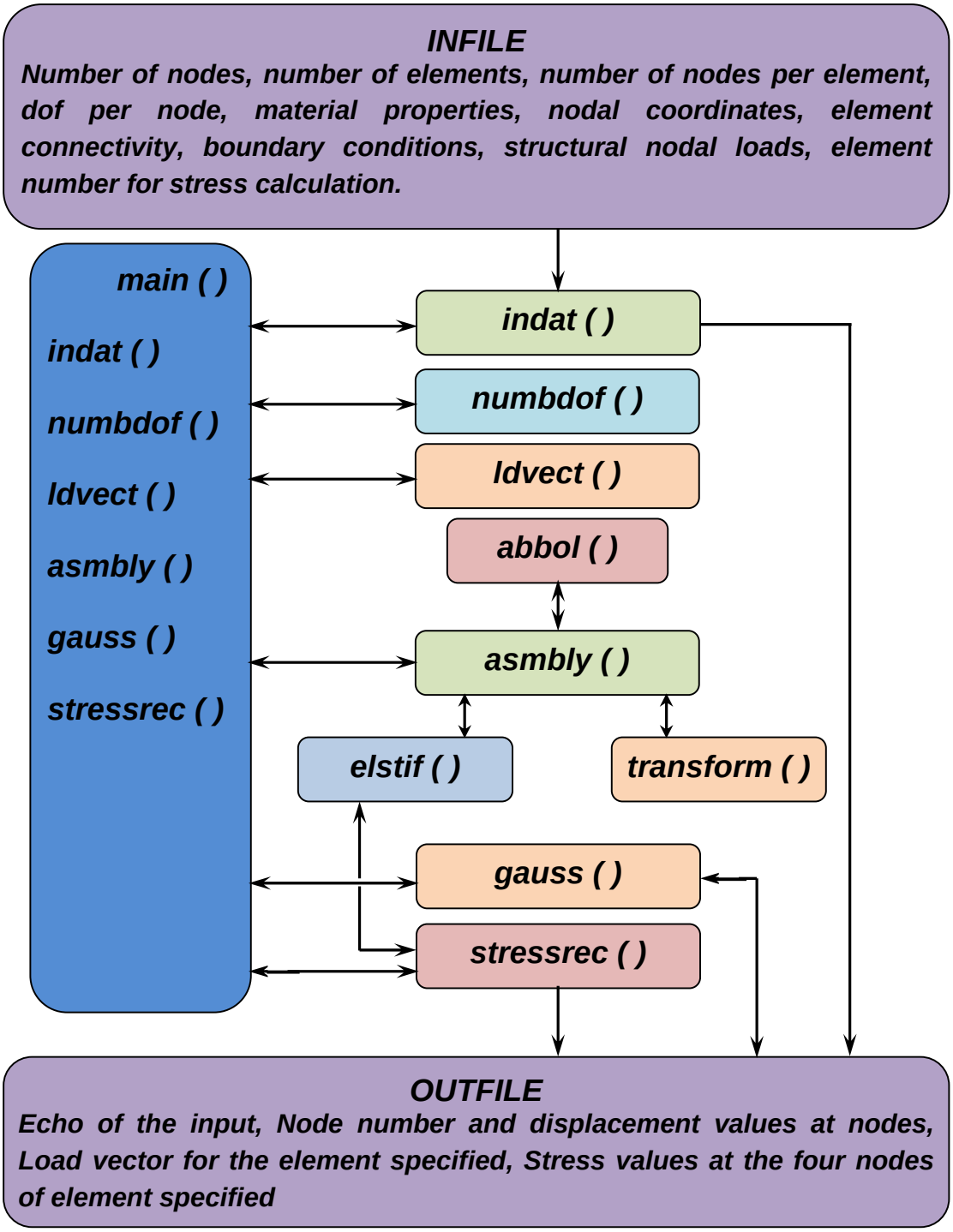

Figure 5.7 Schematic flow diagram of the computer program for the linear elastic Finite Element Analysis using rectangular shell element.

1. **indata ( ):** The detailed description of the problem has been read from the data file ***INFILE***. The problem description contains the following data

- Number of nodes
- Number of elements
- Number of nodes per element
- dof per node
- Material properties – Young's modulus and Poison's ratio
- Nodal coordinates
- Element connectivity and thickness
- Boundary conditions
- Nodal loads of the structure
- Element number for which stresses to be calculated

The echo of the input has been written in the output data file ***OUTFILE***.

2. **numbdof( ):** Boundary conditions has been used by the function to sequentially number the unconstrained structural dof. This global numbering of structural dof has been stored in the one dimensional array **nbdf [ ]**. Zeros have been put at places corresponding to arrested dof. The size of **nbdf [ ]** is equal to the total number of structural dof and the number of non-zero elements in the array is equal to the number of unconstrained dof.

3. **ldvect ( ):** The nodal load data and the global numbering of structural dof have been used by the function to generate the load vector. The load vector has been stored in the one dimensional array **ldv[ ]**. The size of this one dimensional array is equal to number of unconstrained dof.

4. **asmbly ( ):** The assembled stiffness matrix for the entire structure has been generated by the function. Functions **elstif ( )**, **transform ( )** and **abbol ( )** have been called to obtain the elemental stiffness matrix in global coordinates and Boolean matrix. The element connectivity, elemental stiffness matrix and Boolean matrix have been used to assemble elemental stiffness matrices and obtain the structural stiffness matrix. The structural stiffness matrix has been stored in the two dimensional array **astif [ ] [ ].** The number of rows and columns in **astif [ ] [ ]** is equal to the number of unconstrained dof in the structure.

5. **gauss ( ):** The assembled stiffness matrix **astif [ ][ ]** and load vector **ldv[ ]** have been used by the function to determine the displacement vector. The structural eqn. 5.10 has been solved by the function using Gauss elimination method and the displacement vector has been stored in the one dimensional array **def[ ] .** The displacement arrays **w [ ], theetax [ ], theetay [ ], u [ ], v [ ]** and **theetaz [ ]** which contains the nodal values of dof w, θ_X, θ_Y, U, V and θ_Z have been extracted from the array **def [ ].** The structural node numbers and the corresponding displacement values have been written in the data file ***OUTFILE***.

6. **stressrec ( ):** The force vector and the stresses at the four nodes of the specified element have been calculated by the function. The function **elstif ( )** has been called and the element stiffness matrix in local coordinates has been obtained using nodal connectivity, thickness and nodal coordinates of the element specified. The dof at the four nodes of the element specified has been extracted from the displacement arrays **w [ ], theetax [ ], theetay [ ], u [ ], v [ ]** and **theetaz [ ]**. Using the nodal coordinates of the element specified, the direction cosines of its local coordinates have been found out. The dof at the four nodes of the element specified in local coordinate system have been transformed to global coordinate system using eqn. 5.5. The elemental load vector for the element specified has been obtained using eqn. 5.4. The elemental load vector at the four nodes of the element specified has been written in the data file ***OUTFILE***. The stress values in the top and bottom layers at the four nodes of the element specified have been calculated using eqns. 5.11 and 5.12 and these values have been written in the data file ***OUTFILE***.

7. **abbol ( ) :** The Boolean matrix for each element of the structure has been determined using element nodal connectivity and the global numbering of structural dof. The Boolean matrix of an element contains global numbering of dof at the four nodes of the element. The size of the Boolean matrix of an element is twenty four.

8. **elstif ( ) :** The stiffness matrix of an element in local coordinates has been determined by the function. The length along local x and y axis of an element has been calculated by the function using the elemental connectivity and nodal coordinates. The function also uses thickness of the element and the stiffness matrix for the element has been calculated using expressions for stiffness coefficients given in Appendix C and eqns. 5.2 and 5.3.

9. **transform ( ) :** The function determines the direction cosines of the local coordinates of the element using elemental connectivity and nodal coordinates. The elemental stiffness matrix in local coordinates has been transformed to global coordinates using the eqn. 5.7.

5.4.5 Numerical Validation

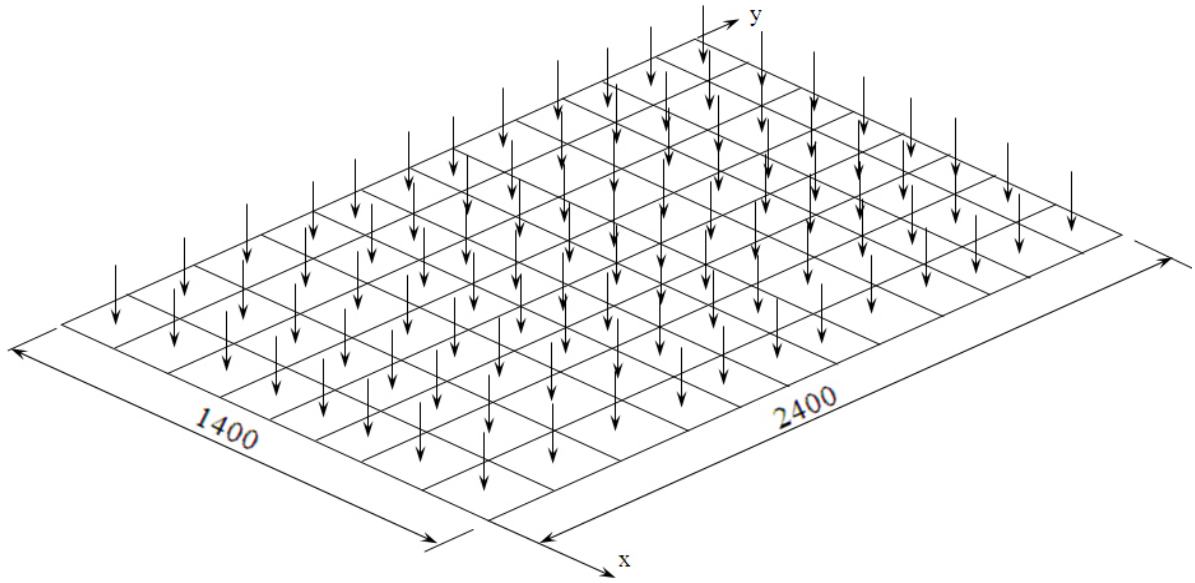

Figure 5.8 Finite element mesh of thin flat plate with uniformly distributed load.

A thin flat rectangular plate has been analyzed using the computer program developed. Analysis has been carried out for two separate boundary conditions viz., all four edges simply supported and all four edges fixed. The flat plate with length, breadth and thickness, 2400 mm, 1400 mm and 6 mm respectively has been discretized with flat rectangular shell element as shown in Figure 5.8. The plate is made with EHS 690 steel. Poisson's ratio of the material is 0.3, the modulus of elasticity is 210 GPa, the density is 7800 kg/m^3 and the yield stress is 690 MPa. A uniform pressure load of 10 kPa is applied on the surface of the plate.

A section of the HSP explained in section 3.2.1 whose geometry given in Figure 3.1 has been analysed using the computer code developed. The material properties of the RUC of HSP have been given in section 3.2.2. A uniform pressure load of 10 kPa is applied on the surface

of the plate and analysis has been carried out for two separate boundary conditions viz., all four edges simply supported and all four edges fixed.

5.4.6 Results and Discussion

The results obtained using the computer code developed has been compared with the same obtained using ANSYS 12. The deflection at the centre of the plate, stresses along the x and y direction at the centre of the plate in the top and bottom layer have been compared. For the thin rectangular plate the results have been tabulated and presented in Tables 5.1 and 5.2. It has been seen that the maximum percentage variation in deflection is 0.39 and the maximum percentage variation in stress is 6.10. For the RUC of HSP the results have been tabulated and presented in Tables 5.3 and 5.4. The maximum percentage variation in deflection is 9.61 and the maximum percentage variation in elemental load is 9.11.

Table 5.1 Displacement and stresses at the centre of the plate for all four edges simply supported boundary condition, analysed using shell element formulated and ANSYS 12

Response	Solution Using Computer Code	Solution Using ANSYS 12	Percentage Variation
Deflection (mm)	-81.8	-81.48	0.39
Stress in the x Direction at the Top Layer (MPa)	-298.8	-300.54	0.58
Stress in the x Direction at the Bottom Layer (MPa)	298.8	300.54	0.58
Stress in the y Direction at the Top Layer (MPa)	-156.58	-161.23	2.88
Stress in the y Direction at the Bottom Layer (MPa)	156.58	161.23	2.88

Table 5.2 Displacement and stresses at the centre of the Plate for all four edges fixed boundary condition, analysed using shell element formulated and ANSYS 12

Response	Solution Using Computer Code	Solution Using ANSYS 12	Percentage Variation
Deflection (mm)	-22.44	-22.47	0.16
Stress in the x Direction at the Top Layer (MPa)	-133.58	-133.2	0.29
Stress in the x Direction at the Bottom Layer (MPa)	133.58	133.2	0.29
Stress in the y Direction at the Top Layer (MPa)	-58.2	-61.98	6.10
Stress in the y Direction at the Bottom Layer (MPa)	58.2	61.98	6.10

Table 5.3 Displacement and elemental loads at the centre of the Hat Stiffened Plate for all edges simply supported boundary condition, analysed using shell element formulated and ANSYS12

Response	Solution Using Computer Code	Solution Using ANSYS 12	Percentage Variation
Deflection at the centre (mm)	-0.6754	-0.7179	5.92
Force in the x Direction at the centre (N)	455.95	453.95	0.44
Force in the y Direction at the centre (N)	1279	1286.1	0.55
Moment about the x axis at the centre (N-mm)	1367	1255.7	8.86
Moment about the y axis at the centre (N-mm)	11085	11175	0.81

Table 5.4 Displacement and elemental loads at the centre of the Hat Stiffened Plate for all four edges fixed boundary condition, analysed using shell element formulated and ANSYS12

Response	Solution Using Computer Code	Solution Using ANSYS 12	Percentage Variation
Deflection at the centre (mm)	-0.3487	-0.3822	9.61
Force in the x Direction at the centre (N)	453.7	449.81	0.86
Force in the y Direction at the centre (N)	1317.7	1326	0.63
Moment about the x axis at the centre (N-mm)	1321.6	1201.2	9.11
Moment about the y axis at the centre (N-mm)	11505	11575	0.60

5.5 FORMULATION OF SUPERELEMENT

The six constituent elements of the Superelement for HSP have been shown in Figure 5.9 (a). Circled numbers indicate element numbers, numbers one to four on the four corners of each element indicate the node numbers of each element and the numbers within square brackets indicate the dof at each node. Superelement of HSP and super dof are shown in Figure 5.9 (b). The numbers one to twelve indicate the node numbers and the numbers within the square brackets indicates the super dof at each node. The stiffness matrices of the six constituent elements of the substructure of HSP have been added according to the nodal connectivity to obtain the stiffness matrix of the Superelement for HSP. The stiffness matrices of elements four and six have been transformed from local coordinates to global coordinates using eqn. 5.7 before assembly. The composition of super dof of the Superelement for HSP has been explained subsequently.

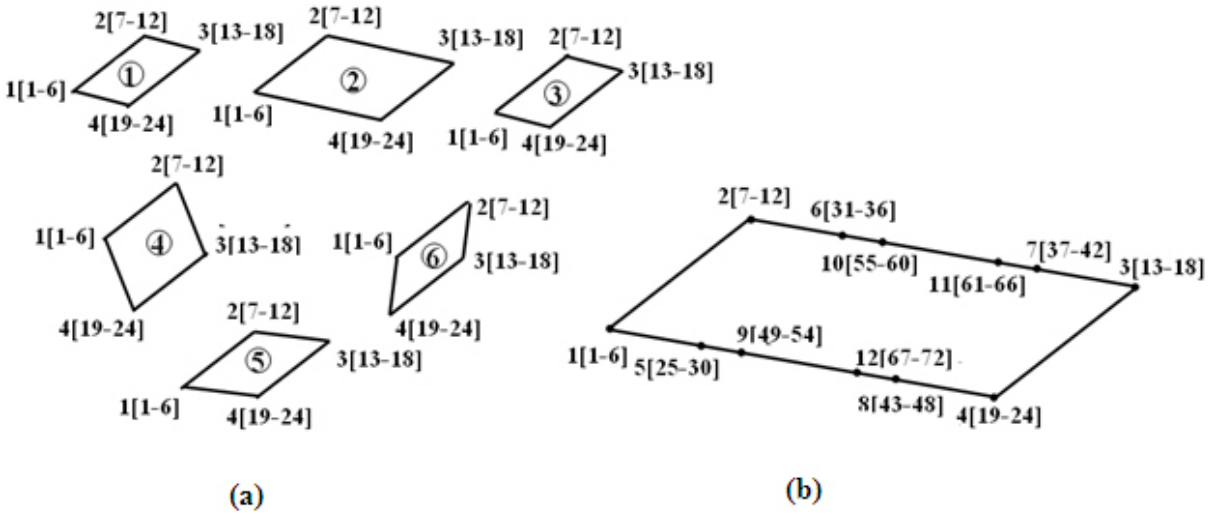

Figure 5.9 Degrees of freedom: (a) Constituent finite elements (b) Superelement

The dof [1 to 6] at node 1 and dof [7 to 12] at node 2 of element one will turn into super dof [1 to 6] at node 1 and super dof [7 to 12] at node 2 of Superelement respectively. The dof [13 to 18] at node 3 of element three and [19 to 24] at node 4 of element three will turn into super dof [13 to 18] at node 3 and super dof [19 to 24] at node 4 of the Superelement respectively. The dof, [19 to 24] at node 4 of element one, dof [1 to 6] at node 1 of element two and transformed dof [1 to 6] at node 1 of element four, will comprise super dof [25 to 30] at node 5 of the Superelement. The dof, [13 to 18] at node 3 of element one, [7 to 12] at node 2 of element two and transformed dof [7 to 12] at node 2 of element four, will comprise super dof [31 to 36] at node 6 of the Superelement. The dof, [13 to 18] at node 3 of element two, dof [7 to 12] at node 2 of element three and transformed dof [7 to 12] at node 2 of element six will comprise super dof [37 to 42] at node 7 of the Superelement. The dof, [19 to 24] at node 4 of element two, dof [1 to 6] at node 1 of element three and transformed dof [1 to 6] at node 1 of element six will comprise super dof [43 to 48] at node 8 of the Superelement. The transformed dof [19 to 24] at node 4 of element four, and dof [1 to 6] at node 1 of element five will comprise super dof [49 to 54] at node 9 of the Superelement. The transformed dof [13 to 18] at node 3 of element four, and dof [7 to 12] at node 2 of element 5 will comprise super dof [55 to 60] at node 10 of the Superelement. The dof [13 to 18] at node 3 of element five, and transformed dof [13 to 18] of element six will comprise super dof [61 to 66] at node 11 of the Superelement. The dof [19 to 24] at node 4 of element five, and transformed dof [19 to 24] at node 4 of element six will comprise super dof [67 to 72] at node 12 of the Superelement.

5.6 FINITE ELEMENT ANALYSIS USING SUPERELEMENTS

The analysis of a HSP shown in Figure 5.2 (a) has been carried out using the Superelement developed. The geometrical parameters of the substructure of HSP shown in Figure 5.1 (a) have been found out from the geometry of HSP. The stiffness matrices of the constituent elements of the Superelement have been calculated and assembled according to the procedure mentioned in section 5.5. The HSP to be analyzed is discretized using the Superelement shown in Figure 5.9 (b). The stiffness matrices of the Superelements have been assembled according to nodal connectivity to obtain the structural stiffness matrix. The loads and boundary conditions are applied at the nodes of the structure discretized using Superelements. While applying the load it may be noted that the node numbers 1 to 8 of the Superelement shown in Figure 5.9 (b) are on the plate and node number 9 to 12 of the Superelement are on the stiffener. A finite element model of the HSP meshed using Superelements is shown in Figure 5.2 (b). The structural equations have been solved using Gauss elimination method to obtain the super dof at each node of the Superelement. For each Superelement the super dof will give the dof at the nodes of the constituent finite elements in global co ordinates. These elemental dof are transformed to local dof using eqn. 5.5. The nodal loads F_z, M_x, M_y, F_x, F_y, M_z and for the element are obtained using eqn. 5.4 and the stresses σ_x and σ_y at the nodal point have been calculated using eqn. 5.11 and 5.12.

5.7 DESCRIPTION OF THE COMPUTER CODE

A computer program for the linear elastic FEA of a HSP using Superelement developed herein has been coded in C programming language. The program can run in a personal computer with Linux operating system. The schematic flow diagram of the software has been shown in Figure 5.10. The computer program consists of a main and ten functions. The program reads the input data from the data file ***INFILE*** and the output has been written in the data file ***OUTFILE***.

The input data file ***INFILE*** contains the detailed problem description viz., the geometric details of substructure shown in Figure 5.1 (a), discretization of HSP using Superelements, loads, boundary conditions and element number whose nodal stress values have to be

calculated. The echo of the input, nodal values of displacements at each structural nodes in global coordinates, force resultants on the twelve nodes of Superelement specified in the local coordinates and stress values in the top and bottom layer at the twelve nodes of the element specified in the local coordinates have been written in the file ***OUTFILE***.

Working of the ten functions has been explained subsequently.

1. **indat ( ) :** The detailed description of the problem has been read from the data file ***INFILE.*** The problem description contains the following data:
    - Material Properties - Young's modulus and Poisson's ratio
    - Geometry of the substructure - a_1, a_2, a_3, h and b as shown in Figure 5.1 (a)
    - Thickness of the six constituent elements of the substructure
    - Number of nodes in the structure
    - Number of elements in the strucuture
    - Number of nodes per Superelement
    - dof per node
    - Element connectivity
    - Boundary condition
    - Structural nodal loads
    - Element number for stress calculation

    The echo of the input has been written in the data file ***OUTFILE***.
2. **superel ( ) :** The stiffness matrix for the Superelement has been calculated by the function using the material properties and geometrical parameters of the substructure of HSP. The procedure explained in section 5.5 has been followed for calculating the stiffness matrix of the Superelement. The four noded shell element having six dof per node formulated in section 5.4 has been used as the constituent elements for the substructure of HSP. The nodal coordinates of the substructure shown in Figure 5.1 (b) has been calculated using the geometrical parameters of the substructure. The function **genstiff ( )** has been called for calculating the stiffness matrix for each of the six constituent element of the substructure in local coordinates. The function **transform ( )** has been called to transform the element stiffness matrix in local coordinates to global coordinates. The stiffness matrices of the six conventional elements have been added according to nodal connectivity to obtain the stiffness matrix of the substructure or the Superelement. The stiffness matrix of the Superelement has been written in a data file ***CK.***

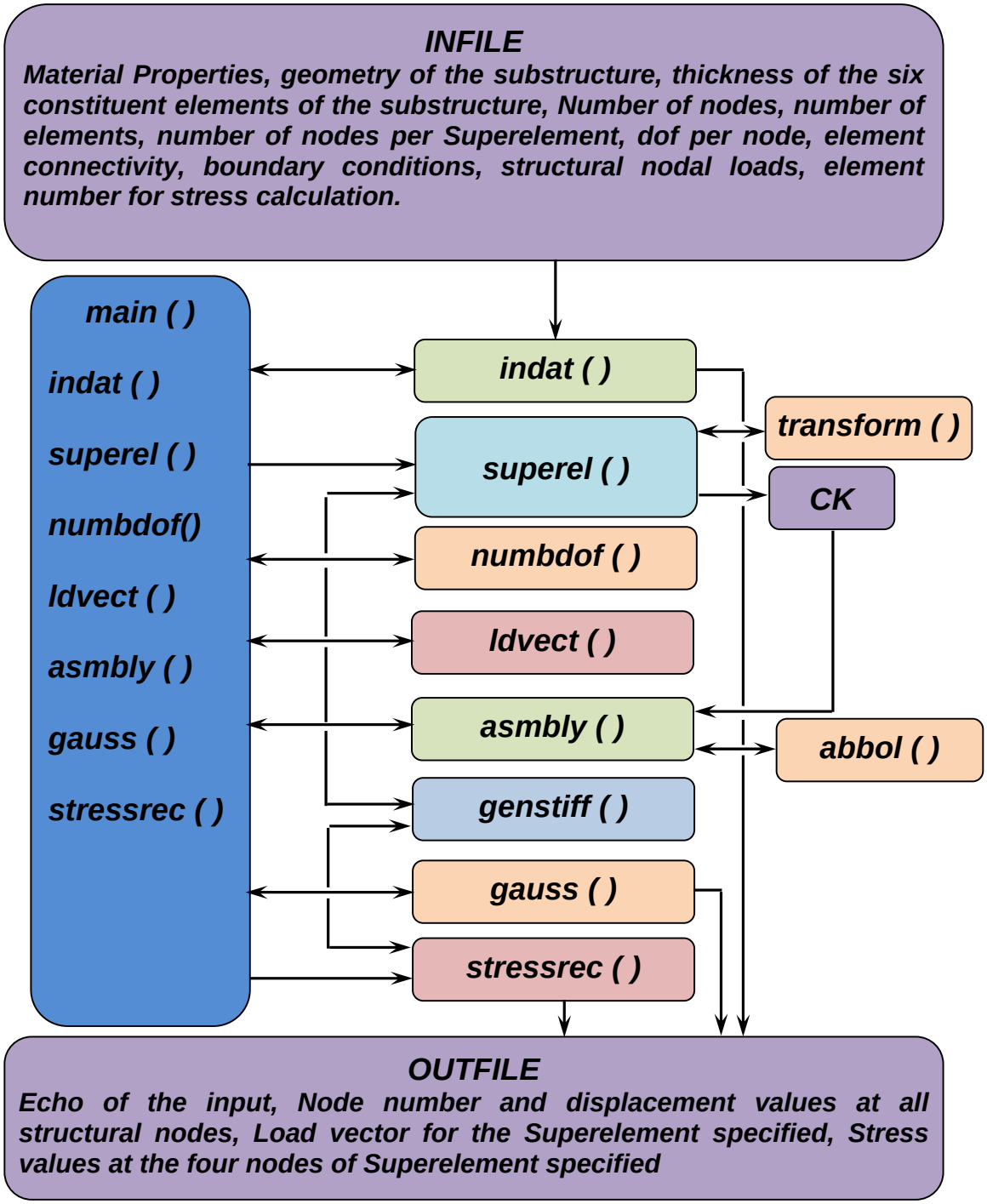

Figure 5.10 Schematic Flow Diagram of the Software for the Finite Element Analysis using the Superelement

3. **numbdof( ):** The function sequentially numbers the unconstrained structural dof considering the boundary conditions. This global numbering of structural dof has been stored in the one dimensional array **nbdf[ ]**. Zeros have been put at places corresponding to arrested dof. The size of **nbdf[ ]** is equal to the total number of structural dof and the number of non-zero elements in the array is equal to the number of unconstrained dof.
4. **ldvect ( ):** The nodal load data and the global numbering of structural dof have been used by the function to generate the load vector. The load vector has been stored in the one dimensional array **ldv[ ]**. The size of this one dimensional array is equal to number of unconstrained dof.
5. **asmbly ( ):** The assembled stiffness matrix for the entire structure has been generated by the function. Function **abbol ( )** have been called to obtain the Boolean matrix for each Superelement. The stiffness matrix for each Superelement is read from the data file **CK**. The element connectivity, elemental stiffness matrix and Boolean matrix have been used to assemble elemental stiffness matrices of Superelements and obtain the structural stiffness matrix. The structural stiffness matrix has been stored in the two dimensional array **sastif[ ][ ].** The number of rows and columns in **sastif[ ][ ]** is equal to the number of unconstrained dof in the structure.
6. **gauss ( ):** The assembled stiffness matrix **sastif[ ][ ]** and load vector **ldv[ ]** have been used by the function to determine the displacement vector. The structural eqn. has been solved by the function using Gauss elimination method and the displacement vector has been stored in the one dimensional array **def[ ].** The displacement arrays **w[ ], theetax[ ], theetay[ ], u[ ], v[ ]** and **theetaz[ ]** which contains the nodal values of dof w, θ_X, θ_Y, U, V and θ_Z have been extracted from the array **def[ ].** The structural node numbers and the corresponding displacement values have been written in the data file ***OUTFILE***.
7. **stressrec ( ):** The function calculates the force vector and the stresses at all the twelve nodes of the Superelement specified. As shown in Figure 5.1, the Superelement has been constituted by 6 conventional shell elements. The stress at the twelve nodes of the Superelement can be obtained by evaluating the stress values at four nodes of constituent elements 1, 3 and 5. The function **genstiff( )** has been called and the element stiffness matrix for the element 1 of the constituent element of the Superelement has been obtained. The nodal values of displacements in global coordinates for this element have

been extracted from the displacement arrays **w [ ], theetax [ ], theetay [ ], u [ ], v [ ]** and **theetaz [ ]**. Using the nodal coordinates of the element one, the direction cosines of its local coordinate system have been found out. The displacement values in global coordinates have been transformed to local coordinates using eqn. 5.5. The force vector for the element specified is obtained using eqn. 5.4. These force vectors for the four nodes of the element one are stored in the force arrays **fz [ ], mx [ ], my [ ], fx [ ],fy [ ]** and **mz [ ]** and these are also written in the data file ***OUTFILE***. From the force vector, stresses at the four nodes of the element specified are calculated using the eqns. 5.11 and 5.12. The stress values in the top and bottom layers at the four nodes of the element specified have been calculated using eqns. 5.11 and 5.12 and these values have been written in the data file ***OUTFILE***. The procedure is repeated for elements three and element five of the Superelement.

8. **abbol ( ) :** The Boolean matrix for each Superelement of the structure has been determined using element nodal connectivity and the global numbering of structural dof. The Boolean matrix of an element contains global numbering of dof at the twelve nodes of the element. The size of the Boolean matrix of a Superelement is seventy two.
9. **genstiff ( ) :** The stiffness matrix of an element in local coordinates has been determined by the function. The length along local x and y axis of an element has been calculated using the nodal coordinates of the element. The function also uses thickness of the element and the stiffness matrix for the element has been calculated using expressions given in Appendix C and eqns. 5.2 and 5.3.
10. **transform ( ) :** The function determines the direction cosines of the local coordinates of the element using nodal coordinates. The elemental stiffness matrix in local coordinates has been transformed to global coordinates using the eqn. 5.7.

5.8 MODIFICATION IN COMPUTER CODE FOR COMPOSITE SUPERELEMENT

The computer code developed for the analysis of isotropic HSP using Superelement can be employed for the analysis of HSP made of composite materials by modifying the function **genstiff( )** to generate the stiffness matrix for composite shell element. This element stiffness matrix can be selected based on the requirement of the structural component and material

(fibre and matrix). This actually is a benefit that the best available or generated composite finite element can be used as the constituent element. Material properties as required by the element stiffness matrix for the composite material have to be given in the input file. As described in section 5.3, the Superelement for composite HSP is a combination of eight conventional four noded rectangular composite shell elements. The thicknesses of these eight conventional composite shell elements have to given in the input file. The stiffness matrix for the composite shell element can be generated using the closed form formulae or using numerical integration. In the function **stressrec( ),** appropriate eqns. for the recovery of stress for composite shell element have to be used instead of eqns. 5.11 and 5.12.

5.9 NUMERICAL INVESTIGATIONS

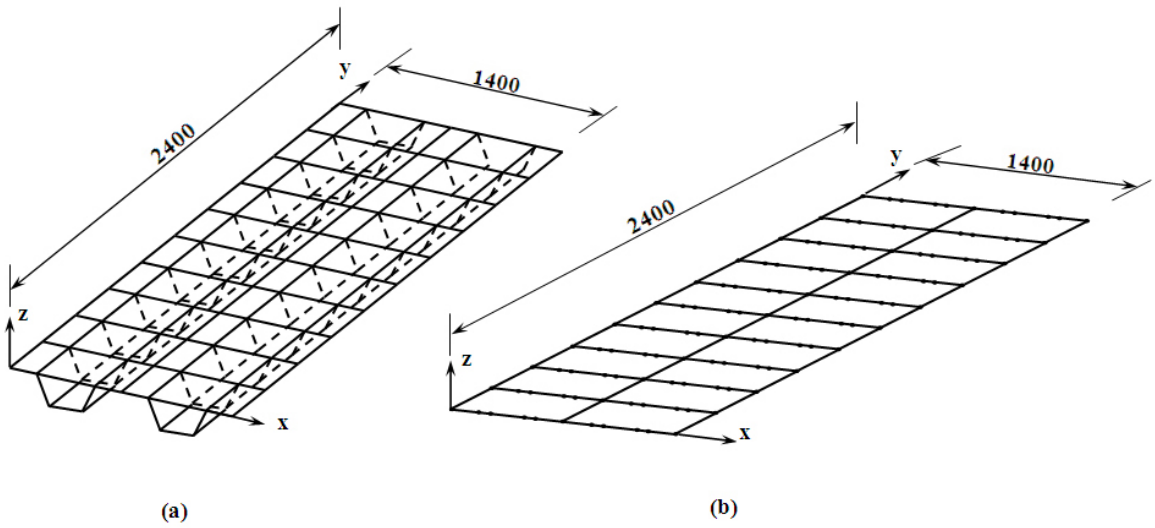

Figure 5.11 Finite element model of Representative Unit Cell of Hat Stiffened Plate modeled using: (a) Conventional rectangular shell element (b) Superelement

A RUC of the HSP with two stiffeners whose geometry and dimensions as shown in Figure 3.2 has been analysed using the software developed. The material properties are given in section 3.2.1. The values of the geometrical parameter a_1, a_2, a_3, h and b have been 175 mm, 350 mm, 210 mm, 150 mm and 240 mm respectively. The thicknesses of the six

conventional elements which constitute the Superelement have been 6 mm, 6 mm, 6 mm, 4 mm, 4 mm and 4 mm. Finite element model of the RUC of HSP modeled using conventional rectangular shell element has been shown in Figure 5.11 (a) and the same modeled using Superelement has been shown in Figure 5.11 (b). The structure has been analysed for two separate boundary conditions viz., all four edges simply supported and all four edges fixed. A uniform pressure load of 10 kPa is applied on the surface of the plate.

5.10 RESULTS AND DISCUSSION

A Superelement for the analysis of HSP that reduces the modeling efforts and storage requirements for the analysis of ship structures made of HSP has been developed. RUC of HSP has been analysed using the computer code which uses the Superelement for the HSP. The results obtained using the Superelement has been compared with that obtained using conventional elements and have been presented in a tabular form in Tables 5.5 and 5.6. It has been seen that the maximum percentage variation in deflection is 0.68% and the maximum variation in stress is 6.6%. The Superelement developed for HSP predicted the deflection and stress for a RUC of HSP with sufficiently good accuracy.

Table 5.5 Displacement and stresses at the centre of the Hat Stiffened Plate for all four edges simply supported boundary condition, analysed using Superelement and conventional finite element

Response	Solution Using Superelement	Solution Using Conventional Element	Percentage Variation
Deflection (mm)	-0.6791	-0.6745	0.68
Stress in the x Direction at the Top Layer (MPa)	-16.03	-16.03	0
Stress in the x Direction at the Bottom Layer (MPa)	14.75	14.76	0.06
Stress in the y Direction at the Top Layer (MPa)	-5.06	-5.04	0.4
Stress in the y Direction at the Bottom Layer (MPa)	0.15	0.16	6.6

Table 5.6 Displacement and stresses at the centre of the Hat Stiffened Plate all four edges fixed boundary condition, analysed using Superelement and conventional finite element

Response	Solution Using Superelement	Solution Using Conventional Element	Percentage Variation
Deflection (mm)	-0.3451	-0.3446	0.14
Stress in the x Direction at the Top Layer (MPa)	-16.44	-16.44	0.00
Stress in the x Direction at the Bottom Layer (MPa)	15.23	15.23	0.00
Stress in the y Direction at the Top Layer (MPa)	-4.93	-4.93	0.00
Stress in the y Direction at the Bottom Layer (MPa)	0	0	0.00

CHAPTER 6

SUMMARY AND CONCLUSIONS

6.1 SUMMARY

Trapezoidal or Hat shaped stiffeners are commonly used in composite ship constructions and are getting popular in the construction of metallic ships because of the efforts for designing light weight ships. Orthotropic plate theory has been identified as a classical method for the analysis of Hat stiffened plate. The expression for the flexural rigidities of Hat Stiffened Plate and analytical solution for bending and buckling of rectangular orthotropic plates have been identified and presented in this thesis. The structural advantages of a Hat Stiffened Plate over other commonly used open section stiffeners have been substantiated in the thesis through numerical investigations. Structural response of Representative Unit Cells of Hat Stiffened Plate and plates stiffened with commonly used open section stiffeners viz., flat bar, angle bar and tee bar has been predicted using ANSYS 12. Investigations have been carried out for simply supported boundary condition and three general types of loading viz., out-of-plane loading, in-plane loading and torsion loading. Comparison of weight, deflection, stress and buckling load has been presented in table form. The comparison shows that HSP exhibit better strength-to-weight ratio as compared to plates stiffened with commonly used open section stiffeners.

An Orthotropic Plate Model has been developed as an efficient structural substitute for Hat Stiffened Plate based on the equal rigidity concept, which makes use of Orthotropic Rescaling Technique. The Orthotropic Plate Model developed for a Representative Unit Cell of Hat Stiffened Plate has been validated with the analytical solution available for orthotropic plate. The stress and deflection of Representative Unit Cell of Hat Stiffened Plate modeled using isotropic thin shell element and its equivalent Orthotropic Plate Model using orthotropic thin shell element have been predicted using ANSYS 12. Analysis has been carried out for a uniform pressure load and the two boundary conditions viz., all four edges simply supported as well as two edges fixed and two edges simply supported. A comparison of results obtained

for Hat stiffened Plate and its equivalent Orthotropic Plate Model has been presented in the table form. For simply supported boundary condition the Orthotropic Plate Model could predict the maximum deflection and stress with sufficiently good accuracy. Linear buckling analysis and ultimate strength analysis of Hat Stiffened Plate and its equivalent Orthotropic Plate Model has been carried out for all four edges simply supported boundary condition and the results have been compared. The Orthotropic Plate Model could predict the linear buckling load with good accuracy and ultimate strength with an accuracy of 18.5% only.

A Superelement for the Finite Element Analysis of Hat Stiffened Plate has been formulated in the thesis. A general shell element having six degrees of freedom per node has been generated using the standard procedure available and validated. The Superelement of Hat Stiffened Plate has been modeled using the general shell element and the stiffness matrices of the shell element constituting the Superelement for the Hat Stiffened Plate have been assembled to obtain the stiffness matrix of the Superelement for Hat Stiffened Plate. The Superelement generated has been used to carry out a linear static analysis of a Representative Unit Cell of Hat Stiffened Plate between two bulkheads. The results obtained using Superelements for Hat Stiffened Plate have been compared with the same obtained using conventional shell elements. The Superelement could predict the deflection and in-plane stress of Hat Stiffened Plate with sufficiently good accuracy for different boundary conditions.

Hat Stiffeners are used in composite stiffened plates. Formulation of Superelement for composite Hat Stiffened Plate has been presented. The computer code developed for the Finite Element Analysis using Superelement for isotropic Hat Stiffened Plate can be modified and used for the analysis using Superelement for composite Hat Stiffened Plate. The modifications in the computer code have also been presented in the thesis.

6.2 CONCLUSIONS AND RECOMMENDATIONS

The conclusions drawn from this research work are listed below.

1. Usage of Hat Stiffened Plate for ship structure can effectively reduce the weight as compared to commonly used open section stiffeners. Light weight structure will result in faster, more economical and environment friendly ships.

2. The Orthotropic Plate Model developed can predict deflection, stress and linear buckling load with sufficiently good accuracy in the case of all four edges simply supported boundary condition.
3. The Finite Element Analysis using the Superelement developed for the Hat Stiffened Plate accurately predicts the stresses and deflection. The usage of Superelement is relatively simple as it does not involve any condensation. Usage of Superelements will reduce the storage requirement and man hour required in the Finite Element Analysis of structures made of Hat Stiffened Plate. The formulation of Superelement has also been applied for Hat Stiffened Plates made of composite materials.

6.3 SIGNIFICANT CONTRIBUTIONS

Orthotropic Plate Model concept is more generic that, any scheme to solve the orthotropic plate equations can be used as a solution strategy for Hat Stiffened Plate. Hat Stiffened Plates are usually employed for ship structural components such as decks and bulkheads. In the Orthotropic Plate Model geometric orthotropy is converted to material orthotropy i.e., the stiffeners are smeared and they vanish from the field of analysis and the structure can be analysed using any conventional Finite Element software which has orthotropic elements in its element library. Therefore, it can be stated that the geometric complexity of ship structure having Hat Stiffened Plates has been reduced largely by this contribution. Hence Orthotropic Plate Model is a novel and efficient structural substitute for such stiffened plates. The Orthotropic Plate Model developed as the structural substitute for Hat Stiffened Plate has the following advantages:

- Reduces the modeling efforts
- Reduces the storage requirement
- Analysis for lateral loads and in-plane loads can be carried out

Superelement developed herein for the analysis of Hat Stiffened Plate is an efficient tool to reduce the modeling efforts in Finite Element Analysis of ship structure made of Hat Stiffened Plate. The option for selecting appropriate finite elements such as confirming, robust etc. as well as isotropic, composite etc. exists which makes this contribution very general. Formulation of Superelement for composite Hat Stiffened Plate has also been demonstrated.

Using Superelement for the Finite Element Analaysis of Representative Unit Cell of Hat Stiffened Plate the number of areas to be generated reduces from seven to one and the number of elements reduces from one hundred twenty to twenty without any compromise in the accuracy. The Superelement developed for the Hat Stiffened Plate has the following advantages:

- Reduces the modeling effort
- Reduce the storage requirement
- Save computation
- Preserve the functional or behavioral identity of the structure
- The procedure used for the Superelement can adopted for the analysis of Hat Stiffened Plate made of any type of material

The capability of both these contributions to handle the typical boundary conditions and characteristic loads in a ship structure has been demonstrated through numerical investigations.

REFERENCES

1. **Adini, A. and Clough, R. W. (1960):** Analysis of Plate Bending by the Finite Element Method, Report submitted to the National Science Foundation, Washington D C.

2. **Bao, G., Jiang, W. and Roberts, J.C. (1997):** Analytical and Finite Element Solutions for Bending of Orthotropic Rectangular Plates, Int. J. Solids Structures, 14, pp. 1797 – 1822.

3. **Bathe, K. J. (2004):** Finite Element Procedures, Prentice Hall of India, New Delhi, pp. 207-209.

4. **Bathe, K. J. and Dvorkin, E. N. (1985):** Short Communication A Four Node Plate Bending Element based on Mindlin/Reissner Plate Theory and a mixed Interpolation, International Journal for Numerical Methods in Engineering, vol. 21, pp. 367-383.

5. **Bediar, O. K. (1997a):** The elastic behavior of multi-stiffened plates under uniform compression, Thin Walled Structures, vol. 27, pp. 311-335.

6. **Bediar, O.K. (1997b):** Analysis of stiffened plates under lateral loading using sequential quadratic programming (SQP), Computers & Structures, vol. 62, pp. 63-80.

7. **Bogner, F. K., Fox, R. L. and Schmit, L. A. Jr. (1965):** The Generation of Inter element Compatible Stffness and Mass Matrices by use of interpolation formulas, Proceedings of 1st conference on Matrix Method in Structural Mechanics, pp. 397-444.

8. **Chen, N. Z. and Soares, C. G. (2007):** Longitudinal Strength analysis of Ship Hulls of Composite Materials Under Sagging Moments, Composite Structures, 77, pp. 36-44.

9. **Clough, R. W. and Tocher, J. L. (1965):** Finite Element Stiffness Matrices for the Analysis of Plate Bending, Proceedings of 1st conference on Matrix Method in Structural Mechanics, pp. 515-545.

10. **Cook, R. D. and Shah, V. N. (1978):** A cost comparison of two static condensation Stress recovery algorithms, International Journal for Numerical Methods in Engineering, vol. 12, pp. 581-588.

11. **Crisfield, M. A.(1983):** A four-noded thin plate bending element using shear constraints – a modified version of Lyon's element, Computer Methods in Applied Mechanics and Engineering, 39, pp. 93–120.

12. **D'Arcangelo, A. M. (1969):** Ship Design and construction, SNAME , New York.

13. **Dubas, P. (1976):** Plated Structure with Closed Section Stiffeners, Proceedings of International conference on Steel Plated Structures, London, pp. 265-279.

14. **Dvorkin, E. N. and Bathe, K. J. (1984):** A continuum mechanics based four-node shell element for general nonlinear analysis, Engineering Computations, 1, 77–88.

15. **Elias, Z . M. (1968):** Duality in Finite Element Methods, Journal of Engineering Mechanics Division, ASCE vol. 94, (EM4), pp. 931-946.

16. **Fattaneh, M and Mohammad R. K. (2014):** Parametric study on average stress-average strain curve of composite stiffened plates using progressive failure method, Latin American Journal of Solids and Structures, vol.11, no. 12.

17. **Gallagher, C. (1975):** Finite Element Analysis: Fundamentals, Prentice Hall, Englewood Cliffs, New Jersy.

18. **Griffiths, D. V. (1994):** Stiffness Matrix of the four node quadrilateral element in closed form, International Journal for numerical methods in engineering, vol. 37, pp. 1027-1038.

19. **Hofmeyer, H. (2005a):** Cross-section crushing behavior of hat-sections (Part I: Numerical modeling, Thin Walled Structures, 43, pp. 1143-1154.

20. **Hofmeyer, H. (2005b):** Cross-section crushing behavior of hat-sectons (Part II: Analytical modeling, Thin Walled Structures, 43, pp. 1155-1165.

21. **Hrabok, M. M. and Hrudey, T. M. (1984):** A Review and Catalogue of Plate Bending Finite Elements, Computer and Structures, 19, pp. 479-495.

22. **Hughes, F. O. (1988):** Ship Structural Design, SNAME, New Jersy, p. 123.

23. **Hughes, T. J. R., Taylor, R. and Kanolkulchai, W. (1977):** A simple and efficient finite element for plate bending, International Journal for numerical methods in engineering, 11, pp. 1529–1543.

24. **IACS (2006a):** Common Structural Rules for Double Hull Oil Tankers, International Association of Classification Societies, London.

25. **IACS (2006b):** Common Structural Rules for Bulk Carriers, International Association of Classification Societies, London.

26. **Ibrahimbegovic, A. and Wilson, E. L. (1991):** A Unified formulation for triangular and quadrilateral Flat shell finite elements with six nodal dof, Communications in Applied Numerical Methods, vol. 7, pp. 1-9.

27. **Irons, B. M. and Draper, K. J. (1965):** Inadequacy of nodal connections in a stiffness solution by Plate Bending, American Institute of Aeronautics and Astronautics Journal, vol. 3(5), p. 961.

28. **ISO 18072-1 (2007):** Ships and Marine Technology – Ship Structures – Part 1: General Requirements for Their Ultimate Limit State Assessment, International Organization for Standardization, Geneva.

29. **Jia, J. and Ulfvarson, A. (2005):** Structural Behavior of a High Tensile Steel Deck Using Trapezoidal Stiffeners and Dynamics of Vehicle – Deck Interactions, Marine Structures, 18, pp. 1-24.

30. **Jiang, W., Bao, G. and Roberts, J. C.(1997):** Finite Element Modeling of Stiffened and Unstiffened Orthotropic Plates, Computers and Structures, vol. 63, pp. 105-117.

31. **Kawai, T. (1973):** The Application of Finite Element Methods to Ship Structures, Computers and Structures, 3, pp. 1175-1194.

32. **Ko, W. L. and Jackson, R. H. (1991):** Compressive Buckling Analysis of Hat Stiffened Panel, NASA Technical Memorandum 4310. Edwards, CA, USA.

33. **Kratzig, W. B. and Zhang, J. W. (1994):** A simple four noded quadrilateral finite element for plates, Journal of Computational and Applied Mathematics, 50, pp. 361-373.

34. **Kumar, S. M., Alagusundramoorthy, P. and Sundaravadivelu, R. (2004):** Stability of Stiffened Plates Under Axial Compression, Proceedings of ASCE Conference on Civil Engineering in the Oceans VI, Baltimore, USA., pp. 319-328.

35. **MacNeal, R. H. (1978):** A simple quadrilateral shell element, Computers & Structures, 8, 175–183.

36. **MacNeal, R. H. (1982):** Derivation of stiffness matrices by assumed strain distributions, Nuclear Engineering and Design, 70, 3–12.

37. **Melosh, R. J. (1961):** A Stiffness Matrix for the Analysis of Thin Plates in Bending, Journal of the Aeronautical Sciences, vol. 28(1), pp. 34-42.

38. **Mittelstedt, C. and Schroder, K. U. (2010):** Local post buckling of hat-stringer-stiffened composite laminated plates under transverse compression, Composite Structures, vol. 92, pp. 2830-2844.

39. **Morley, L. S. D. (1967):** A Triangular Equilibrium Element With Linearly Varying Bending Moments for Plate Bending Problems, The Aeronautical Journal, Royal Aeronautical Society vol. 71, pp. 715-719.

40. **Morley, L. S. D. (1968):** The Triangular Equilibrium Element in the Solution of Plate Bending Problems, The Aeronautical Quarterly, vol. 19, pp. 149-169.

41. **Paik, J. K. and Seo, J. K. (2009a):** Nonlinear Finite Element Method Models for Ultimate Strength Analysis of Steel Stiffened Plate Structures under Combined Biaxial

Compression and Lateral Pressure Actions - Part I: plate elements, Thin Walled Structures, 47, pp. 1008-1017.

42. **Paik, J. K. and Seo, J. K. (2009b):** Nonlinear Finite Element Method Models for Ultimate Strength Analysis of Steel Stiffened Plate Structures under Combined Biaxial Compression and Lateral Pressure Actions - Part II: stiffened panels, Thin Walled Structures, 47, pp. 998-1007.

43. **Paik, J. K., Kim, B. J. and Seo, J. K. (2008a):** Methods for Ultimate Limit State Assessment of Ships and Ship Shaped Offshore Structures: Part I: unstiffened Plates, Ocean Engineering, 35, pp. 261-270.

44. **Paik, J. K., Kim, B. J. and Seo, J. K. (2008b):** Methods for Ultimate Limit State Assessment of Ships and Ship Shaped Offshore Structures: Part II: stiffened Panels, Ocean Engineering, 35, pp. 271-280.

45. **Paik, J. K., Kim, B. J. and Seo, J. K. (2008c):** Methods for Ultimate Limit State Assessment of Ships and Ship Shaped Offshore Structures: Part III: hull girders, Ocean Engineering, 35, pp. 281-286.

46. **Paik, J. K., Thayamballi, A. K. and Kim, B. J. (2001):** Large Deflection orthotropic plate approach to develop ultimate strength formulations for stiffened panels under combined biaxial compression tension and lateral pressure, Thin Walled Structures, 39, pp. 215-246.

47. **Paik, J. K.and Thayamballi, A. K. (2003):** An experimental investigation on the dynamic ultimate compressive strength of ship plating, International Journal of Impact Engineering, 28, pp. 803-811.

48. **Park, K. C. and Stanley, G. M. (1986):** A Curved C0 shell element based on assumed natural-coordinate strains, Journal of Applied Mechanics, 108, pp. 278–286.

49. **Prusty, B. G. and Ray, C. (2004):** Free vibration analysis of composite Hat Stiffened panels by method of finite elements, Journal of Reinforced Plastics and Composites, vol. 23, pp. 533-547.

50. **Prusty, B. G. (2003):** Linear Static Analysis of Composite Hat Stiffened Laminated Shells Using Finite Elements, Finite Elements in Analysis and Design, 39, pp.1125-1138.

51. **Prusty, B. G. (2008):** Free Vibration and Buckling Response of Hat Stiffened Composite Panels under General Loading, International journal of Mechanical Sciences, 50, pp. 1326-1333.

52. **Prusty, B. G. and Satsangi, S. K. (2001):** Analysis of stiffened Shell for ships and ocean structures by finite element method, Ocean Engineering, 28, pp. 621-638.

53. **Przemieniecki, J. S. (1968):** Theory of Matrix Structural Analysis, New York: McGraw-Hill, pp. 96-121.

54. **Pu, Y., Das P. K. and Faulkner D. (1997):** Ultimate Compression Strength and Probabilistic Analysis of Stiffened Plates, Journal of Offshore Mechanics and Arctic Engineering, vol. 119, pp. 270-275.

55. **Pugh, E. D., Hinton, E. and Zienkiewicz, O. C. (1978):** A study of quadrilateral plate bending elements with reduced integration, International Journal for numerical methods in engineering, 12, 1059–1078.

56. **Rajagopalan, K. and Chettiar, C. G. (1984):** The Usefulness of Static Condensation in the Finite Element analysis of stiffened submersible cylindrical hulls, Computers and Structures, vol. 18, no. 4, pp. 733-738.

57. **Roberts, J. C., Bao G. and White, G. J.(1999):** Experimental, numerical and analytical results for bending and buckling of rectangular orthotropic plates, Composite Structures, 43, pp. 289-299.

58. **Satish Kumar, Y. V. and Mukopadhyay, M. (2000):** Finite Element Analysis of Ship Structures Using a new stiffened plate element, Applied Ocean research, 22, pp. 361-374.

59. **Schade, H. A. (1951):** The effective breadth of stiffened plating under bending loads, Trans. SNAME, 59.

60. **Schade H. A. (1953):** The effective breadth concept in ship design, Trans. SNAME, 61, pp. 410-430

61. **Stanley, G. M.(1985):** Continuum-based shell elements, Ph. D. Thesis, Department of Mechanical Engineering, Stanford University.

62. **Sun, H. H. and Soares, C. G. (2003):** An experimental study of ultimate torsional strength of a ship-type hull girder with a large deck opening, Marine Structures, 16, pp. 51-67.

63. **Tessler, A. and Hughes, T. J. R. (1985):** A three-node Mindlin plate element with improved transverse shear, Computer Methods in Applied Mechanics and Engineering, 50, 71–101.

64. **Timoshenko, S. P. and Woinowsky-Krieger, S. (1959):** Theory of plates and shells, McGraw-Hill, New York.

65. **Tocher, J. L. (1962):** Analysis of Plate Bending Using Triangular Elements, Ph.D. Thesis, Dept. of Civil Engineering, University of California, Berkley.

66. **Torbe, I. and Church, K. (1975):** A General Quadrilateral Plate Element, International Journal for Numerical Methods in Engineering, vol. 9, pp. 855-868, 1975.

67. **Troitsky M. S. (1976):** Stiffened Plates Bending, Stability and Vibrations, Elsevier Scientific Publishing Company, New York.

68. **Wang, X. and Rammerstorfer, F. G. (1996):** Determination of Effectve Breadth and Effective Width of stiffened plates by finite strip analyses, Thin Walled Structures, vol. 26, no. 4, pp. 261-286.

69. **Wilson, E. L. (1974):** The Static Condensation Algorithm, International Journal for Numerical Methods, 8, pp. 198-203.

70. **Yao, T. (2003):** Hull Girder Strength, Marine Structures, 16, pp. 1-13.

71. **Zhou, C. E. and Vecchio, F. J. (2006):** Closed form Stiffness Matrix for the four node quadrilateral Element with a fully populated Material Stiffness" Journal of Engineering Mechanics, ASCE, pp. 1392-1395.

72. **Zienckiewicz, C. (1977):** The Finite Element Method in Engineering Science, McGraw-Hill, New York.

APPENDIX – A

ORTHOTROPIC PLATE THEORY

The orthotropic plate approach has two simplifying assumptions viz., the stiffeners are uniformly spaced over the plate and the normal stresses in the stiffened plate are some average of plate stress and stiffener stress (Timoshenko, 1959). A thin orthotropic plate subjected to uniform lateral load is shown in Figure A1. The plate is perfectly elastic, continuous, homogeneous, obeys Hooke's law and its elastic properties in orthogonal directions x and y, differ.

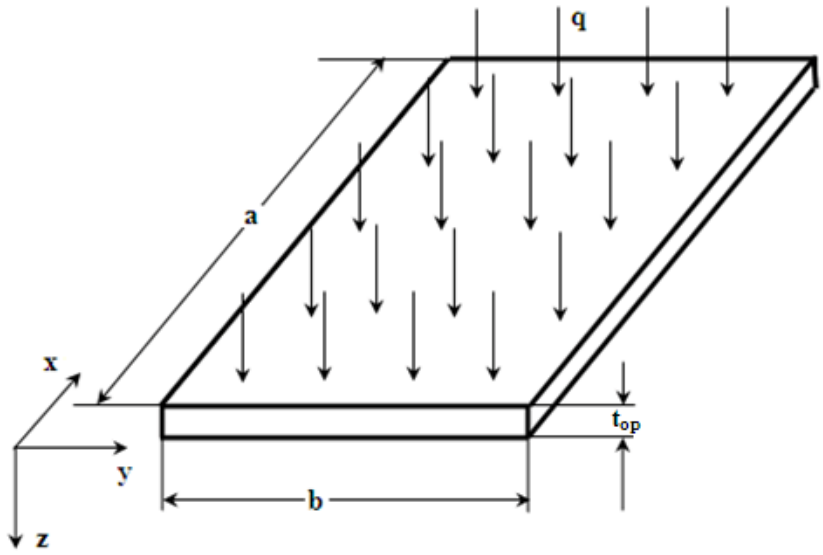

Figure A1. Orthotropic rectangular plate under uniform lateral load.

Based on the usual assumptions in the theory of bending of thin plates, the governing equation for displacement w of the plate in the z direction is available (Troitsky, 1976) as follows.

$$D_x \frac{\partial^4 w}{\partial x^4} + 2H \frac{\partial^4 w}{\partial x^2 \partial y^2} + D_y \frac{\partial^4 w}{\partial y^4} = q(x, y) \qquad \text{(A1)}$$

where,

$$D_x = \frac{E_x {t_{op}}^3}{12(1-\nu_x \nu_y)} \quad \text{(A2 a)}$$

$$D_y = \frac{E_y {t_{op}}^3}{12(1-\nu_x \nu_y)} \quad \text{(A2 b)}$$

The effective torsional rigidity is given by equation A3 as,

$$2H = D_x \nu_y + D_y \nu_x + 4D_{xy} \quad \text{(A3)}$$

where,

$$D_{xy} = \frac{G_{xy} {t_{op}}^3}{12} \quad \text{(A4)}$$

For the equivalent OPM, H and G_{xy} are given by the following expressions,

$$H = \sqrt{D_x D_y} \text{ and } G_{xy} = \frac{\sqrt{E_x E_y}}{2(1+\nu_{xy})} \quad \text{(A5)}$$

Following Betti's reciprocal theorem,

$$D_x.\nu_y = D_y.\nu_x \quad \text{(A6)}$$

$$D_x.\nu_z = D_z.\nu_x \quad \text{(A7)}$$

Besides,

$$\left.\begin{aligned} \nu_{xy} &= \sqrt{\nu_x \nu_y} \\ \nu_{xz} &= \sqrt{\nu_x \nu_z} \\ \nu_{yz} &= \sqrt{\nu_y \nu_z} \end{aligned}\right\} \quad \text{(A8)}$$

APPENDIX – B

ANALYTICAL SOLUTION FOR BENDING OF ORTHOTROPIC PLATE

Bao et al. (1997) has presented an analytical solution for bending of flat, rectangular, orthotropic thin plate shown in Figure A1. The material orthotropy has been characterized by two non-dimensional parameters, defined as

$$\lambda = \frac{D_y}{D_x} \quad \text{and} \quad \eta = \frac{H}{\sqrt{D_x D_y}} \tag{B1}$$

and the modified aspect ratio for the orthotropic plate as

$$R = \lambda^{1/4}\, a/b \tag{B2}$$

The exact solution for the maximum deflection of the plate with all edges simply supported under uniform lateral load has been given by

$$\frac{\Delta}{\Delta_0} = \frac{16.R^4}{\pi^6} \sum_{m=1,3,\ldots..}^{\infty} \sum_{n=1,3,\ldots.}^{\infty} \frac{(-1)^{(m+n+2)/2}}{D_{mn}}. \tag{B3}$$

where,

Δ_0 is a reference deflection, $\Delta_0 = \frac{qb^4}{D_y}$. (B4)

$$D_{mn} = m^4 + 2\eta(mnR)^2 + (nR)^4$$

The maximum in-plane stress σ_x occurs at the centre of the plate. For a plate with $-1 < \eta < 1$, the maximum in-plane stress σ_x has been given by

$$\frac{\sigma_x {t_{op}}^2}{qb^2} = \frac{3\nu_x}{4} + \frac{24}{\pi^3 \lambda \lambda_1 \lambda_2} \sum_{m=1,3,\ldots..}^{\infty} \frac{(-1)^{\frac{m-1}{2}}}{m^3 \phi_m} x$$

$$\left[\left(\sqrt{\lambda} - \nu_y \eta\right) \sinh \frac{m\pi\lambda_1 R}{2} \sin \frac{m\pi\lambda_2 R}{2} - 2\nu_y \lambda_1 \lambda_2 \cosh \frac{m\pi\lambda_1 R}{2} \cos \frac{m\pi\lambda_2 R}{2}\right] \tag{B5}$$

where,

$$\Phi_m = \cosh m\pi\lambda_1 R + \cos m\pi\lambda_2 R$$

$$\lambda_1 = \sqrt{\frac{1+\eta}{2}} \text{ and } \lambda_2 = \sqrt{\frac{1-\eta}{2}} \tag{B6}$$

and for plate with $\eta > 1$, the maximum in-plane stress σ_x has been given by

$$\frac{\sigma_x t_{op}^2}{qb^2} = \frac{3\nu_x}{4} + \frac{24}{\pi^3\lambda(\lambda_1^2 - \lambda_2^2)} \sum_{m=1,3,..}^{\infty} \frac{(-1)^{\frac{m-1}{2}}}{m^3} x \left[\frac{\lambda_2^2 (\nu_y - \lambda_1^2\sqrt{\lambda})}{\cosh \frac{m\pi\lambda_1 R}{2}} - \frac{\lambda_1^2 (\nu_y - \lambda_2^2\sqrt{\lambda})}{\cosh \frac{m\pi\lambda_2 R}{2}} \right] \tag{B7}$$

where,

$$\lambda_1 = \sqrt{\eta + \sqrt{\eta^2 - 1}} \quad \text{and} \quad \lambda_2 = \sqrt{\eta - \sqrt{\eta^2 - 1}} \tag{B8}$$

For a plate fixed along edges parallel to the y axis and simply supported along the other two edges, with $-1 < \eta < 1$, the maximum deflection and the in-plane stress σ_x at the centre have been given by

$$\frac{\Delta}{\Delta_0} = \frac{5}{384} - \frac{8}{\pi^5} \sum_{m=1,3...}^{\infty} \frac{(-1)^{\frac{(m-1)}{2}}}{m^5 \Psi_m} \quad x$$

$$\left[\lambda_1 \cosh \frac{m\pi\lambda_1 R}{2} \sin \frac{m\pi\lambda_2 R}{2} + \lambda_2 \sinh \frac{m\pi\lambda_2 R}{2} \cos \frac{m\pi\lambda_2 R}{2} \right] \tag{B9}$$

$$\frac{\sigma_x t_{op}^2}{qb^2} = \frac{3\nu_x}{4} - \frac{48}{\pi^3\lambda} \sum_{m=1,3..}^{\infty} \frac{(-1)^{\frac{(m-1)}{2}}}{m^3 \Psi_m} \quad x$$

$$\left[(\nu_y - \sqrt{\lambda})\lambda_1 \cosh \frac{m\pi\lambda_1 R}{2} \sin \frac{m\pi\lambda_2 R}{2} + (\nu_y + \sqrt{\lambda})\lambda_2 \sinh \frac{m\pi\lambda_1 R}{2} \cos \frac{m\pi\lambda_2 R}{2} \right] \tag{B10}$$

where,

$$\Psi_m = \lambda_2 \sinh m\pi\lambda_1 R + \lambda_1 \sinh m\pi\lambda_2 R$$

λ_1 and λ_2 have been given by Eq. (B6) and Δ_0 has been given by Eq. (B4).

For a plate with $1 < \eta < \infty$, the maximum deflection and the maximum in-plane stress σ_x at the centre of the orthotropic plate has been given by

$$\frac{\Delta}{\Delta_0} = \frac{5}{384} - \frac{4}{\pi^5}\sum_{m=1,3\ldots}^{\infty}\frac{(-1)^{(m-1)/2}}{m^5\zeta_m}\left[\lambda_1 \sinh\frac{m\pi\lambda_1 R}{2} - \lambda_2 \sinh\frac{m\pi\lambda_2 R}{2}\right] \quad \text{(B11)}$$

$$\frac{\sigma_x {t_{op}}^2}{qb^2} = \frac{3\nu_x}{4} + \frac{24}{\pi^3\lambda}\sum_{m=1,3..}^{\infty}\frac{(-1)^{\frac{m-1}{2}}}{m^3\zeta_m} \quad x$$

$$\left[(\nu_y - \lambda_1^2\sqrt{\lambda})\lambda_2 \sinh\frac{m\pi\lambda_2 R}{2} - (\nu_y - \lambda_2^2\sqrt{\lambda})\lambda_1 \sinh\frac{m\pi\lambda_1 R}{2}\right] \quad \text{(B12)}$$

where,

$$\zeta_m = \lambda_1 \sinh\frac{m\pi\lambda_1 R}{2}\cosh\frac{m\pi\lambda_2 R}{2} - \lambda_2 \cosh\frac{m\pi\lambda_1 R}{2}\sinh\frac{m\pi\lambda_2 R}{2}$$

λ_1 and λ_2 have been given by Eq. (B8) and $\Delta_0$has been given by Eq. (B4).

APPENDIX – C

EXPRESSIONS FOR STIFFNESS COEFFICIENTS

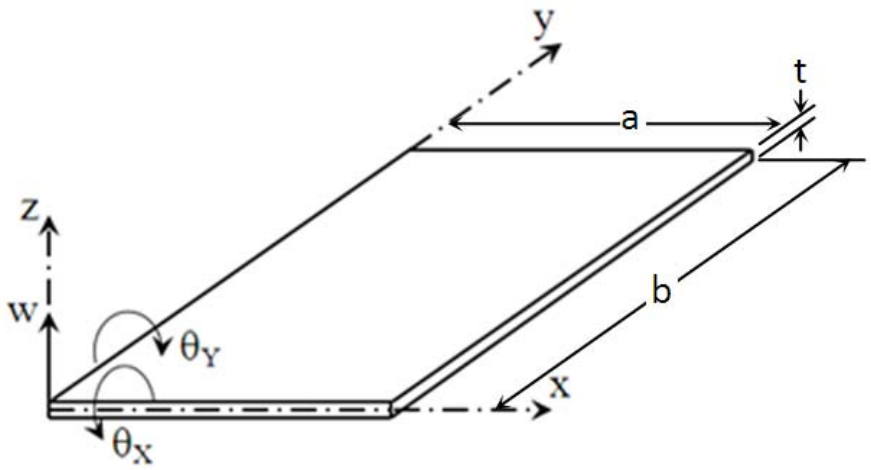

Figure C1 Geometry of rectangular plate bending element.

For a rectangular plate bending element shown in Figure C1, the expressions for the Stiffness Coefficients have been given below:

$$\beta = \frac{b}{a}$$

$$k_{11} = \left[4(\beta^2 + \beta^{-2}) + \frac{1}{5}(14 - 4\nu)\right] \text{ x } \frac{Et^3}{12(1-\nu^2)ab}$$

$$k_{21} = \left[2\beta^{-2} + \frac{1}{5}(1 + 4\nu)\right] b \text{ x } \frac{Et^3}{12(1-\nu^2)ab}$$

$$k_{22} = \left[\frac{4}{3}\beta^{-2} + \frac{1}{5}(1 - \nu)\right] b^{-2} \text{ x } \frac{Et^3}{12(1-\nu^2)ab}$$

$$k_{31} = -\left[2\beta^{-2} + \frac{1}{5}(1 + 4\nu)\right] a \text{ x} \frac{Et^3}{12(1-\nu^2)ab}$$

$$k_{32} = -\nu ab \text{ x } \frac{Et^3}{12(1-\nu^2)ab}$$

$$k_{33} = \left[\frac{4}{3}\beta^2 + \frac{4}{15}(1 - \nu)a^2\right] \text{x } \frac{Et^3}{12(1-\nu^2)ab}$$

$$k_{41} = \left[2(\beta^2 - 2\beta^{-2}) - \frac{1}{5}(14 - 4\nu)\right] \text{x } \frac{Et^3}{12(1-\nu^2)ab}$$

$$k_{42} = -\left[2\beta^{-2} + \frac{1}{5}(1 - \nu)\right] \text{b x } \frac{Et^3}{12(1-\nu^2)ab}$$

$$k_{43} = \left[-\beta^2 + \frac{1}{5}(1 + 4\nu)\right] a \text{ x } \frac{Et^3}{12(1-\nu^2)ab}$$

$$k_{44} = \left[4(\beta^2 + \beta^{-2}) + \frac{1}{5}(14 - 4\nu)\right] \text{x } \frac{Et^3}{12(1-\nu^2)ab}$$

$$k_{51} = \left[2\beta^{-2} + \frac{1}{5}(1 - \nu)\right] \text{bx } \frac{Et^3}{12(1-\nu^2)ab}$$

$$k_{52} = \left[\frac{2}{3}\beta^{-2} - \frac{1}{15}(1 - \nu)\right] b^{-2} \text{ x } \frac{Et^3}{12(1-\nu^2)ab}$$

$$k_{53} = 0$$

$$k_{54} = -\left[2\beta^{-2} + \frac{1}{5}(1 + 4\nu)\right] b \text{ x } \frac{Et^3}{12(1-\nu^2)ab}$$

$$k_{55} = \left[\frac{4}{3}\beta^{-2} + \frac{4}{15}(1 - \nu)b^2\right] \text{x } \frac{Et^3}{12(1-\nu^2)ab}$$

$$k_{61} = \left[-\beta^2 + \frac{1}{5}(1 + 4\nu)\right] a \text{ x} \frac{Et^3}{12(1-\nu^2)ab}$$

$$k_{62} = 0$$

$$k_{63} = \left[\frac{2}{3}\beta^2 - \frac{4}{15}(1 - \nu)\right] a^2 \text{ x } \frac{Et^3}{12(1-\nu^2)ab}$$

$$k_{64} = -\left[2\beta^2 + \frac{1}{5}(1 + 4\nu)\right] a \text{ x } \frac{Et^3}{12(1-\nu^2)ab}$$

$$k_{65} = \nu ab \text{ x } \frac{Et^3}{12(1-\nu^2)ab}$$

$$k_{66} = \left[\frac{4}{3}\beta^2 + \frac{4}{15}(1 - \nu)a^2\right] \text{x } \frac{Et^3}{12(1-\nu^2)ab}$$

$$k_{71} = \left[-2(\beta^2 - 2\beta^{-2}) + \frac{1}{5}(14 - 4\nu)\right] \text{x } \frac{Et^3}{12(1-\nu^2)ab}$$

$$k_{72} = \left[-\beta^{-2} + \frac{1}{5}(1 - \nu)\right] \text{bx } \frac{Et^3}{12(1-\nu^2)ab}$$

$$k_{73} = \left[\beta^2 - \frac{1}{5}(1 - \nu)\right] a \text{ x} \frac{Et^3}{12(1-\nu^2)ab}$$

$$k_{74} = \left[2(2\beta^2 - \beta^{-2}) - \frac{1}{5}(14 - 4\nu)\right] \text{x } \frac{Et^3}{12(1-\nu^2)ab}$$

$$k_{75} = \left[-\beta^2 + \frac{1}{5}(1+4\nu)\right] b \text{ x } \frac{Et^3}{12(1-\nu^2)ab}$$

$$k_{76} = \left[2\beta^2 + \frac{1}{5}(1-\nu)\right] a \text{ x} \frac{Et^3}{12(1-\nu^2)ab}$$

$$k_{77} = \left[4(\beta^2 + \beta^{-2}) + \frac{1}{5}(14-4\nu)\right] \text{x } \frac{Et^3}{12(1-\nu^2)ab}$$

$$k_{81} = \left[\beta^{-2} - \frac{1}{5}(1-\nu)\right] bx \frac{Et^3}{12(1-\nu^2)ab}$$

$$k_{82} = \left[\frac{1}{3}\beta^{-2} + \frac{1}{15}(1-\nu)\right] b^2 \text{ x } \frac{Et^3}{12(1-\nu^2)ab}$$

$$k_{83} = 0$$

$$k_{84} = \left[-\beta^2 + \frac{1}{5}(1+4\nu)\right] b \text{ x } \frac{Et^3}{12(1-\nu^2)ab}$$

$$k_{85} = \left[\frac{2}{3}\beta^{-2} - \frac{4}{15}(1-\nu)\right] b^2 \text{ x } \frac{Et^3}{12(1-\nu^2)ab}$$

$$k_{86} = 0$$

$$k_{87} = -\left[2\beta^{-2} + \frac{1}{5}(1+4\nu)\right] b \text{ x } \frac{Et^3}{12(1-\nu^2)ab}$$

$$k_{88} = \left[\frac{4}{3}\beta^{-2} + \frac{4}{15}(1-\nu)\right] b^2 \text{ x } \frac{Et^3}{12(1-\nu^2)ab}$$

$$k_{91} = \left[-\beta^2 + \frac{1}{5}(1-\nu)\right] a \text{ x } \frac{Et^3}{12(1-\nu^2)ab}$$

$$k_{92} = 0$$

$$k_{93} = \left[\frac{1}{3}\beta^{-2} + \frac{1}{15}(1-\nu)\right] a^2 \text{ x } \frac{Et^3}{12(1-\nu^2)ab}$$

$$k_{94} = -\left[2\beta^2 + \frac{1}{5}(1-\nu)\right] a \text{ x } \frac{Et^3}{12(1-\nu^2)ab}$$

$$k_{95} = 0$$

$$k_{96} = \left[\frac{2}{3}\beta^2 - \frac{1}{15}(1-\nu)\right] a^2 \text{ x } \frac{Et^3}{12(1-\nu^2)ab}$$

$$k_{9\,7} = \left[2\beta^2 + \frac{1}{5}(1+4\nu)\right] a \times \frac{Et^3}{12(1-\nu^2)ab}$$

$$k_{9\,8} = -\nu ab \times \frac{Et^3}{12(1-\nu^2)ab}$$

$$k_{9\,9} = \left[\frac{4}{3}\beta^2 + \frac{4}{15}(1-\nu)\right] a^2 \times \frac{Et^3}{12(1-\nu^2)ab}$$

$$k_{10\,1} = \left[-2(2\beta^2 - \beta^{-2}) - \frac{1}{5}(14-4\nu)\right] \times \frac{Et^3}{12(1-\nu^2)ab}$$

$$k_{10\,2} = \left[\beta^{-2} - \frac{1}{5}(1+4\nu)\right] b \times \frac{Et^3}{12(1-\nu^2)ab}$$

$$k_{10\,3} = \left[2\beta^2 + \frac{1}{5}(1-\nu)\right] a \times \frac{Et^3}{12(1-\nu^2)ab}$$

$$k_{10\,4} = \left[2(\beta^2 + \beta^{-2}) + \frac{1}{5}(14-4\nu)\right] \times \frac{Et^3}{12(1-\nu^2)ab}$$

$$k_{10\,5} = \left[\beta^2 - \frac{1}{5}(1-\nu)\right] b \times \frac{Et^3}{12(1-\nu^2)ab}$$

$$k_{10\,6} = \left[\beta^2 - \frac{1}{5}(1-\nu)\right] a \times \frac{Et^3}{12(1-\nu^2)ab}$$

$$k_{10\,7} = \left[2(\beta^2 - 2\beta^{-2}) - \frac{1}{5}(14-4\nu)\right] \times \frac{Et^3}{12(1-\nu^2)ab}$$

$$k_{10\,8} = \left[2\beta^{-2} + \frac{1}{5}(1-\nu)\right] b \times \frac{Et^3}{12(1-\nu^2)ab}$$

$$k_{10\,9} = \left[\beta^2 - \frac{1}{5}(1-\nu)\right] a \times \frac{Et^3}{12(1-\nu^2)ab}$$

$$k_{10\,10} = \left[4(\beta^2 + \beta^{-2}) + \frac{1}{5}(14-4\nu)\right] \times \frac{Et^3}{12(1-\nu^2)ab}$$

$$k_{11\,1} = \left[\beta^{-2} - \frac{1}{5}(1+4\nu)\right] b \times \frac{Et^3}{12(1-\nu^2)ab}$$

$$k_{11\,2} = \left[\frac{2}{3}\beta^{-2} - \frac{4}{15}(1-\nu)\right] b^2 \times \frac{Et^3}{12(1-\nu^2)ab}$$

$$k_{11\,3} = 0$$

$$k_{11\,4} = \left[-\beta^2 - \frac{1}{5}(1-\nu)\right] a \times \frac{Et^3}{12(1-\nu^2)ab}$$

$$k_{11\,5} = \left[\frac{1}{3}\beta^{-2} + \frac{1}{15}(1-\nu)\right] b^2 \times \frac{Et^3}{12(1-\nu^2)ab}$$

$$k_{11\,6} = 0$$

$$k_{11\,7} = -\left[2\beta^{-2} + \frac{1}{5}(1-\nu)\right] b \times \frac{Et^3}{12(1-\nu^2)ab}$$

$$k_{11\,8} = \left[\frac{2}{3}\beta^{-2} - \frac{1}{15}(1-\nu)\right] b^2 \times \frac{Et^3}{12(1-\nu^2)ab}$$

$$k_{11\,9} = 0$$

$$k_{11\,10} = \left[2\beta^{-2} + \frac{1}{5}(1+4\nu)\right] b \times \frac{Et^3}{12(1-\nu^2)ab}$$

$$k_{11\,11} = \left[\frac{4}{3}\beta^{-2} + \frac{4}{15}(1-\nu)\right] b^2 \times \frac{Et^3}{12(1-\nu^2)ab}$$

$$k_{12\,1} = -\left[2\beta^2 + \frac{1}{5}(1-\nu)\right] a \times \frac{Et^3}{12(1-\nu^2)ab}$$

$$k_{12\,2} = 0$$

$$k_{12\,3} = \left[\frac{2}{3}\beta^2 - \frac{1}{15}(1-\nu)\right] a^2 \times \frac{Et^3}{12(1-\nu^2)ab}$$

$$k_{12\,4} = \left[-\beta^2 + \frac{1}{5}(1-\nu)\right] a \times \frac{Et^3}{12(1-\nu^2)ab}$$

$$k_{12\,5} = 0$$

$$k_{12\,6} = \left[\frac{1}{3}\beta^2 + \frac{1}{15}(1-\nu)\right] a^2 \times \frac{Et^3}{12(1-\nu^2)ab}$$

$$k_{12\,7} = \left[\beta^2 - \frac{1}{5}(1+4\nu)\right] a \times \frac{Et^3}{12(1-\nu^2)ab}$$

$$k_{12\,8} = 0$$

$$k_{12\,9} = \left[\frac{2}{3}\beta^2 - \frac{4}{15}(1-\nu)\right] a^2 \times \frac{Et^3}{12(1-\nu^2)ab}$$

$$k_{12\,10} = \left[2\beta^{-2} + \frac{1}{5}(1+4\nu)\right] a \text{ x } \frac{Et^3}{12(1-\nu^2)ab}$$

$$k_{12\,11} = \nu ab \text{ x } \frac{Et^3}{12(1-\nu^2)ab}$$

$$k_{12\,12} = \left[\frac{4}{3}\beta^2 + \frac{4}{15}(1-\nu)\right] a^2 \text{ x } \frac{Et^3}{12(1-\nu^2)ab}$$

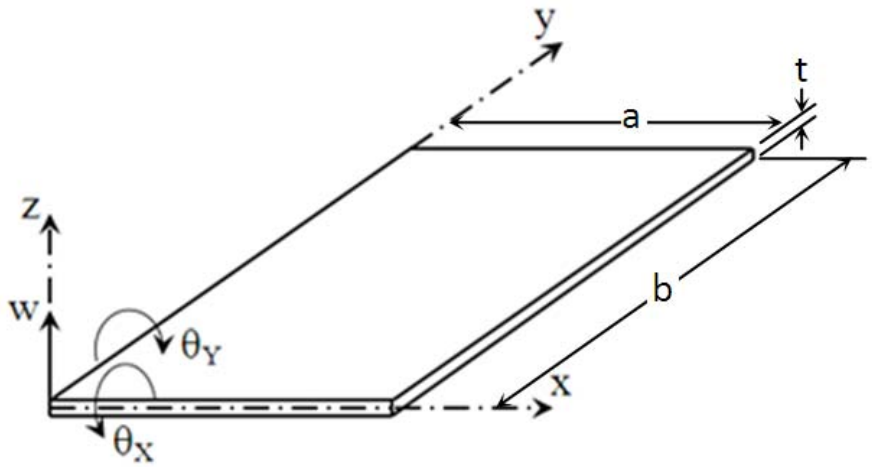

Figure C2 Geometry of rectangular plane stress element.

For a rectangular plane stress element shown in Figure C2, the expressions for the Stiffness Coefficient have been given below:

$$\beta = \frac{b}{a}$$

$$k_{11} = \left[(4-\nu^2)\beta + \frac{3}{2}(1-\nu)\right] \text{ x } \frac{Et}{12(1-\nu^2)}$$

$$k_{21} = \left[\frac{3}{2}(1+\nu)\right] \text{ x } \frac{Et}{12(1-\nu^2)}$$

$$k_{22} = \left[(4-\nu^2)\beta^{-1} + \frac{3}{2}(1-\nu)\beta\right] \text{ x } \frac{Et}{12(1-\nu^2)}$$

$$k_{31} = \left[(2+\nu^2)\beta - \frac{3}{2}(1-\nu)\beta^{-1}\right] \text{ x } \frac{Et}{12(1-\nu^2)}$$

$$k_{32} = \left[-\frac{3}{2}(1-3\nu)\right] \text{ x } \frac{Et^3}{12(1-\nu^2)ab}$$

$$k_{33} = \left[(4-\nu^2)\beta + \frac{3}{2}(1-\nu)\beta^{-1}\right] \text{x } \frac{Et}{12(1-\nu^2)}$$

$$k_{41} = \left[\frac{3}{2}(1-3\nu)\right] x \frac{Et}{12(1-\nu^2)}$$

$$k_{42} = \left[-(4-\nu^2)\beta^{-1} + \frac{3}{2}(1-\nu)\beta\right] x \frac{Et}{12(1-\nu^2)}$$

$$k_{43} = \left[-\frac{3}{2}(1+\nu)\right] x \frac{Et}{12(1-\nu^2)}$$

$$k_{44} = \left[(4-\nu^2)\beta^{-1} + \frac{3}{2}(1-\nu)\beta\right] x \frac{Et}{12(1-\nu^2)}$$

$$k_{51} = \left[-(2+\nu^2)\beta - \frac{3}{2}(1-\nu)\beta^{-1}\right] x \frac{Et}{12(1-\nu^2)}$$

$$k_{52} = \left[-\frac{3}{2}(1+\nu)\right] x \frac{Et}{12(1-\nu^2)}$$

$$k_{53} = \left[-(4-\nu^2)\beta + \frac{3}{2}(1-\nu)\beta^{-1}\right] x \frac{Et}{12(1-\nu^2)}$$

$$k_{54} = \left[-\frac{3}{2}(1-3\nu)\right] x \frac{Et}{12(1-\nu^2)}$$

$$k_{55} = \left[(4-\nu^2)\beta + \frac{3}{2}(1-\nu)\beta^{-1}\right] x \frac{Et}{12(1-\nu^2)}$$

$$k_{61} = \left[-\frac{3}{2}(1+\nu)\right] x \frac{Et}{12(1-\nu^2)}$$

$$k_{62} = \left[-(2+\nu^2)\beta^{-1} - \frac{3}{2}(1-\nu)\beta\right] x \frac{Et}{12(1-\nu^2)}$$

$$k_{63} = \left[\frac{3}{2}(1-3\nu)\right] x \frac{Et}{12(1-\nu^2)}$$

$$k_{64} = \left[(2+\nu^2)\beta^{-1} - \frac{3}{2}(1-\nu)\beta\right] x \frac{Et}{12(1-\nu^2)}$$

$$k_{65} = \left[\frac{3}{2}(1+\nu)\right] x \frac{Et}{12(1-\nu^2)}$$

$$k_{66} = \left[(4-\nu^2)\beta^{-1} + \frac{3}{2}(1-\nu)\beta\right] x \frac{Et}{12(1-\nu^2)}$$

$$k_{71} = \left[-(4-\nu^2)\beta + \frac{3}{2}(1-\nu)\beta^{-1}\right] x \frac{Et}{12(1-\nu^2)}$$

$$k_{72} = \left[\frac{3}{2}(1-3\nu)\right] x \frac{Et}{12(1-\nu^2)}$$

$$k_{73} = \left[-(2+\nu^2)\beta - \frac{3}{2}(1-\nu)\beta^{-1}\right] x \frac{Et}{12(1-\nu^2)}$$

$$k_{74} = \left[\frac{3}{2}(1+\nu)\right] x \frac{Et}{12(1-\nu^2)}$$

$$k_{75} = \left[(2+\nu^2)\beta - \frac{3}{2}(1-\nu)\beta^{-1}\right] x \frac{Et}{12(1-\nu^2)}$$

$$k_{76} = \left[-\frac{3}{2}(1-3\nu)\right] x \frac{Et}{12(1-\nu^2)}$$

$$k_{77} = \left[(4-\nu^2)\beta + \frac{3}{2}(1-\nu)\beta^{-1}\right] x \frac{Et}{12(1-\nu^2)}$$

$$k_{81} = \left[-\frac{3}{2}(1-3\nu)\right] x \frac{Et}{12(1-\nu^2)}$$

$$k_{82} = \left[(2+\nu^2)\beta^{-1} - \frac{3}{2}(1-\nu)\beta\right] x \frac{Et}{12(1-\nu^2)}$$

$$k_{83} = \left[\frac{3}{2}(1+\nu)\right] x \frac{Et}{12(1-\nu^2)}$$

$$k_{84} = \left[-(2+\nu^2)\beta^{-1} - \frac{3}{2}(1-\nu)\beta\right] x \frac{Et}{12(1-\nu^2)}$$

$$k_{85} = \left[\frac{3}{2}(1-3\nu)\right] x \frac{Et}{12(1-\nu^2)}$$

$$k_{86} = \left[-(4-\nu^2)\beta^{-1} + \frac{3}{2}(1-\nu)\beta\right] x \frac{Et}{12(1-\nu^2)}$$

$$k_{87} = \left[-\frac{3}{2}(1+\nu)\right] x \frac{Et}{12(1-\nu^2)}$$

$$k_{88} = \left[(4-\nu^2)\beta^{-1} + \frac{3}{2}(1-\nu)\beta\right] x \frac{Et}{12(1-\nu^2)}$$

APPENDIX – D

CALCULATION OF WEIGHT RATIO AND SECTION MODULUS

Section Modulus of HSP:

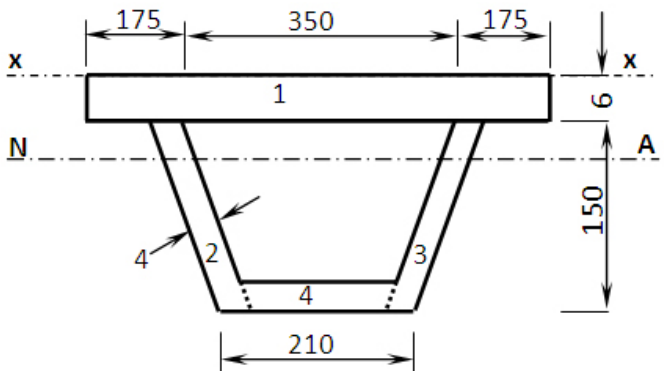

Figure D1 Geometry of one hat stiffener and attached plate. Two such units constitute RUC of HSP

Area No:	Area	Distance to centroid from xx d1	First Moment q = A x d1	Height h	M.I. about local centroid $I_C = Ax\ h^2/2$	Distance to local centroid from NA d2	M.I. about NA $I = Ic+Axd2^2$
	cm^2	cm	cm^3	cm	cm^4	cm	cm^4
1	42	0.3	12.6	0.6	1.26	3.61	548.61
2	6.6	8.1	53.46	15	123.75	4.20	240.17
3	6.6	8.1	53.46	15	123.75	4.20	240.17
4	8.4	15.4	129.36	0.4	0.112	11.49	1109.08
Area	63.6	First Moment	248.88		Total Moment of Inertia		2138.03

Distance to NA from xx	3.91 cm
Farthest distance from Neutral Axis	11.69 cm
Section modulus of one stiffener and attached plate	182.89 cm^3
Section modulus of complete RUC of hat stiffend plate	**365.78 cm^3**
Area of one stiffener and attached plate	63.6 cm^2
Total Cross sectional Area of HSP	**127.2 cm^2**

Section Modulus plate stiffened with bar stiffener:

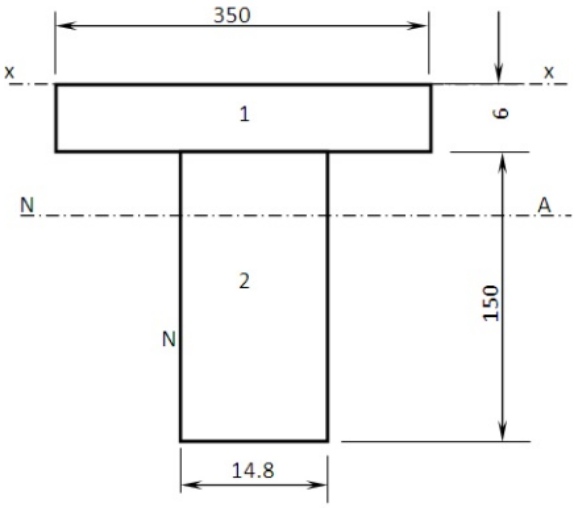

Figure D2 Geometry of one bar stiffener and attached plate. Four such units constitute RUC of plate stiffened with bar stiffener

Area No:	Area	Distance to centroid from xx d1	First Moment q = A x d1	Height h	M.I. about local centroid $I_C = Ax\,h^2/2$	Distance to local centroid from NA d2	M.I. about NA $I = Ic+Axd2^2$
	cm^2	cm	cm^3	cm	cm^4	cm	cm^4
1	21	0.3	6.3	0.6	0.63	4.01	338.31
2	22.2	8.1	179.82	15	416.25	3.79	735.13
Area	43.2	First Moment	186.12		Total Moment of Inertia		1073.44

Distance to NA from xx	4.31 cm
Farthest distance from Neutral Axis	11.29 cm
Section modulus of one stiffener and attached plate	95.07 cm^3
Section modulus of complete RUC of plate stiffened with bar	**380.28 cm^3**
Area of one stiffener and attached plate	43.2 cm^2
Total Cross sectional Area of plate stiffened with bar	**172.8 cm^2**

Section Modulus plate stiffened with angle stiffener:

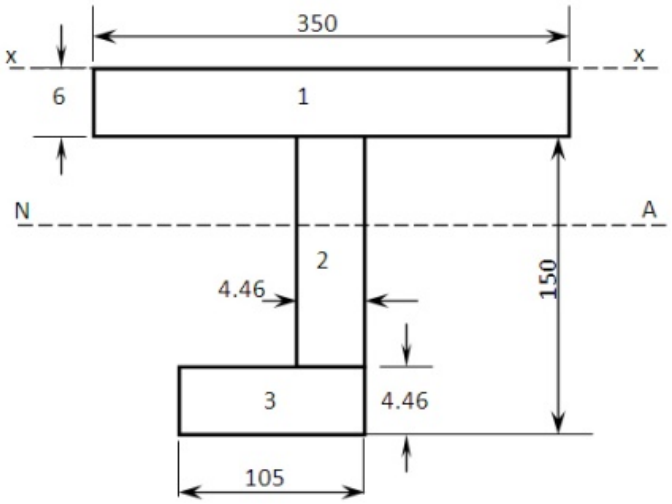

Figure D3 Geometry of one angle stiffener and attached plate. Four such units constitute RUC of plate stiffened with angle stiffener

Area No:	Area	Distance to centroid from xx d1	First Moment q = A x d1	Height h	M.I. about local centroid $I_C = Ax\ h^2/2$	Distance to local centroid from NA d2	M.I. about NA $I = Ic+Axd2^2$
	cm^2	cm	cm^3	cm	cm^4	cm	cm^4
1	21	0.3	6.3	0.6	0.63	3.72	291.24
2	6.49	7.877	51.129	14.55	114.57	3.86	211.13
3	4.68	15.377	72.01	0.446	0.0776	11.360	604.09
Area	32.17	First Moment	129.44	Total Moment of Inertia			1106.46

Distance to NA from xx	4.02 cm
Farthest distance from Neutral Axis	11.58 cm
Section modulus of one stiffener and attached plate	95.54 cm^3
Section modulus of complete RUC of plate stiffened with angle	**382.2 cm^3**
Area of one stiffener and attached plate	32.17 cm^2
Total Cross sectional Area of plate stiffened with angle	**128.68 cm^2**

Section Modulus plate stiffened with Tee stiffener:

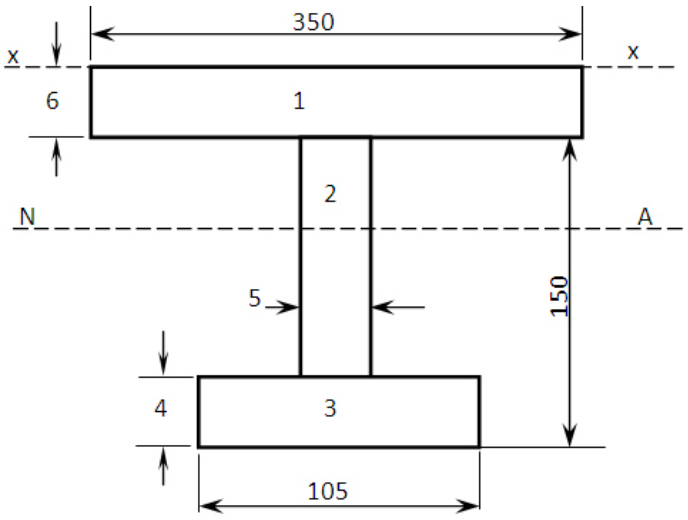

Figure D4 Geometry of one Tee stiffener and attached plate. Four such units constitute RUC of plate stiffened with Tee stiffener

Area No:	Area	Distance to centroid from xx d1	First Moment q = A x d1	Height h	M.I. about local centroid $I_c = Ax\ h^2/2$	Distance to local centroid from NA d2	M.I. about NA $I = Ic+Axd2^2$
	cm^2	cm	cm^3	cm	cm^4	cm	cm^4
1	21	0.3	6.3	0.6	0.63	3.66	281.94
2	7.3	7.9	57.67	14.6	129.67	3.94	242.99
3	4.2	15.4	64.68	0.4	0.056	11.44	549.725
Area	32.5	First Moment	128.65		Total Moment of Inertia		1074.65

Distance to NA from xx	3.96
Farthest distance from Neutral Axis	11.64 cm
Section modulus of one stiffener and attached plate	92.32 cm^3
Section modulus of complete RUC of plate stiffened with Tee	**369.28 cm^3**
Area of one stiffener and attached plate	32.5 cm^2
Total Cross sectional Area of plate stiffened with Tee	**130 cm^2**

Weight Ratio Calculation:

$$\text{Weight Ratio} = \frac{\text{Weight of Stiffened Plate}}{\text{Weight of HSP}}$$

Weight of stiffened plate = Cross sectional area of stiffened plate x length x material density

Length and Material Density is the same for all four types of stiffened plates

$$\text{Weight ratio} = \frac{\text{Cross sectional area of stiffened plate}}{\text{Cross sectional area of HSP}}$$

Sl No	Type of Stiffener	Total Cross sectional Area A (cm^2)	Weight Ratio A/A_{HSP}
1	HSP	127.2	1
2	Flat Bar	172.8	1.36
3	Angle Bar	128.68	1.01
4	Tee Bar	130	1.02

APPENDIX – E

CALCULATION OF STRESS FROM THE LOAD VECTOR

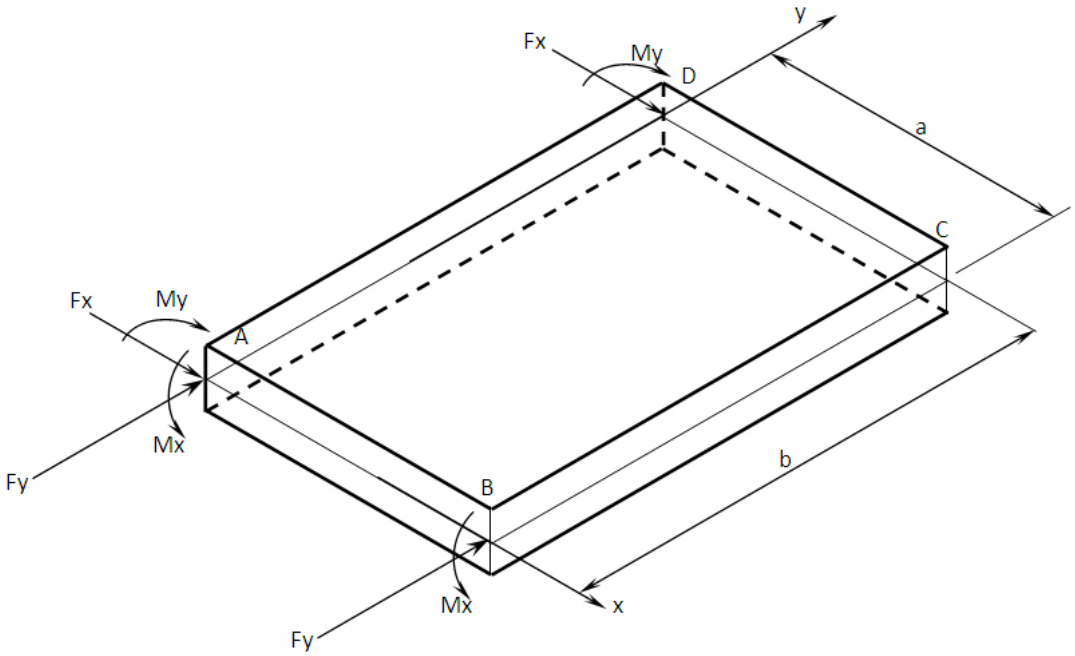

Figure E1 Rectangular Element with load vectors

Total moment on face AB = 2Mx

Section Modulus of face AB = $\frac{at^2}{6}$

On face AB, stress in the y direction on top layer due to BM = $\sigma_y = \frac{2M_x}{\frac{at^2}{6}} = + \frac{12M_x}{at^2}$

On face AB, stress in y direction on the bottom layer due to BM $\sigma_y = - \frac{12M_x}{at^2}$

On face AB total force in y direction = 2Fy

Stress in y direction on face AB due to force in y direction $\sigma_y = -\frac{2F_y}{at}$

Total stress in the y direction on face AB, top layer $\sigma_y = + \frac{12M_x}{at^2} - \frac{2F_y}{at}$

Total stress in the y direction on face AB, bottom layer $\sigma_y = -\frac{12M_x}{at^2} - \frac{2F_y}{at}$

Similarly on face CD

Total stress in the y direction on face AB, top layer $\sigma_y = -\frac{12M_x}{at^2} + \frac{2F_y}{at}$

Total stress in the y direction on face AB, bottom layer $\sigma_y = \frac{12M_x}{at^2} + \frac{2F_y}{at}$

Similarly on face AD

Total stress in the y direction on face AD, top layer $\sigma_x = -\frac{12M_y}{bt^2} - \frac{2F_x}{bt}$

Total stress in the y direction on face AD, bottom layer $\sigma_x = +\frac{12M_y}{bt^2} - \frac{2F_x}{bt}$

Similarly on face BC

Total stress in the y direction on face BC, top layer $\sigma_x = \frac{12M_y}{bt^2} + \frac{2F_x}{bt}$

Total stress in the y direction on face BC, bottom layer $\sigma_x = -\frac{12M_y}{bt^2} + \frac{2F_x}{bt}$

PUBLICATIONS BASED ON THE RESEARCH WORK.

1. Manoj G. T. and Nandakumar C. G. (2012), Ultimate Strength Predictions of Hat Stiffened Plates, Proceedings of International Conference on Recent Innovations in Technology (ICRIT 2012), RIT, Kottayam, Kerala, pp. 39-45.

2. Manoj G. T. and Nandakumar C. G. (2013), Hat Stiffened Plates for Ship Building, International Journal of Applied Engineering Research and Development, vol. 3, pp. 1-10.

3. Manoj G. T. and Nandakumar C. G. (2014), Orthotropic Plate Model for Hat Stiffened Plate, Proceedings of Institution of Mechanical Engineers, Part M: Journal of Engineering for the Maritime Environment, vol. 228(3), pp. 262-271.

4. Manoj G. T. and Nandakumar C. G. Superelement for Hat Stiffened Plate, Communicated to the journal Engineering Computations.

AUTHOR'S RESUME

Manoj G Tharian completed B.Tech in Mechanical Engineering from Govt. Engineering College, Thrissur. He worked as project associate in Ocean Engineering Research Centre, IIT Madras in 1995. He Completed Marine Engineering diploma from Marine Engineering Research Institute, Mumbai. He worked as a Marine Engineer in Chevron Shipping Company, San Francisco and Anglo Eastern Ship Management, Hong Kong from 1996 to 2002. He has sailed as fourth engineer and third engineer onboard tanker ships and container ships. He has done his M.Tech in Computer Aided Structural Analysis and Design from the Department of Ship Technology, Cochin University of Science and Technology, Kochi. From 2003 to 2005 and 2007 to 2012, he worked as Assistant Professor in Viswajyothi college of Engineering and Technology. Currently he is working as HoD, Mechanical Engineering Department at Rajagiri School of Engineering and Technology, Kochi.